DEVELOPMENT OF 3-D PRINTED EXOHAND FOR MIRROR THERAPY

A THESIS SUBMITTED TO
THE GRADUATE SCHOOL OF NATURAL AND APPLIED SCIENCES
OF
MIDDLE EAST TECHNICAL UNIVERSITY

BY

TUNAHAN YILMAZ

IN PARTIAL FULFILLMENT OF THE REQUIREMENTS
FOR
THE DEGREE OF MASTER OF SCIENCE
IN
MECHANICAL ENGINEERING

NOVEMBER 2022

Approval of the thesis:

DEVELOPMENT OF 3-D PRINTED EXOHAND FOR MIRROR THERAPY

submitted by **TUNAHAN YILMAZ** in partial fulfillment of the requirements for the degree of **Master of Science in Mechanical Engineering Department, Middle East Technical University** by,

Prof. Dr. Halil Kalıpçılar
Dean, Graduate School of **Natural and Applied Sciences** _____

Prof. Dr. M. A. Sahir Arıkan
Head of Department, **Mechanical Engineering** _____

Assoc. Prof. Dr. Ali Emre Turgut
Supervisor, **Mechanical Engineering, METU** _____

Assist. Prof. Dr. Kutluk Bilge Arıkan
Co-supervisor, **Mechanical Engineering, TEDU** _____

Examining Committee Members:

Assoc. Prof. Dr. Mehmet Bülent Özer
Mechanical Engineering, METU _____

Assoc. Prof. Dr. Ali Emre Turgut
Mechanical Engineering, METU _____

Assist. Prof. Dr. Kutluk Bilge Arıkan
Mechanial Engineering, TEDU _____

Assoc. Prof. Dr. Ender Yıldırım
Mechanical Engineering, METU _____

Assoc. Prof. Dr. Can Ulaş Doğruer
Mechanical Engineering, Hacettepe University _____

Date: 24.11.2022

I hereby declare that all information in this document has been obtained and presented in accordance with academic rules and ethical conduct. I also declare that, as required by these rules and conduct, I have fully cited and referenced all material and results that are not original to this work.

Name, Surname: Tunahan Yılmaz

Signature :

ABSTRACT

DEVELOPMENT OF 3-D PRINTED EXOHAND FOR MIRROR THERAPY

Yılmaz, Tunahan
M.S., Department of Mechanical Engineering
Supervisor: Assoc. Prof. Dr. Ali Emre Turgut
Co-Supervisor: Assist. Prof. Dr. Kutluk Bilge Arıkan

November 2022, 131 pages

This thesis presents the modeling and design of a family of exoskeleton mechanisms to be used in post-stroke rehabilitation therapy. The mechanism in question is an exoskeleton worn on the index finger, and it aims to support the fingers of patients who have lost their mobility after paralysis, like a physiotherapist, and to improve motor learning in the patient in this process. Based on motor learning principles, an under-actuated mechanism design has been created for this purpose, allowing the patient to make mistakes while also encouraging him to expand the search space. A wide range of phalanges sizes was considered within the design function to reduce the effect of finger sizes on the mechanism. Within the mechanism family, there are fully-actuated and under-actuated versions. While obtaining a fully-actuated design output, it is desired to keep the task space of the mechanism wide. The Global Isotropy Index was used as the metric controlling the end effector's manipulability for this purpose. The Genetic Algorithm toolbox of the MATLAB program was used for mechanism optimization. After obtaining the output for the fully-actuated mechanism, the evolution of this obtained design into the under-actuated versions was carried out. The Virtual Work method is used to analyze the under-actuated mechanism by obtaining force

equations. A method for this transition that is expected to be easily realized is also presented. Following the design, the mechanism was manufactured and tested.

Keywords: exoskeleton, global isotropy index, fully-actuation, under-actuation, genetic algorithm

ÖZ

AYNA TERAPİSİNDE KULLANILMAK ÜZERE 3D BASILMIŞ EL İSKELETİNİN GELİŞTİRİLMESİ

Yılmaz, Tunahan
Yüksek Lisans, Makina Mühendisliği Bölümü
Tez Yöneticisi: Doç. Dr. Ali Emre Turgut
Ortak Tez Yöneticisi: Dr. Öğr. Üyesi. Kutluk Bilge Arıkan

Kasım 2022 , 131 sayfa

Bu tez, inme sonrası rehabilitasyon tedavisinde kullanılacak bir harici iskelet mekanizmaları ailesinin modellemesini ve tasarımını sunmaktadır. Söz konusu mekanizma, işaret parmağına takılan bir dış iskelet olup, felç sonrası hareket kabiliyetini kaybetmiş hastaların parmaklarını bir fizyoterapist gibi desteklemeyi ve bu süreçte hastada motor öğrenmeyi geliştirmeyi amaçlamaktadır. Bu amaçla, motor öğrenme ilkelerine dayalı olarak, hastanın hata yapmasına izin verecek ve aynı zamanda arama alanını artırmaya teşvik edecek, eksik-tahrikli bir mekanizma tasarımı yapılmıştır. Parmak boyutlarının mekanizma üzerindeki etkisini azaltmak için, tasarım fonksiyonunda çok çeşitli falanks boyutları düşünülmüştür. Mekanizma ailesinde, tam-tahrikli ve eksik-tahrikli sınıflar mevcuttur. Tam tahrikli tasarım çıktısı elde edilirken mekanizmanın çalışma alanı geniş tutulmak istenmiştir. Bu amaçla, uç noktasının manipüle edilebilirliğini kontrol eden metrik olarak Global İzotropi Endeks'i kullanılmaktadır. Mekanizma optimizasyonu için MATLAB programının Genetik Algoritma araç kutusu kullanılmıştır. Tam-tahrikli mekanizmanın çıktısı elde edildikten sonra, bu çık-

tının eksik-tahrikli versiyonlara evirilmesi gerçekleştirilmiştir. Sanal İş yöntemi ile eksik-tahrikli mekanizma analizi kuvvet denklemleri ile yapılmıştır. Ayrıca bu geçiş için kolaylıkla gerçekleştirilebileceği öngörülen bir yöntem sunulmuştur. Tasarımın ardından mekanizmanın imalat ve testleri gerçekleştirildi.

Anahtar Kelimeler: dış iskelet, global izotropi endeksi, tam-tahrik, eksik-tahrik, genetik algoritma

For the sake of Science

ACKNOWLEDGMENTS

First of all, I am grateful to my supervisor Assoc. Prof. Dr. Ali Emre Turgut for his always constructive and positive attitude during the process. It was very valuable to be his student.

Secondly, I would like to thank to my co-advisor Assist. Prof. Dr. Kutluk Bilge Arıkan. I worked with him almost more than I worked with Mr. Turgut. I was pushed forward and supported by Mr. Arıkan during the process and that made me bring out my potential. It was very enjoyable to work with him.

Then, I would like to thank my family. I am their product. Seeing and knowing that they are by my side whenever I need a hand makes me feel strong. Be happy!

Friends, my tribe, I thank you all for the moral support that you all give. Kick the bottom of the pool and let the water lift you up. Now it is time to rise!

I would like to thank my coworkers and boss for their patience and understanding throughout the process. They made this one easier than it would have been.

Dear sister, I wish you a long and fruitful life. Don't let a stone touch your feet. Hopefully, you meet nice people. I am always by your side.

Last but not least, I want to thank me. I want to thank me for believing in me, for doing all this hard work, for having no days off, for never quitting, for always being a giver and trying to give more than I recieve. I want to thank me for trying to do more right than wrong. I want to thank me for just being me at all times. Tunafish, you are a bad mf!

Everything has an end. And here it comes. "Anyway the wind blows, does not really matter to me."

This work is funded by the Scientific and Technological Research Council of Turkey under grant number TUBİTAK 121E107.

TABLE OF CONTENTS

LIST OF TABLES

TABLES

LIST OF FIGURES

FIGURES

LIST OF ABBREVIATIONS

WHO	World Health Organization
DOF	Degree of Freedom
DOA	Degree of Actuation
GII	Global Isotropy Index
N.A.	Not Available
MCP	Metacarpophalangeal joint
PIP	Proximal Interphalangeal joint
DIP	Distal Interphalangeal joint
GA	Genetic Algorithm

CHAPTER 1

INTRODUCTION

1.1 Motivation and Problem Definition

A stroke may occur at any time. In the world, 15 million people have a stroke every year. It happens when a blood vessel that feeds blood to a portion of the brain is blocked or when its blood flow is restricted, depriving the brain tissue of oxygen and nutrients. After that, minutes later, brain cells start to die. Rapid therapy is required right away after a stroke. Otherwise, months or years of difficult recuperation are required. "Get up, stand up, and don't give up the fight." should be the motto. Stroke patients must relearn how to perform all these motor functions, much like a baby learns to sit up and walk.

Motor learning is essential for the production of motor functions. Like elite athletes, the more practice one puts in, the better the results. Exploration entails looking for new paths. Exploration is required for the learning process to take place. When a motor function is well examined, the user wishes to exploit that movement. When exploitation outnumbers exploration, motor learning nears completion.

Rehabilitation has been used to treat stroke patients for thousands of years. The identical movements must be repeated hundreds or thousands of times throughout therapy. Physiotherapists guide patients while they practice for this reason. These repetitious operations are now guided by robots. If an exoskeleton mechanism is attached to the body and powered by motors, it can cause bodily components to move. Rehabilitation robots is a new era with great promise. Unfortunately, they are highly expensive, and the majority of patients are unable to pay their recuperation procedure.

Fine motor skills are more difficult to improve than gross motor skills. They require more time to gain. This thesis describes a 3D-printed exo-finger mechanism that is incredibly inexpensive in comparison to rehabilitation robots, focuses on fine motor skill improvement, and has a durable construction that allows it to be utilized by a diverse spectrum of users.

1.2 The Outline of the Thesis

A literature review is provided in Chapter 2. To begin, stroke, motor learning, and rehabilitation robots are discussed. The anatomy of the index finger is then introduced. Third, the mechanism kinds are described in detail: fully actuated and under-actuated. Following that, performance measurements are provided, which are used to obtain the perfect mechanism by selecting optimal structural parameters. Then, optimization approaches such as single objective function and multi-objective function are discussed (Pareto Optimality). In addition, a manufacturing technology, 3D printing, is described in detail for prototype purposes. Finally, the thesis study's contribution is at the end of the Literature Survey chapter.

The mathematical modeling of mechanisms and the construction of optimization algorithms are acquired in Chapter 3. First, the fully-actuated mechanism's kinematic synthesis is developed. Second, a transition methodology is developed for analyzing an under-actuated mechanism. Finally, an under-actuated mechanism family is created by modifying an already specified fully-actuated mechanism. To ensure that the needed motor torques of the mechanisms are within the valid range, required motor torques are calculated for all mechanism types using the Virtual Work Theorem. In addition, the mechanism's sensitivity to human index finger size is tested to ensure that it works for a wide range of finger phalanges sizes. MATLAB is used to identify the best solutions utilizing the genetic algorithm methodology.

The results of fully actuated, transition part, and under-actuated mechanism family are presented in Chapter 4. There are three distinct sections in the fully-actuated part, each distinguished by the optimization problem-solving method. The fully-actuated portion is chosen from among the options. Then, in the transition section, the most

basic under-actuated mechanism findings, a 5-bar mechanism, are shown, so that the force equations can be used to derive the necessary equation to solve the problem. Finally, utilizing the selected fully-actuated mechanism, an under-actuated mechanism family is constructed in the final section. Following that, a selection from that family is made.

The mechanical design and printed mechanism are presented in Chapter 5. A constructed torsional spring is also depicted. Within this chapter, the assembly is completed. The mechanism is then attached to a healthy individual in order to capture user data. In Chapter 6, there is a discussion part. The challenges of creating an underactuated mechanism are highlighted. The conclusion is then delivered. Finally, future work that will advance this research is described and explored.

CHAPTER 2

LITERATURE SURVEY

2.1 Stroke, Motor Learning and Rehabilitation Robotics

Stroke occurs when any veil that feeds blood to brain is blocked or fractured so that an area of the brain dies in minutes. There is no way to heal the dead part. If that part was at the motor cortex which deals with the motor functions, there might be loss of motion. According to World Health Organization, annually 15 million people worldwide suffer a stroke[1]. While one-third of them overcome with tiny disorders, unfortunately another one-third pass away. The last one-third experiences paralysis. The paralysis types are given in Figure 2.1, which is adapted from [2].

Motor function is generated by triggered motor neurons which are in motor cortex. Motor function is the basic understanding of movement or activity through the motor neurons[3]. The learning process of a motor function is called as motor learning. The user explores for an efficient motor function by making mistakes with a feedback

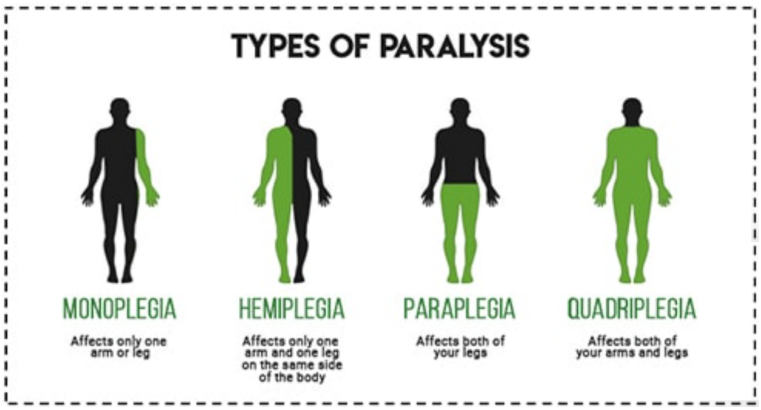

Figure 2.1: Paralysis Types [2]

mechanism just like in reinforcement learning process. When the motor function is gained permanently, the user exploits that motion and motor learning is completed. When exploitation starts, exploration stops. Then the user makes the same outputs for the same inputs. Motor control is defined as the process of initiating, directing, and grading purposeful voluntary movement[3]. In motor learning process, the skill acquisition and progress is done by neural-plasticity[4]. Neural plasticity, also known as brain plasticity, is the ability of neural networks in the brain to change through growth and reorganization[3]. The dead part of the brain can not be healed, unfortunately. However, another parts of the brain can take the place of dead parts under favour of neural-plasticity. Psychotherapists have been dealing with the cure of this illness. They guide patients to obtain motor functions with learning process. Just like how parents teach babies to walk, the therapists teach patients to improve the deficiencies after stroke. Motor recovery is the improvement in the performance of a fatigued muscle or in the movement of a group of muscles paralyzed by stroke or injury[5]. The purpose of the therapy is motor recovery. The recovery of a lost ability after stroke works with the similar neural mechanism as motor learning[5].

Mirror neurons are good to trigger for motor learning. The name of these neurons come from their working principle. The observed action seems to be reflected, as in a mirror, in the motor representation for the same action of the observer[6]. There is a therapy type namely, mirror therapy, in which the stronger body part is used to trick the brain into thinking that the weaker part is moving[6]. This action observation and imitation is a tool for neuro-rehabilitation for learning new skills. The action observation and imitation has a positive impact on recovery of motor functions after stroke[6].

According to the motor learning principles, in order to improve motor learning, there are some things to be considered[7]. Firstly, practice time is important. The more it is practiced, the better the results are. Secondly, the feedback which is given to the patient should not be a lot, but sufficient. Knowledge of performance and knowledge of results should be given to the patient in order to make sure that the patient is aware its situation. Thirdly, motivation is a very helpful for neural-plasticity to occur. A goal in the practice promotes the patient for the result. Fourthly, mental practice before session is another helpful tool to use in therapies. Finally, the most important thing is

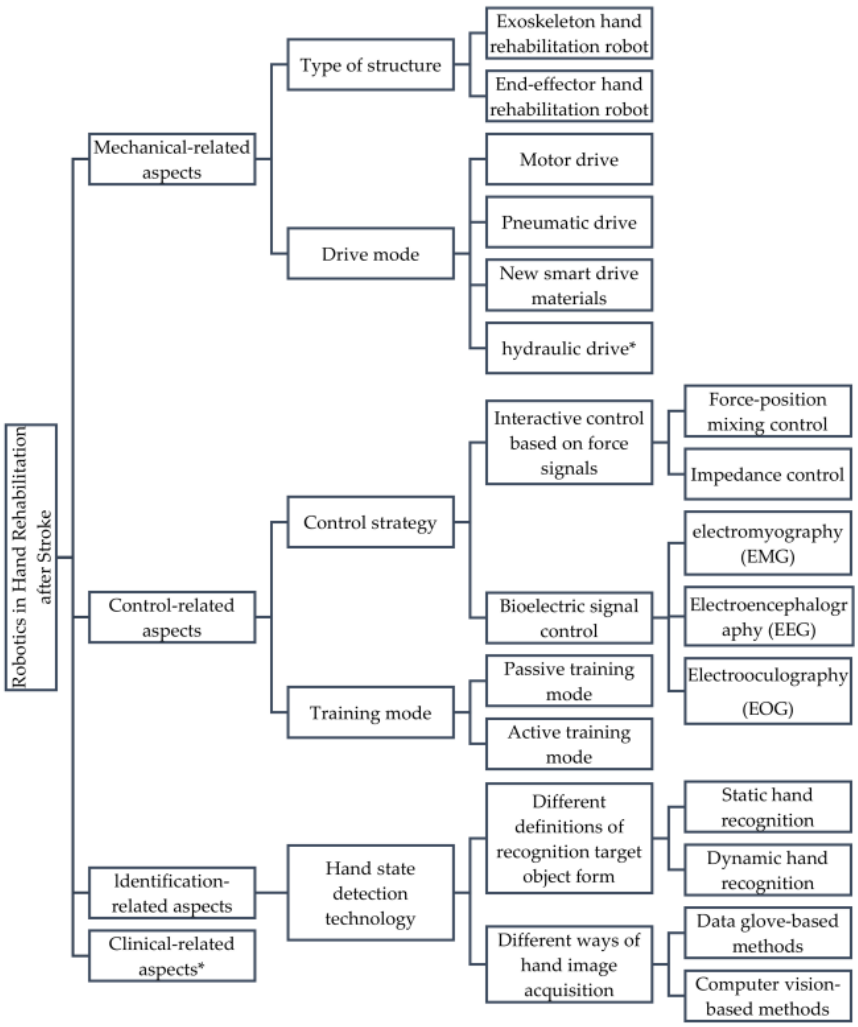

Figure 2.2: Hand Rehabilitation Robotics Overview [8]

allowing patient making mistakes. The patient must be guided surely but the guidance should not be limiting. Otherwise, slacking might occur, which is unwanted in motor recovery process since it falters motor learning. The patient must explore and make mistakes so that see the results of those mistakes. In this thesis, a mechanism model, under-actuated mechanism, is considered, which allows the user to make mistakes due to its nature.

Nowadays, physiotherapists are substituted with robots. Rehabilitation robotics is a developing industry. Robots guide patients in rehabilitation processes. The general overview of the hand rehabilitation robots are given in Figure 2.2, which is taken from [8].

2.2 Finger Anatomy

The index finger has 4 degrees of freedom as in Figure 2.3, which is taken from [9].

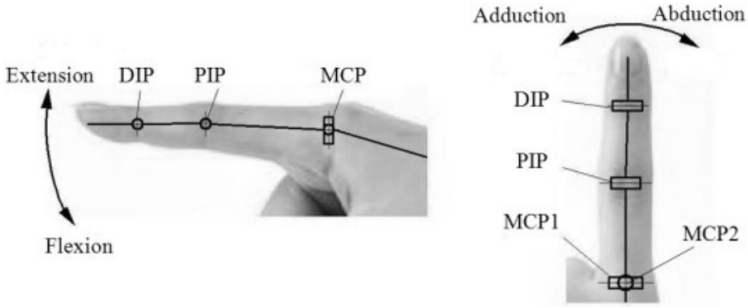

Figure 2.3: 4 DOF Finger model [9]

When it is considered in planar motion, the adduction-abduction movement can be eliminated, only extension-flexion movement can be considered. Thus, the *dof* is decreased to 3. The planar skeleton model is given in Figure 2.4 which is taken from literature[10].

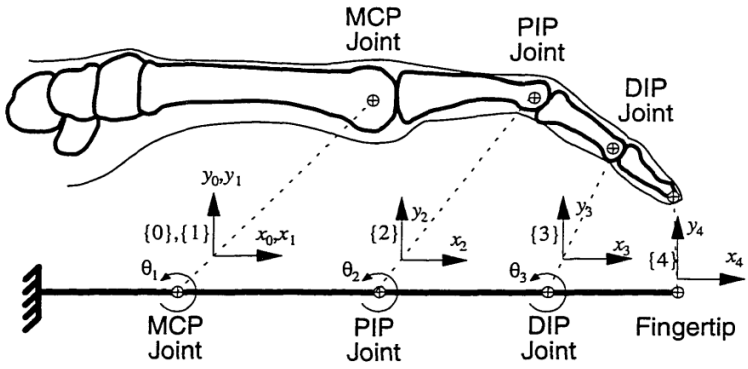

Figure 2.4: Planar skeleton model of the human finger [10]

Although the finger segment sizes differ too much due to age, gender, ethnicity and some other differences, the average sizes are found from the literature[11] as in Table 2.1.

The joint motion range for the index finger is given in Table 2.2, which is adapted from [12]. These are the boundaries for an index finger to work safely. Working out

Table 2.1: Human finger phalanges sizes [11]

Finger Segment	Length (SD) $[cm]$	Mass $[g]$	Moment of inertia $[g/cm^2]$
Distal	2.4 (0.1)	3.8	2.0
Middle	3.1 (0.2)	6.3	5.8
Proximal	4.9 (0.3)	19.6	45.4

of these boundaries is neither recommended nor achievable. Thus, a task space will be constructed within these boundaries.

Table 2.2: Finger Joint Motion Range [12]

Finger Joint	Angular Relative Motion Range
MCP	$-90^\circ < \theta_1 < 45^\circ$
PIP	$-120^\circ < \theta_2 < 0^\circ$
DIP	$-90^\circ < \theta_3 < 50^\circ$

The reachable workspace for a human index finger is given in Figure 2.5, which is taken from literature[13].

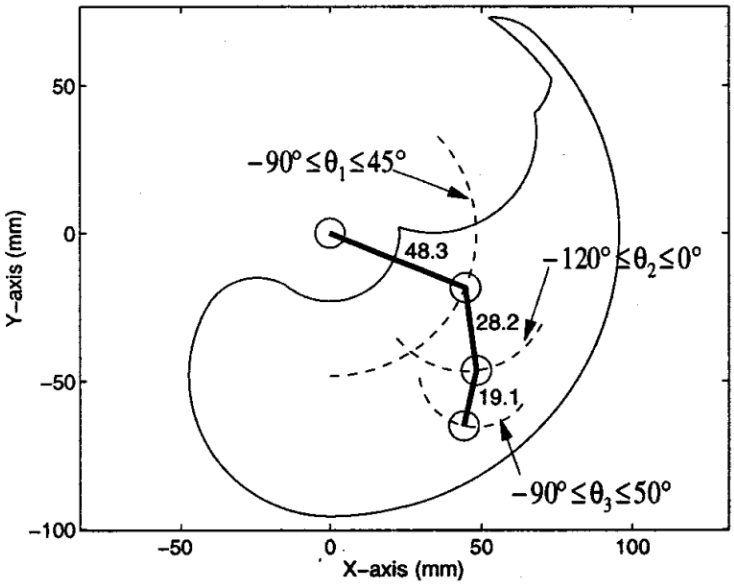

Figure 2.5: Human finger reachable task space [13]

Table 2.3: Static Passive Torque [11]

Joint	τ^s [Nm]
DIP	$-0.103\theta^3 + 0.102\theta^2 - 0.052\theta - 0.019$
PIP	$0.056\theta^3 + 0.016\theta^2 - 0.132\theta + 0.015$
MCP	$-0.071\theta^3 + 0.145\theta^2 - 0.154\theta - 0.029$

Table 2.4: Stiffness and Damping Coefficients [11]

Joint	K [Nm/rad]	B [Nms/rad]
DIP	$0.38\theta^2 - 0.09\theta + 0.13$	0.0081
PIP	$1.06\theta^2 - 0.76\theta + 0.4$	0.0105
MCP	$1.02\theta^2 - 0.54\theta + 0.45$	0.0142

Finger passive joint torques are calculated according to the equations in Tables 2.3 and 2.4 which are taken from [11].

The equations in Table 2.3 are to calculate the static passive torque that occurs in the finger joints at rest. For the torque that is produced by the finger in the motion, the formula is as follows[11]:

$$\tau_j = {\tau_j}^s - B_j\dot{\theta}_j - K_j(\theta_j)\Delta\theta_j \tag{2.1}$$

where τ is the passive joint torque, τ_s is the static passive torque, and K and B are the spring and damping coefficient for the joint[11].

2.3 Mechanism Types

2.3.1 Fully-Actuated Mechanisms

If there exists an independent input for each degree of freedom, the system is fully actuated [14]. In a fully-actuated mechanism, the degree of actuation(*doa*) is equal to the degree of freedom(*dof*).

2.3.2 Under-Actuated Mechanisms

In under-actuated mechanisms, the *doa* less than *dof*. In order to define the mechanism kinematically, there needs to be number of independent passive elements, such as springs, equal to the missing number of actuators. Under-actuated systems are able to flexible. They are sensitive to external forces.

In order to define an under-actuated mechanism kinematically, there needs to implement force equations.

2.4 Performance Metrics

In all design procedures, finding best is desired. The question is, "with respect to what?". The answer is "a measure". In order to find an optimal mechanism or system, performance metrics have been used. At least one performance metric has to be defined to be minimized or maximized. Some of the design metrics that have been used so far are given in the below subsections.

2.4.1 Transmission Angles

Transmission angle calculation has been used as a performance measure in mechanism optimization. In an ideal mechanism, a smooth motion throughout the task space is desired, in which the transmission ratios do not change continuously. This measure might help to choose the best mechanism so that the force transmission is uniform[15]. The desired value for the transmission angle is 90° since the force transmission occurs in that orientation the most effectively.

2.4.2 Required Motor Torques

In some designs, minimizing the required motor torque values is considered as a measure[16]. For this purpose, the Virtual Work method can be used in order to estimate the motor torque value. Newtonian formulation of the dynamics of the mecha-

nism can also be used in order to evaluate the motor torque value[17]. These methods are applied by some assumptions.

2.4.3 Global Isotropy Index

Isotropy means having equal properties in all directions. In kinematic perspective, it is explained as being the furthest possible distance from singularity[18]. Having an isotropic mechanism is a desired feature. When a mechanism is isotropic, the following items are accomplished as explained in [18, 19] as follows:

- High performance is achieved as minimizing waste energy.
- Best servo accuracy can be obtained by the availability of invertability of kinematic equations for control.
- Error is equal in all directions.
- Equal forces may be exerted in all directions.
- Equal ease to move in any direction exists.

The history of Global Isotropy Index(GII) begins with Yoshikawa[20]. He proposed a measure metric for manipulability as in Equation 2.2.

$$W = \sqrt{det(J(\theta)J^T(\theta))} \tag{2.2}$$

where J is the Jacobian matrix and θ is the state. Although this metric is used for obtaining the largest manipulability measure at a given state of end-effector in the taskspace, it depends on the scale of a manipulator[18]. For a metric to be used in the design, it is required to be independent from scale[21].

After Yoshikawa, Klein and Blaho examined several performance metrics[22]. They introduced minimum singular value of Jacobian. However, the expression was not analytically.

Then, Kim and Khosla indicated 2 problems of Yoshikawa's manipulability which are having scale and order dependencies[23]. The scale dependency prevents to compare

different sized manipulators and the order dependency does not help to understand physical meaning of the manipulability[18]. In order to overcome this misconception, they defined a new measure metric, namely isotropy, in which the ratio of geometric mean and arithmetic mean of the eigenvalues of JJ^T is considered as in Equation 2.3[23].

$$\Delta = \frac{W}{\Psi}$$
$$\Psi = \frac{\text{trace}(JJ^T)}{\text{order m}} \tag{2.3}$$

where Δ is the measure of isotropy and W is the Yoshikawa's manipulability measure. This metric is dimensionless as it is not dependent on the scale.

Klein and Miklos defined "Spatial Isotropy" in which positional and orientational isotropy of the end-effector is combined to one. They believe that it would be a relatively weak and artificial condition if the Jacobian is considered as a measure of whole isotropy in one term.[24]

Gosselin reconceived Jacobian matrix by eliminating end-effector angular velocity. If the end-effector is defined as a single point, the velocity explanation needs the angular velocity. However, usage of more than one point for the end-effector allows to subtract the angular velocity to define the velocity of the end-effector. Thus, dimensionally homogenous Jacobian is obtained.[25].

Ma and Angeles defined "Dynamic Conditioning Index(DCI)" which measures the dynamical coupling and numerical stability of the generalized inertia matrix. Results are well suited for particular positions, however, satisfactory performance is not guaranteed for whole workspace. Consequently, it was not stated for optimal global performance when the manipulator works in a large task space.[26]

Angeles is defined "Conditioning index(CI)" in terms of the minimum condition num-

ber on the proper choice of the joint variables[27]. It is regarded as a local property.

All the condition indices mentioned so far, which are regarding to Jacobian, depend on the operating point and the location of the point is critical in obtaining a good kinematic manipulation performance. Hence they fail to give a reliable measure of global performance throughout the whole workspace.
Gosselin and Angeles proposed "Global Conditioning Index(GCI)" in which the whole workspace is considered by the condition number is scaled over the workspace, as in Equation 2.4.

$$GCI = \frac{\int_W \frac{dW}{k}}{\int_W dW} \tag{2.4}$$

where k is the local performance measure such as the condition number as in Equation 2.5:

$$k = \sqrt{\frac{\lambda_{max}(G(x,p)G^T(x,p))}{\lambda_{min}(G(x,p)G^T(x,p))}} = \frac{\sigma_{max}(G(x,p))}{\sigma_{min}(G(x,p))} \tag{2.5}$$

At first, GCI might seem as a good global performance metric. However, since it averages the results, some poor results might be ignored.

Stocco defined a measurement metric for global isotropy namely GII, which stands for "Global Isotropy Index"[28]. It is the ratio of the smallest singular value of the Jacobian matrix to the largest singular value of the Jacobian matrix in the whole workspace as shown in Equation 2.6.

$$\mu = \frac{\sigma_{min}(J(\Theta))}{\sigma_{max}(J(\Theta))} \quad , \quad 0 \leq \mu \leq 1 \tag{2.6}$$

where μ is the mechanism isotropy, $\sigma_{min}(J(\Theta))$ is the minimum singular value decomposition value of the Jacobian matrix, $\sigma_{max}(J(\Theta))$ is the maximum singular value decomposition value of the Jacobian matrix and $J(\Theta)$ is the Jacobian matrix that describes the mechanism.

GII compares the largest and smallest singular values in the entire workspace. Every position in whole workspace is checked with all possible configurations, then minimum and maximum singular values are found. The ratio gives a scalar num-

ber. As this number(μ) gets closer to 1, mechanism is more isotropic. When $\mu = 1$, mechanism is perfectly isotropic. Good servo accuracy and singularity avoidance is obtained. Otherwise, when $\mu = 0$, losing 1 or more *dof* occurs and inverse kinematics can not be defined. In the literature, some studies has been examined with the GII metric[12, 29].

2.4.4 Sensitivity Index

Sensitivity can be explained as the change in an original value of a system when the variables of that system varies[30]. For design purposes, the sensitivity analysis is examined in order to determine how the variation of the variables affects the designed mechanism[31].

Sensitivity analysis has been used to obtain robust systems in which the variation of some parameters becomes insignificant. This analysis is applied either in the design procedure as a part of a performance measure[32] or after the design process in order to check the designed mechanism is appropriate[31].

In this thesis, a robust mechanism is desired. The mechanism is wanted to be used by different patients. For this purpose, the mechanism is required to be less sensitive to human finger phalanges sizes.

2.4.5 Collision Prevention

In complex mechanisms, where several loops are included in the mechanism, the joints might collide with each other. In order to prevent that, a collision prevention measurement has been used[33]. In this metric, joint positions are checked if they crash in the task space. For some complicated mechanisms, especially spatial systems, if the task space is limited, this design metric might be very helpful to obtain the optimal solution.

2.5 Optimization methods

Optimization is a way to find a destination in which minimum sources are consumed.

In order to find the best solution, some methods have been used. A straightforward one is the Brute Force approach. In this method, all possible solutions are calculated, then the best one is decided. Although this technique guarantees finding the best solution, it requires a considerable computational power[34]. This method is suitable for small search spaces.

Another optimization technique is the Gradient Descent method. The idea behind this procedure is to follow a gradient up or down in order to find the maximum or minimum of response surface[35]. This procedure is much faster than the brute-force method since all possibilities are not checked. However, a global optimum is not guaranteed. The solution is dependent on the initial starting point.

A different procedure is the Monte Carlo simulation. When the search space is unknown, this method might be good to use. In this technique, a huge number of random points are generated. Then, the frequency distribution of those points is investigated[36].

The advantages of deterministic and random-search methods are combined in the Genetic Algorithm(GA). Principles of genetics are exploited in GA for the optimization theory[37]. First of all, the creation of an initial population of "explorers", which are positioned in the search space occurs. Then, each explorer discovers the value of the response function at its particular place and supplies it to a fitness function. The algorithm repeatedly modifies a population with respect to the value of the fitness function. At each step, the genetic algorithm randomly selects individuals from the current population and uses them as parents to produce the children for the next generation. Over consecutive generations, the population "evolves" toward an optimal solution[38]. The "evolution" process creates three types of children for the next generation as itemized below:[39]

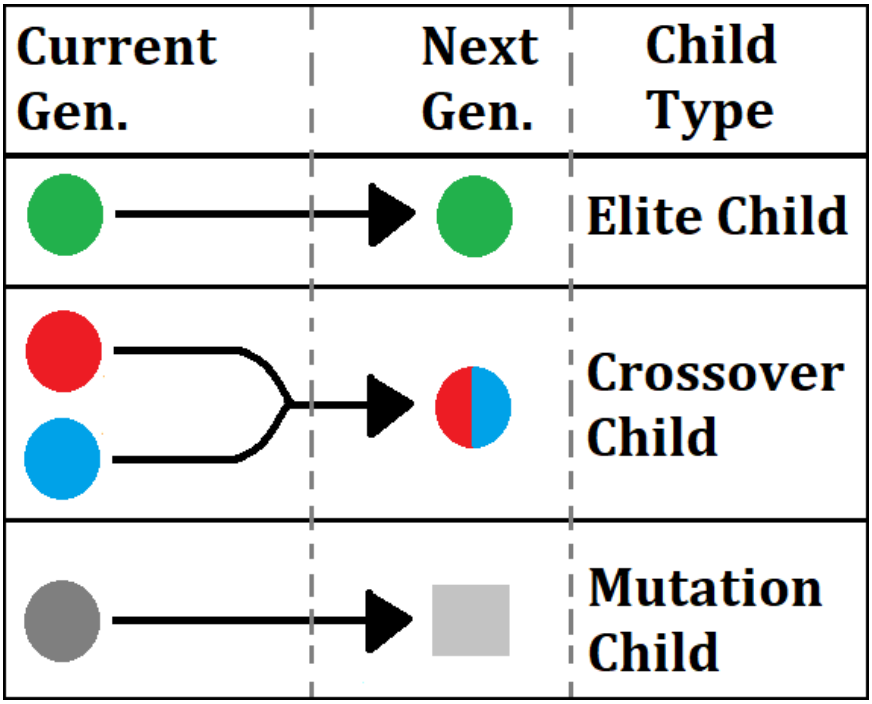

Figure 2.6: GA Children Creation

- Elite child: Current generation's best fitness valued individuals survive.

- Crossover child: A pair of parents are combined. The idea is to create a child which has better properties (in terms of fitness function) than the two parents.

- Mutation child: A single parent becomes the child by introducing random fluctuations.

The creation procedure of the children is illustrated in Figure 2.6

The average performance of individuals in a population is expected to be increased since the ones with the good results are kept and the bad results are eliminated. A basic genetic algorithm flowchart is represented in the Figure 2.7 which taken from [40].

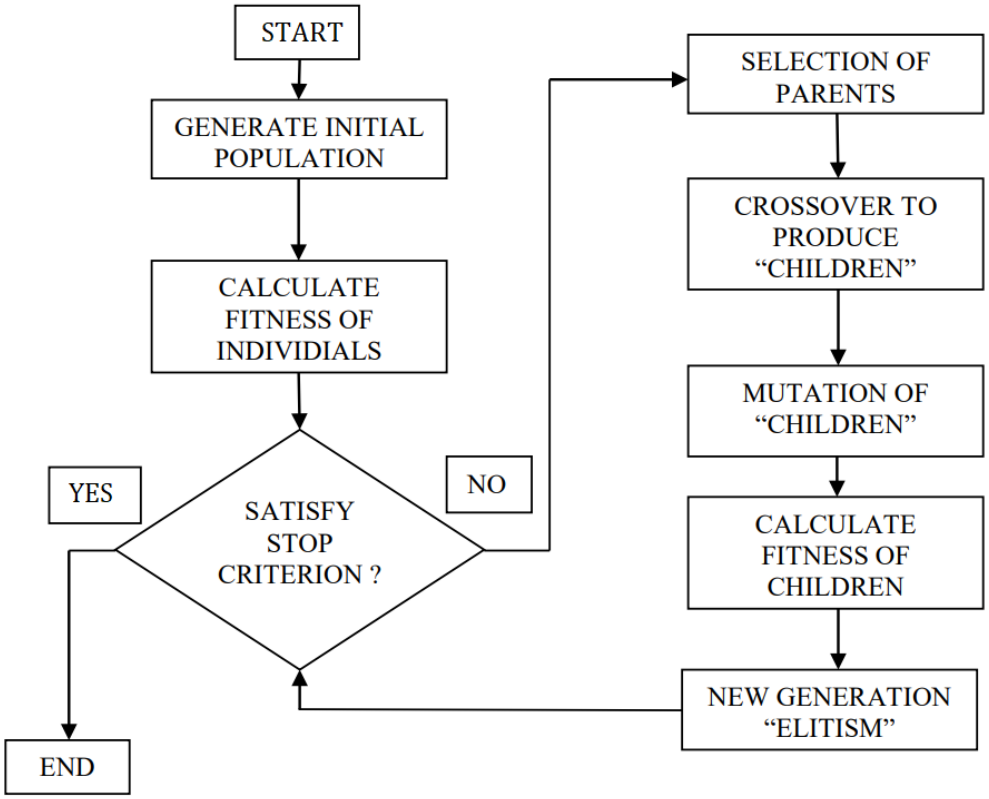

Figure 2.7: GA Children Creation [40]

GA is highly advantageous when solving problems that are not well suited for standard optimization algorithms, including problems in which the objective function is discontinuous, non-differentiable, stochastic, or highly nonlinear[38]. This method is able to find an optimum in huge search spaces. The differences from traditional optimization methods are given below[41]:

- GAs do not search only a single point but a population of points in parallel.
- GAs do not use deterministic transition rules but probabilistic ones.
- GAs work on an encoding of the design variable set rather than on the variables themselves
- GAs do not require derivative information or other auxiliary knowledge. Only the objective function and corresponding fitness levels influence the search.

2.5.1 Single-Objective Function

In the design procedure, more than one performance measure might be desired to be checked simultaneously. Then, these metrics can be implemented in the fitness function either together or separately. When different performance measures are united, it becomes a single-objective optimization problem. A single optimization problem with several metrics can be expressed as a weighted sum as in expression 2.7.

$$F(x) = \alpha_1 f_1(x) + \alpha_2 f_2(x) + ... + \alpha_n f_n(x) \tag{2.7}$$

where x is a design parameter set, $F(x)$ is a combined fitness function, $f_i(x)$ is the i'th objective function and α_i is a constant weight factor for $f_i(x)$.

GA has been mainly applied to single-objective optimization problems[42]. Although this is easy to use, there are some drawbacks. First of all, some undesired solution set might be chosen as the optimal result by the algorithm if the weights are not selected carefully. Secondly, the direction of search in the GA is fixed in the multi-dimensional objective space[42]. At the end of the algorithm, a single result is given as the best result to the user.

2.5.2 Multi Objective Function (Pareto Optimality)

When more than one performance measure is considered, another option is to design the fitness function as a multi-objective problem. In this method, independent fitness functions are combined into one vector instead of representing a scalar value. A multi-objective optimization problem is expressed in 2.8.

$$G(x) = [g_1(x), g_2(x), ..., g_n(x)] \tag{2.8}$$

where x is a design parameter set, $G(x)$ is a multi-objective fitness function, $g_i(x)$ is the i'th objective function.

Multi-Objective optimization does not give a single result like single-optimization but a set of optimal result values. The user is supposed to select from that set.

2.6 Manufacturing Method

3D printing is an easy and fast way to manufacture the part that is going to be manufactured is relatively small-sized. In the mechanism that this thesis focuses on, the possible maximum length of any part is less than 7 mm due to boundaries. Also, the required internal stresses that would occur while the mechanism is in motion will not be high. So, from the viewpoint of material, plastics will be suitable, especially PLA. There are some examples in the literature where these types of products are printed in 3D[43].

2.7 Contributions

- The mechanism synthesis is done with the Global Isotropy Index(GII) index.
- The under-actuated mechanism synthesis with the usage of the Virtual Work method.
- Easy way to transition to under-actuation: breaking a linkage.

CHAPTER 3

METHODOLOGY

In this chapter, mathematical modeling of the considered index finger mechanisms is given. At first, a fully-actuated mechanism is introduced. Then, a methodology, "Transition to the Under-actuation" is given with an easy example; from a 4-bar mechanism to a 5-bar mechanism. Finally, an under-actuated mechanism family which is generated from the designed and tested fully-actuated mechanism is presented. Position, velocity, and force equations are derived for the purpose of mechanism synthesis, and the design methodology and design metrics are detailed in both fully-actuated and under-actuated mechanisms. The mechanism types are shown in Table 3.1.

Table 3.1: Mechanism Types

Mechanism Type	*dof*	*doa*	Focused Parameter
Fully-actuated	2	2	N.A.
Under-actuated ver.1	3	2	a_6
Under-actuated ver.2	3	2	a_8
Under-actuated ver.3	3	2	a_3
Under-actuated ver.4	3	2	β_2

3.1 Fully-Actuated Mechanism

3.1.1 Description of the Mechanism

The fully-actuated mechanism considered in the thesis is given in Figure 3.1. It is a planar mechanism including a human index finger. The represented proximal, middle

and distal phalanges are the links B_0E_0, E_0F_0 and F_0K_0, respectively. The mechanism has 11 links, 14 joints, and 4 loops. All links are connected with revolute joints.

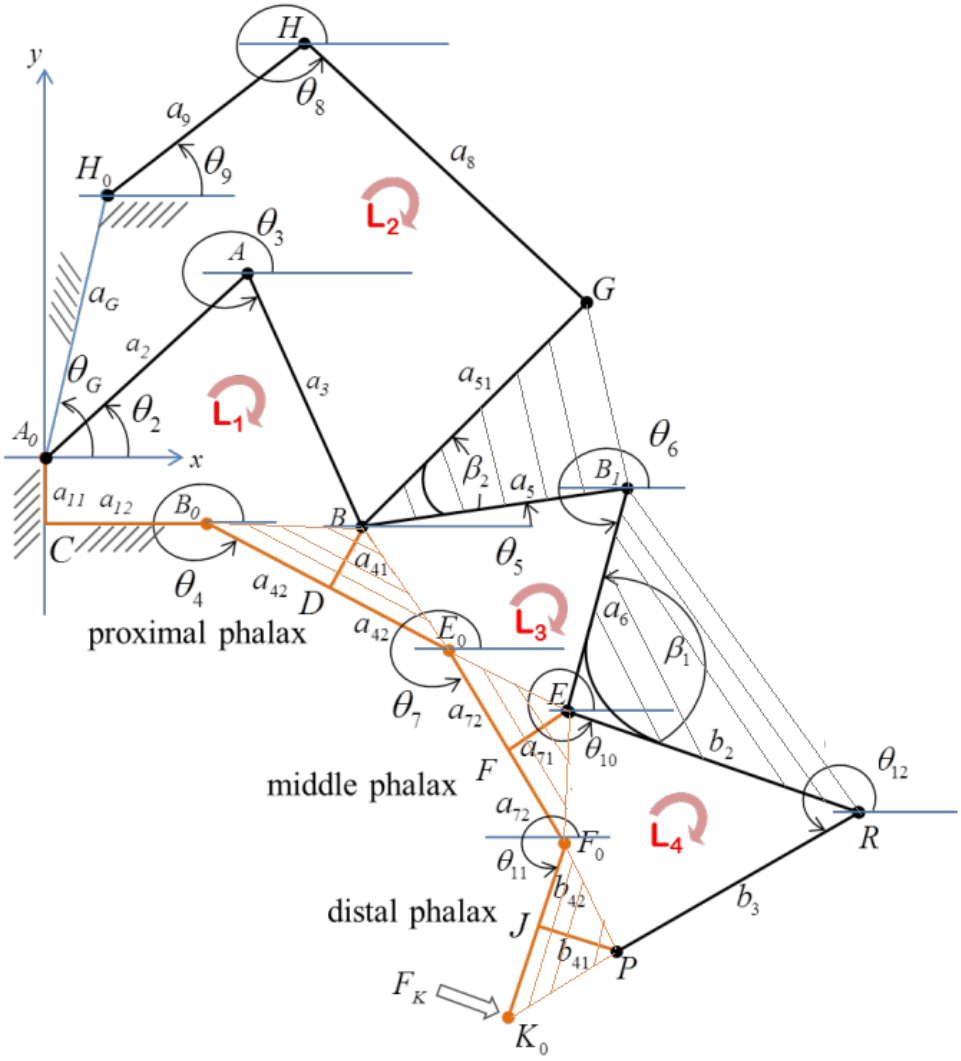

Figure 3.1: Fully actuated index exoskeleton mechanism - 2 dof 3 phalanges

By using Kutzbach Grübler's Formula for planar mechanisms[44], the degree of freedom (*dof*) of the mechanism can be found as below:

$$\begin{aligned} N &= 3(l-1) - 2j \\ &= 3(11-1) - (2)(14) = 2 \end{aligned} \tag{3.1}$$

where

l: number of links

j: number of joints.

The number of Loops can be found below:

$$L = j - l + 1 = 14 - 11 + 1 = 4 \tag{3.2}$$

The number of independent variables can be found below:

$$V = 2L + N = (2)(4) + 2 = 10 \tag{3.3}$$

For a fully-actuated system, the degree of actuation(*doa*) of the mechanism should be equal to the number of *dof* of the mechanism. For this purpose, 2 rotary actuators are placed at points A_0 and H_0.

The position variables of the defined mechanism in Figure 3.1 can be shown as follows:

$$V^* = [\theta_2, \theta_3, \theta_4, \theta_5, \theta_6, \theta_7, \theta_8, \theta_9, \theta_{11}, \theta_{12}] \tag{3.4}$$

Also, the design vector can be shown as follows:

$$S = [a_{11}, a_{12}, a_2, a_3, a_{41}, a_{42}, a_5, a_{51}, a_6, a_{71}, a_{72}, a_8, a_9, b_2, b_3, b41, b_{42}, \beta_1, \beta_2, \theta_G] \tag{3.5}$$

In the mechanism, the human index finger phalanges angles θ_4, θ_7 and θ_{11} are defined as primary variables. To reduce the *dof* and *doa*, the last phalanx joint, namely DIP, is considered to have a relationship with its previous joints θ_4 and θ_7, namely MCP and PIP, respectively. The Equation (3.6) is complied from [11, 45, 46]. While θ_4 and θ_7 can be controlled independently, θ_{11} is defined as a function of θ_4 and θ_7 as follows:

$$\theta_{11} = \frac{5}{3}(\theta_7) - \frac{2}{3}(\theta_4) \tag{3.6}$$

Hence, the consequent primary and secondary variables are shown in Equations 3.7 and 3.8, respectively.

$$V_1{}^* = [\theta_4, \theta_7, \theta_{11}] \tag{3.7}$$

$$V_2{}^* = [\theta_2, \theta_3, \theta_5, \theta_6, \theta_8, \theta_9, \theta_{12}] \tag{3.8}$$

The dependent variable θ_{10} is a function of θ_6 and β_1.

$$\theta_{10} = f(\theta_6, \beta_1) = \theta_6 + \pi - \beta_1 \tag{3.9}$$

3.1.2 Design Methodology

In the design, the structure parameters are optimized, which are given in Equation 3.5. The pseudo-code of the design procedure is given in the Figures 3.2 and 3.3. In the flow chart, there are two separate parts. In the first part, the design for the first 2 finger segments, proximal and middle phalanges are completed. The first part is shown in the Figure 3.2. Then generation for the distal phalange is completed as in the Figure 3.3. The mechanism schema that is going to be designed only for the fully actuated part is given in Figure 3.4. The design parameters are:

$$S_1 = [a_{11}, a_{12}, a_2, a_3, a_{41}, a_{42}, a_5, a_{51}, a_6, a_{71}, a_{72}, a_8, a_9, \beta_2, \theta_G] \tag{3.10}$$

where a_{42} and a_{72} are given as inputs, since they are the half lengths of the human index finger proximal and distal phalanges, respectively. Then, in the second part of the design, the algorithm works for the 3. phalanx, distal phalanx, in which the design parameters are:

$$S_2 = [b_2, b_3, b_{41}, \beta_1] \tag{3.11}$$

where b_{42} is given as input since it is the half length of the human index finger distal phalanx.

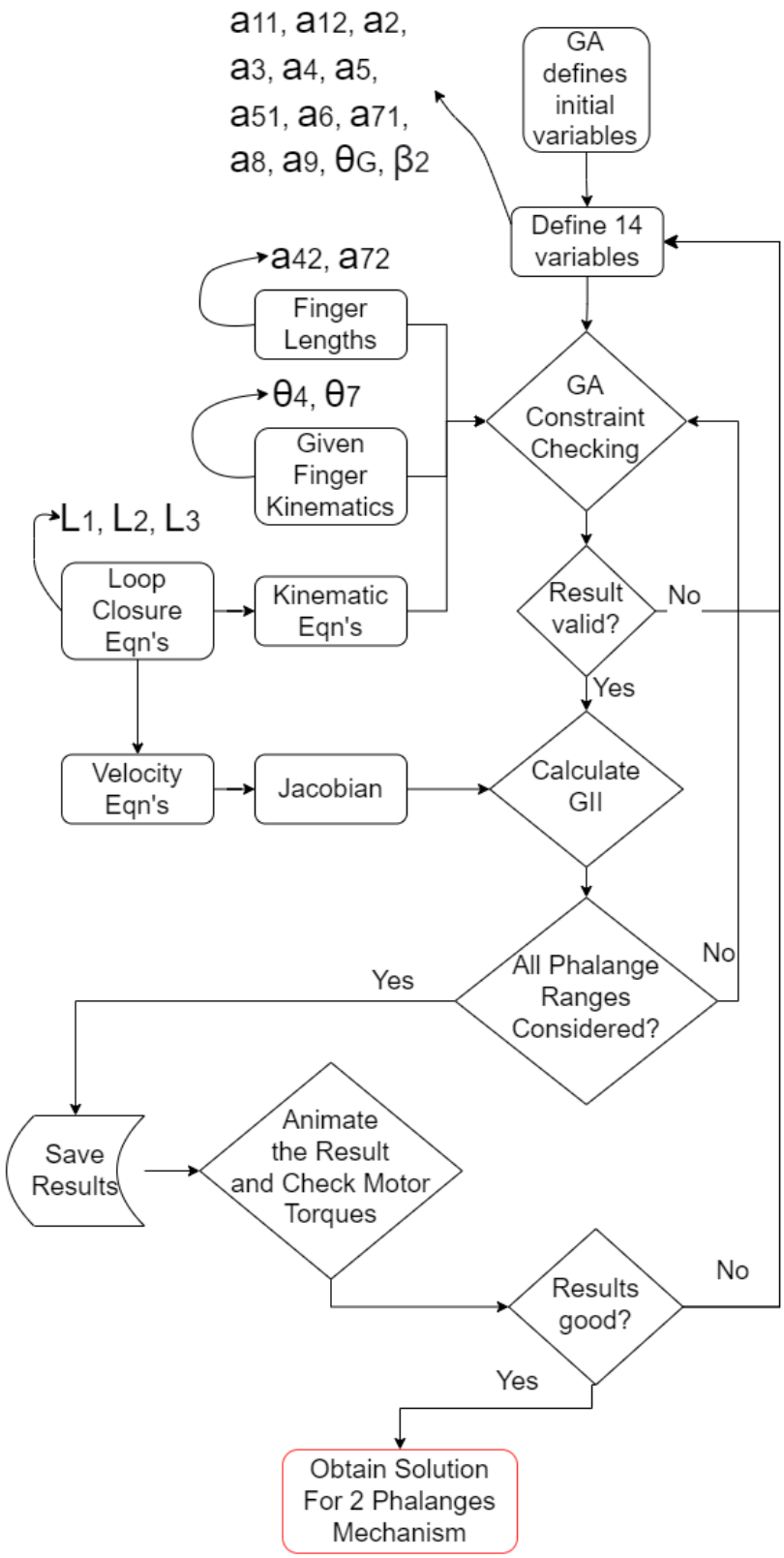

Figure 3.2: Design Flow Chart for Fully-Actuated Mechanism, Part 1

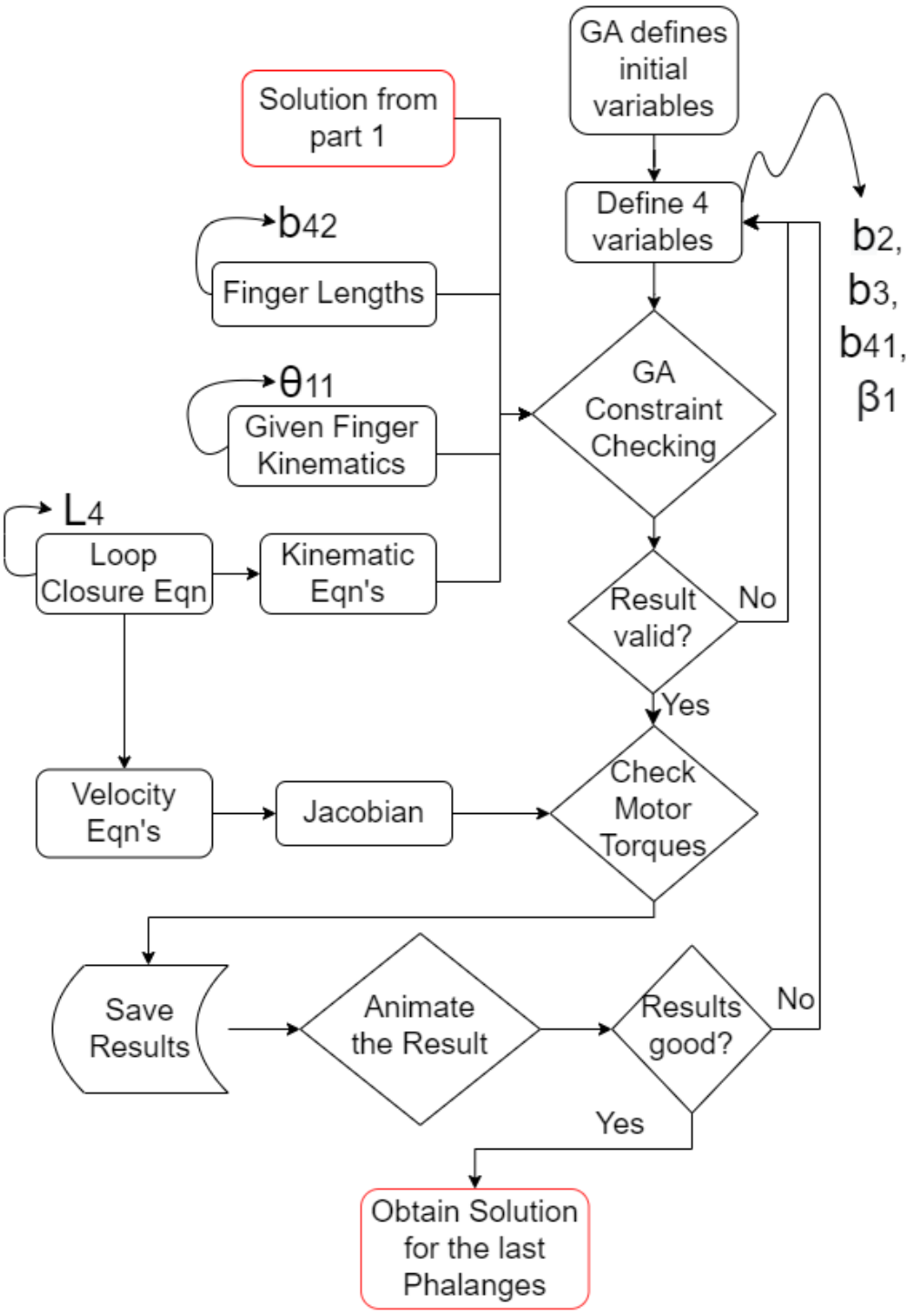

Figure 3.3: Design Flow Chart for Fully-Actuated Mechanism, Part 2

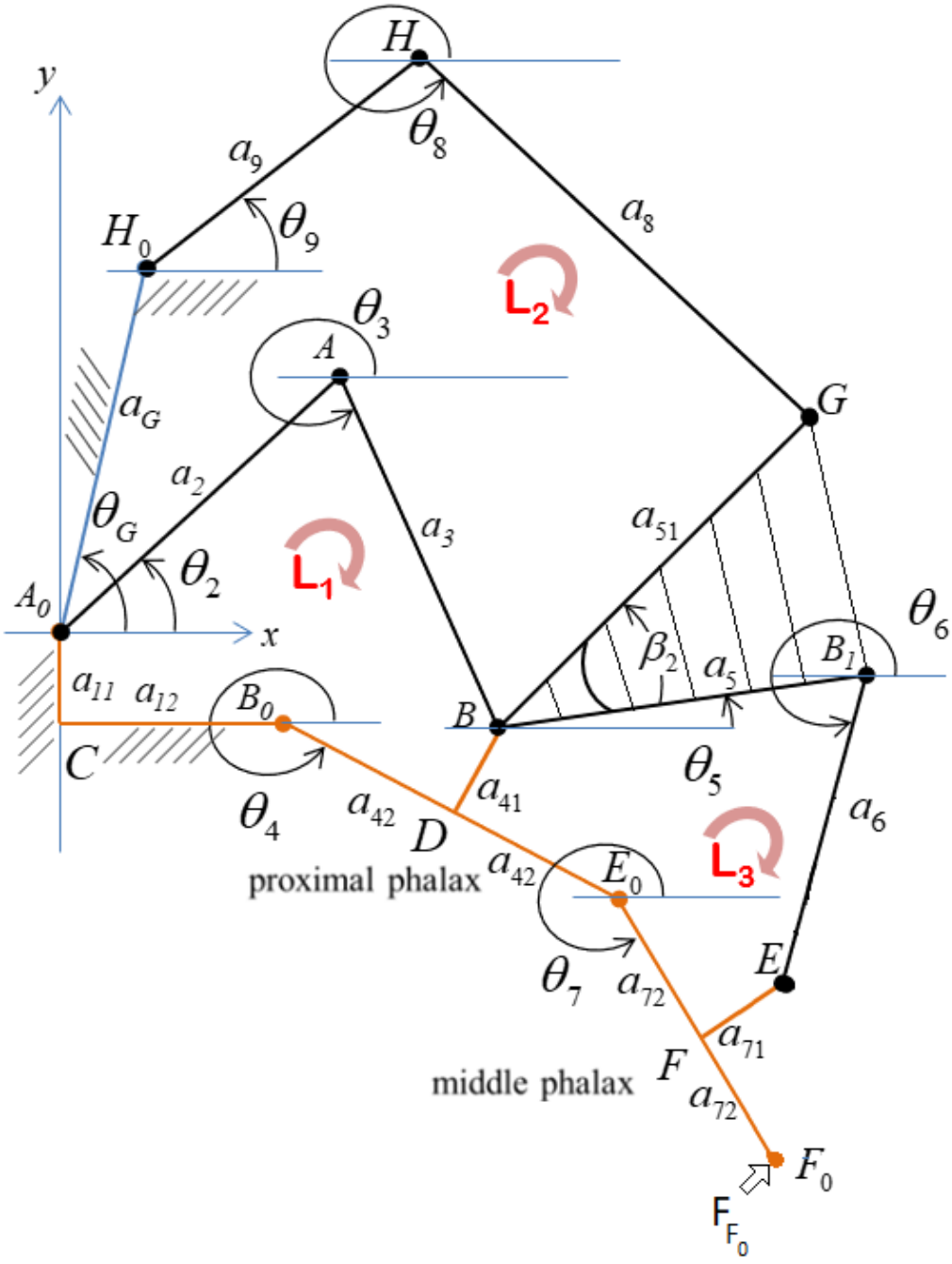

Figure 3.4: Fully actuated index exoskeleton mechanism - 2 dof 2 phalanges

3.1.3 Mechanism Synthesis

This section deals with the derivation of mathematical models for the fully-actuated mechanism.

Note that the *dof* of the revised 2 phalanges mechanism is the same as the 3 phalanges mechanism. In this revised mechanism, there are 9 links and 11 joints. The number of loops is decreased to 3. Mathematical proof is given below:

$$\begin{aligned} N &= 3(l-1) - 2j \\ &= 3(9-1) - (2)(11) = 2 \end{aligned} \tag{3.12}$$

where

l: number of links
j: number of joints.

The number of Loops can be found below:

$$L = j - l + 1 = 11 - 9 + 1 = 3 \tag{3.13}$$

The number of independent variables can be found below:

$$V = 2L + N = (2)(3) + 2 = 8 \tag{3.14}$$

3.1.3.1 Position Analysis

The following complementary equations can be written in order to express the position of the end-effector in terms of the relevant primary and secondary variables and to set up all the necessary relationships among the primary and secondary variables.

$$\overline{P} = \overline{f}(\overline{x}, \overline{y}) \tag{3.15}$$

$$\overline{G}(\overline{x}, \overline{y}) = \overline{0} \tag{3.16}$$

The symbols in the above equations have the following meanings[47]. $\overline{P}$ is a column matrix that represents the position of the end-effector in the task space, $\overline{x}$ is the primary variable vector, $\overline{y}$ is the secondary variable vector, and $\overline{G}$ is a differentiable and continuous function.

Loop Closure Equations

The Loop Closure Equations (LCE's) are written in Equations 3.17.

$$\begin{aligned} L1 &\Rightarrow \overrightarrow{A_0AB} = \overrightarrow{A_0CB_0DB} \\ L2 &\Rightarrow \overrightarrow{A_0H_0HG} = \overrightarrow{A_0ABG} \\ L3 &\Rightarrow \overrightarrow{DBB_1FE} = \overrightarrow{DE_0FE} \\ L4 &\Rightarrow \overrightarrow{FERP} = \overrightarrow{FF_0JPR} \end{aligned} \tag{3.17}$$

Thus, detailed equations can be written as follows:

$$L1 \Rightarrow a_2e^{i\theta_2} + a_3e^{i\theta_3} = (-a_{11}i + a_{12}) + a_{42}e^{i\theta_4} + a_{41}e^{i(\theta_4+\frac{\pi}{2})} \tag{3.18}$$

$$L2 \Rightarrow a_Ge^{i\theta_G} + a_9e^{i\theta_9} + a_8e^{i\theta_8} = a_2e^{i\theta_2} + a_3e^{i\theta_3} + a_{51}e^{i(\theta_5+\beta_2)} \tag{3.19}$$

$$L3 \Rightarrow a_{41}e^{i(\theta_4+\frac{\pi}{2})} + a_5e^{i\theta_5} + a_6e^{i\theta_6} = a_{42}e^{i\theta_4} + a_{72}e^{i\theta_7} + a_{71}e^{i(\theta_7+\frac{\pi}{2})} \tag{3.20}$$

$$L4 \Rightarrow a_{71}e^{i(\theta_7+\frac{\pi}{2})} + b_2e^{i\theta_{10}} + b_3e^{i\theta_{12}} = a_{72}e^{i\theta_7} + b_{42}e^{i\theta_{11}} + b_{41}e^{i(\theta_{11}+\frac{\pi}{2})} \tag{3.21}$$

It is possible to write the above LCE's(3.18, 3.19, 3.20, 3.21) in a matrix form as below:

$$\overline{G} = \begin{bmatrix} 0 \\ 0 \\ 0 \\ 0 \\ 0 \\ 0 \\ 0 \\ 0 \end{bmatrix} = \begin{bmatrix} \delta_1 \\ \delta_2 \\ \delta_3 \\ \delta_4 \\ \delta_5 \\ \delta_6 \\ \delta_7 \\ \delta_8 \end{bmatrix} \tag{3.22}$$

where

$$
\begin{aligned}
\delta_1 &= +\, a_{12} - a_2\cos(\theta_2) - a_3\cos(\theta_3) + a_{42}\cos(\theta_4) - a_{41}\sin(\theta_4) \\
\delta_2 &= -\, a_{11} - a_2\sin(\theta_2) - a_3\sin(\theta_3) + a_{42}\sin(\theta_4) + a_{41}\cos(\theta_4) \\
\delta_3 &= +\, a_2\cos(\theta_2) + a_3\cos(\theta_3) + a_{51}\cos(\theta_5+\beta_2) - a_G\cos(\theta_G) \\
&\quad - a_8\cos(\theta_8) - a_9\cos(\theta_9) \\
\delta_4 &= +\, a_2\sin(\theta_2) + a_3\sin(\theta_3) + a_{51}\sin(\theta_5+\beta_2) - a_G\sin(\theta_G) \\
&\quad - a_8\sin(\theta_8) - a_9\sin(\theta_9) \\
\delta_5 &= +\, a_{41}\sin(\theta_4) + a_{42}\cos(\theta_4) - a_5\cos(\theta_5) - a_6\cos(\theta_6) \\
&\quad + a_{72}\cos(\theta_7) - a_{71}\sin(\theta_7) \\
\delta_6 &= -\, a_{41}\cos(\theta_4) + a_{42}\sin(\theta_4) - a_5\sin(\theta_5) - a_6\sin(\theta_6) \\
&\quad + a_{72}\sin(\theta_7) + a_{71}\cos(\theta_7) \\
\delta_7 &= +\, a_{71}\sin(\theta_7) + a_{72}\cos(\theta_7) - b_2\cos(\theta_{10}) - b_3\cos(\theta_{12}) \\
&\quad + b_{42}\cos(\theta_{11}) - b_{41}\sin(\theta_{11}) \\
\delta_8 &= -\, a_{71}\cos(\theta_7) + a_{72}\sin(\theta_7) - b_2\sin(\theta_{10}) - b_3\sin(\theta_{12}) \\
&\quad + b_{42}\sin(\theta_{11}) + b_{41}\cos(\theta_{11})
\end{aligned}
$$

Position of the End Effector

In the 2 *dof* - 3 phalanges mechanism, which is shown in Figure 3.1, the end-effector is point K_0. The position of that point is given in Equation 3.23.

$$
\overline{P}^* = \begin{bmatrix} {p_1}^* \\ {p_2}^* \end{bmatrix} = \begin{bmatrix} +a_{12} + 2a_{42}\cos(\theta_4) + 2a_{72}\cos(\theta_7) + 2b_{42}\cos(\theta_{11}) \\ -a_{11} + 2a_{42}\sin(\theta_4) + 2a_{72}\sin(\theta_7) + 2b_{42}\sin(\theta_{11}) \end{bmatrix} \tag{3.23}
$$

However, the mechanism is simplified to the 2 phalanges as in Figure 3.4. Thus, the position of the considered end-effector is point F_0. The position of the end-effector that is going to be used in the first part of the design procedure is given in the expression 3.24.

$$
\overline{P} = \begin{bmatrix} p_1 \\ p_2 \end{bmatrix} = \begin{bmatrix} +a_{12} + 2a_{42}\cos(\theta_4) + 2a_{72}\cos(\theta_7) \\ -a_{11} + 2a_{42}\sin(\theta_4) + 2a_{72}\sin(\theta_7) \end{bmatrix} \tag{3.24}
$$

In the mechanism, the angles θ_4 and θ_7 are defined as primary variables. For the second part of the design methodology that is shown in Figure 3.3, the angle θ_{11} is calculated in order to find the structure parameters for the second part of the design procedure. Hence, the consequent secondary variables are found as follows:

From 3.18, real and imaginary parts can be written as follows:

$$a_2 \cos\theta_2 + a_3 \cos\theta_3 = +a_{12} + a_{42} \cos\theta_4 - a_{41} \sin\theta_4 \tag{3.25}$$

$$a_2 \sin\theta_2 + a_3 \sin\theta_3 = -a_{11} + a_{42} \sin\theta_4 + a_{41} \cos\theta_4 \tag{3.26}$$

Then,

$$a_3 \cos\theta_3 = x_1 - a_2 \cos\theta_2 \tag{3.27}$$

$$a_3 \sin\theta_3 = y_1 - a_2 \sin\theta_2 \tag{3.28}$$

where

$$x_1 = +a_{12} + a_{42} \cos\theta_4 - a_{41} \sin\theta_4$$

$$y_1 = -a_{11} + a_{42} \sin\theta_4 + a_{41} \cos\theta_4$$

Then, θ_2 is derived as follows:

$$\theta_2 = \Psi_1 + \sigma_1 \gamma_1 \tag{3.29}$$

where

$$\Psi_1 = atan_2(y_1, x_1)$$

$$f_1 = ({x_1}^2 + {y_1}^2 + {a_2}^2 - {a_3}^2)/(2a_2)$$

$$g_1 = \sqrt{{x_1}^2 + {y_1}^2 - {f_1}^2}$$

$$\gamma_1 = atan_2(g_1, f_1)$$

$$\sigma_1 = \pm 1$$

With the availability of θ_2, Eqs. 3.27 and 3.28, θ_3 can be found without any additional sign variable as follow:

$$\theta_3 = atan_2[(y_1 - a_2 \sin\theta_2), (x_1 - a_2 \cos\theta_2)] \tag{3.30}$$

From 3.20, real and imaginary parts can be written as follows:

$$-a_{41} \sin\theta_4 + a_5 \cos\theta_5 + a_6 \cos\theta_6 = a_{42} \cos\theta_4 + a_{72} \cos\theta_7 - a_{71} \sin\theta_7 \tag{3.31}$$

$$+a_{41}\cos\theta_4 + a_5\sin\theta_5 + a_6\sin\theta_6 = a_{42}\sin\theta_4 + a_{72}\sin\theta_7 + a_{71}\cos\theta_7 \tag{3.32}$$

Then,

$$a_6\cos\theta_6 = x_3 - a_5\cos\theta_5 \tag{3.33}$$

$$a_6\sin\theta_6 = y_3 - a_5\sin\theta_5 \tag{3.34}$$

where

$$x_3 = +a_{41}\sin\theta_4 + a_{42}\cos\theta_4 + a_{72}\cos\theta_7 - a_{71}\sin\theta_7$$

$$y_3 = -a_{41}\cos\theta_4 + a_{42}\sin\theta_4 + a_{72}\sin\theta_7 + a_{71}\cos\theta_7$$

Then, θ_5 is derived as follows:

$$\theta_5 = \Psi_3 + \sigma_3\gamma_3 \tag{3.35}$$

where

$$\Psi_3 = atan_2(y_3, x_3)$$

$$f_3 = ({x_3}^2 + {y_3}^2 + {a_5}^2 - {a_6}^2)/(2a_5)$$

$$g_3 = \sqrt{{x_3}^2 + {y_3}^2 - {f_3}^2}$$

$$\gamma_3 = atan_2(g_3, f_3)$$

$$\sigma_3 = \pm 1$$

With the availability of θ_5, Eqs. 3.33 and 3.34, θ_6 can be found without any additional sign variable as follow:

$$\theta_6 = atan_2[(y_3 - a_5\sin\theta_5), (x_3 - a_5\cos\theta_5)] \tag{3.36}$$

From 3.19, real and imaginary parts can be written as follows:

$$a_G\cos\theta_G + a_9\cos\theta_9 + a_8\cos\theta_8 = +a_2\cos\theta_2 + +a_3\cos\theta_3 + a_{51}\cos(\theta_5 + \beta_2) \tag{3.37}$$

$$a_G\sin\theta_G + a_9\sin\theta_9 + a_8\sin\theta_8 = +a_2\sin\theta_2 + +a_3\sin\theta_3 + a_{51}\sin(\theta_5 + \beta_2) \tag{3.38}$$

Then,

$$a_9\cos\theta_9 = x_2 - a_8\cos\theta_8 \tag{3.39}$$

$$a_9\sin\theta_9 = y_2 - a_8\sin\theta_8 \tag{3.40}$$

where

$$x_2 = +a_2\cos\theta_2 + +a_3\cos\theta_3 + a_{51}\cos(\theta_5+\beta_2) - a_G\cos\theta_G$$

$$y_2 = +a_2\sin\theta_2 + +a_3\sin\theta_3 + a_{51}\sin(\theta_5+\beta_2) - a_G\sin\theta_G$$

Then, θ_8 is derived as follows:

$$\theta_8 = \Psi_2 + \sigma_2\gamma_2 \tag{3.41}$$

where

$$\Psi_2 = atan_2(y_1, x_1)$$

$$f_2 = ({x_2}^2 + {y_2}^2 + {a_8}^2 - {a_9}^2)/(2a_8)$$

$$g_2 = \sqrt{{x_2}^2 + {y_2}^2 - {f_2}^2}$$

$$\gamma_2 = atan_2(g_2, f_2)$$

$$\sigma_2 = \pm 1$$

With the availability of θ_8, Eqs. 3.39 and 3.40, θ_9 can be found without any additional sign variable as follow:

$$\theta_9 = atan_2[(y_2 - a_8\sin\theta_8), (x_2 - a_8\cos\theta_8)] \tag{3.42}$$

From 3.21, real and imaginary parts can be written as follows:

$$-a_{71}\sin\theta_7 + b_2\cos\theta_{10} + b_3\cos\theta_{12} = a_{72}\cos\theta_7 + b_{42}\cos\theta_{11} - b_{41}\sin\theta_{11} \tag{3.43}$$

$$+a_{71}\cos\theta_7 + b_2\sin\theta_{10} + b_3\sin\theta_{12} = a_{72}\sin\theta_7 + b_{42}\sin\theta_{11} + b_{41}\cos\theta_{11} \tag{3.44}$$

Then, with the use of the Equation 3.9,

$$b_3\cos\theta_{12} = x_4 + b_{42}\cos\theta_{11} - b_{41}\sin\theta_{11} \tag{3.45}$$

$$b_3\sin\theta_{12} = y_4 + b_{42}\sin\theta_{11} + b_{41}\cos\theta_{11} \tag{3.46}$$

where

$$x_4 = +a_{71}\sin\theta_7 - b_2\cos\theta_{10} + a_{72}\cos\theta_7$$

$$y_4 = -a_{71}\cos\theta_7 - b_2\sin\theta_{10} + a_{72}\sin\theta_7$$

Then, θ_{11} is derived as follows:

$$\theta_{11} = \Psi_4 + \sigma_4\gamma_4 \tag{3.47}$$

where

$$
\begin{aligned}
x_4^* &= +x_4 b_{42} + y_4 b_{41} \\
y_4^* &= -x_4 b_{41} + y_4 b_{42} \\
\Psi_4 &= atan_2(y_4^*, x_4^*) \\
f_4 &= ({x_4}^2 + {y_4}^2 + {b_{42}}^2 + {b_{41}}^2 - {b_3}^2)/(2) \\
g_4 &= \sqrt{(x_4^*)^2 + ({y_4}^*)^2 - {f_4}^2} \\
\gamma_4 &= atan_2(g_4, f_4) \\
\sigma_4 &= \pm 1
\end{aligned}
$$

With the availability of θ_{11} and Equations 3.45 and 3.46, θ_{12} can be found without any additional sign variable as follow:

$$\theta_{12} = atan_2[(y_4 + b_{42}\sin\theta_{11} + b_{41}\cos\theta_{11}), (x_4 + b_{42}\cos\theta_{11} - b_{41}\sin\theta_{11})] \quad (3.48)$$

3.1.3.2 Velocity Analysis

The velocity equations are obtained by taking the derivative of position equations with respect to time. Just like previously done in the position analysis chapter, the 2 *dof* - 3 phalanges mechanism, which is shown in Figure 3.1, the end-effector is point K_0. Then, velocity of that point is expressed in the expression 3.49.

$$\frac{d}{dt}(\overline{P}^*) = \begin{bmatrix} {v_1}^* \\ {v_2}^* \end{bmatrix} = 2\begin{bmatrix} -(a_{42}\sin\theta_4)\dot{\theta}_4 - (a_{72}\sin\theta_7)\dot{\theta}_7 - (b_{42}\sin\theta_{11})\dot{\theta}_{11} \\ +(a_{42}\cos\theta_4)\dot{\theta}_4 + (a_{72}\cos\theta_7)\dot{\theta}_7 + (b_{42}\cos\theta_{11})\dot{\theta}_{11} \end{bmatrix} \quad (3.49)$$

However, the mechanism is simplified to the 2 phalanges as in Figure 3.4. Thus, the velocity of the considered end-effector is given in the expression 3.50.

$$\frac{d}{dt}(\overline{P}^*) = \begin{bmatrix} {v_1}^* \\ {v_2}^* \end{bmatrix} = 2\begin{bmatrix} -(a_{42}\sin\theta_4)\dot{\theta}_4 - (a_{72}\sin\theta_7)\dot{\theta}_7 \\ +(a_{42}\cos\theta_4)\dot{\theta}_4 + (a_{72}\cos\theta_7)\dot{\theta}_7 \end{bmatrix} \quad (3.50)$$

The velocity equation for all loops can be written easily by taking the derivation of Equation 3.22. The result is given in Equation 3.51.

$$\frac{d}{dt}(\overline{G}) = \ = \begin{bmatrix} 0 \\ 0 \\ 0 \\ 0 \\ 0 \\ 0 \\ 0 \\ 0 \end{bmatrix} = \begin{bmatrix} \gamma_1 \\ \gamma_2 \\ \gamma_3 \\ \gamma_4 \\ \gamma_5 \\ \gamma_6 \\ \gamma_7 \\ \gamma_8 \end{bmatrix} \tag{3.51}$$

where

$$\begin{aligned}
\gamma_1 &= +(a_2\sin\theta_2)\dot{\theta}_2 + (a_3\sin\theta_3)\dot{\theta}_3 - (a_{42}\sin\theta_4 + a_{41}\cos\theta_4)\dot{\theta}_4 \\
\gamma_2 &= -(a_2\cos\theta_2)\dot{\theta}_2 - (a_3\cos\theta_3)\dot{\theta}_3 + (a_{42}\cos\theta_4 - a_{41}\sin\theta_4)\dot{\theta}_4 \\
\gamma_3 &= -(a_2\sin\theta_2)\dot{\theta}_2 - (a_3\sin\theta_3)\dot{\theta}_3 - (a_{51}\sin(\theta_5+\beta_2))\dot{\theta}_5 \\
&\quad + (a_8\sin\theta_8)\dot{\theta}_8 + (a_9\sin\theta_9)\dot{\theta}_9 \\
\gamma_4 &= +(a_2\cos\theta_2)\dot{\theta}_2 + (a_3\cos\theta_3)\dot{\theta}_3 + (a_{51}\cos(\theta_5+\beta_2))\dot{\theta}_5 \\
&\quad - (a_8\cos\theta_8)\dot{\theta}_8 - (a_9\cos\theta_9)\dot{\theta}_9 \\
\gamma_5 &= +(a_{41}\cos\theta_4 - a_{42}\sin\theta_4)\dot{\theta}_4 + (a_5\sin\theta_5)\dot{\theta}_5 + (a_6\sin\theta_6)\dot{\theta}_6 \\
&\quad - (a_{72}\sin\theta_7 + a_{71}\cos\theta_7)\dot{\theta}_7 \\
\gamma_6 &= +(a_{41}\sin\theta_4 + a_{42}\cos\theta_4)\dot{\theta}_4 - (a_5\cos\theta_5)\dot{\theta}_5 - (a_6\cos\theta_6)\dot{\theta}_6 \\
&\quad + (a_{72}\cos\theta_7 - a_{71}\sin\theta_7)\dot{\theta}_7 \\
\gamma_7 &= +(a_{71}\cos\theta_7 - a_{72}\sin\theta_7)\dot{\theta}_7 + (b_2\sin\theta_{10})\dot{\theta}_{10} + (b_3\sin\theta_{12})\dot{\theta}_{12} \\
&\quad - (b_{42}\sin\theta_{11} + b_{41}\cos\theta_{11})\dot{\theta}_{11} \\
\gamma_8 &= +(a_{71}\sin\theta_7 + a_{72}\cos\theta_7)\dot{\theta}_7 - (b_2\cos\theta_{10})\dot{\theta}_{10} - (b_3\cos\theta_{12})\dot{\theta}_{12} \\
&\quad + (b_{42}\cos\theta_{11} - b_{41}\sin\theta_{11})\dot{\theta}_{11}
\end{aligned}$$

From 3.51, velocity equations can be written as follows:

Velocity equation for Loop 1:

$$\begin{bmatrix} +a_3\sin\theta_3 & -(a_{42}\sin\theta_4 + a_{41}\cos\theta_4) \\ -a_3\cos\theta_3 & +(a_{42}\cos\theta_4 - a_{41}\sin\theta_4) \end{bmatrix} \begin{bmatrix} \dot{\theta}_3 \\ \dot{\theta}_4 \end{bmatrix} = \begin{bmatrix} -a_2\sin\theta_2 \\ +a_2\cos\theta_2 \end{bmatrix} \begin{bmatrix} \dot{\theta}_2 \end{bmatrix} \tag{3.52}$$

Velocity equation for Loop 2:

$$\begin{bmatrix} +a_{51}\sin(\theta_5+\beta_2) & -a_8\sin\theta_8 \\ -a_{51}\cos(\theta_5+\beta_2) & +a_8\cos\theta_8 \end{bmatrix} \begin{bmatrix} \dot{\theta}_5 \\ \dot{\theta}_8 \end{bmatrix} = \begin{bmatrix} -a_2\sin\theta_2 & -a_3\sin\theta_3 & +a_9\sin\theta_9 \\ +a_2\cos\theta_2 & +a_3\cos\theta_3 & -a_9\cos\theta_9 \end{bmatrix} \begin{bmatrix} \dot{\theta}_2 \\ \dot{\theta}_3 \\ \dot{\theta}_9 \end{bmatrix} \tag{3.53}$$

Velocity equation for Loop 3:

$$\begin{bmatrix} +a_6\sin\theta_6 & -(a_{72}\sin\theta_7+a_{71}\cos\theta_7) \\ -a_6\cos\theta_6 & +(a_{72}\cos\theta_7-a_{71}\sin\theta_7) \end{bmatrix} \begin{bmatrix} \dot{\theta}_6 \\ \dot{\theta}_7 \end{bmatrix} = \begin{bmatrix} -(a_{41}\cos\theta_4-a_{42}\sin\theta_4) & -a_5\sin\theta_5 \\ -(a_{41}\sin\theta_4+a_{42}\cos\theta_4) & +a_5\cos\theta_5 \end{bmatrix} \begin{bmatrix} \dot{\theta}_4 \\ \dot{\theta}_5 \end{bmatrix} \tag{3.54}$$

Velocity equation for Loop 4:

$$\begin{bmatrix} -(b_{42}\sin\theta_{11}+b_{41}\cos\theta_{11}) & +b_3\sin\theta_{12} \\ +(b_{42}\cos\theta_{11}-b_{41}\sin\theta_{11}) & -b_3\cos\theta_{12} \end{bmatrix} \begin{bmatrix} \dot{\theta}_{11} \\ \dot{\theta}_{12} \end{bmatrix} = \begin{bmatrix} -(a_{71}\cos\theta_7-a_{72}\sin\theta_7) & -b_2\sin\theta_{10} \\ -(a_{71}\sin\theta_7+a_{72}\cos\theta_7) & +b_2\cos\theta_{10} \end{bmatrix} \begin{bmatrix} \dot{\theta}_7 \\ \dot{\theta}_{10} \end{bmatrix} \tag{3.55}$$

The purpose of the velocity derivation is to use them in the Jacobian matrix. Thus, each velocity variable must be defined in terms of motor velocities which are θ_2 and θ_9.

From Equation 3.52, velocity equations for Loop 1 are derived as follows:

$$\begin{bmatrix} \dot{\theta}_3 \\ \dot{\theta}_4 \end{bmatrix} = \begin{bmatrix} j_1 \\ j_2 \end{bmatrix} \begin{bmatrix} \dot{\theta}_2 \end{bmatrix} \tag{3.56}$$

where

$$\begin{bmatrix} j_1 \\ j_2 \end{bmatrix} = \begin{bmatrix} +a_3\sin\theta_3 & -(a_{42}\sin\theta_4+a_{41}\cos\theta_4) \\ -a_3\cos\theta_3 & +(a_{42}\cos\theta_4-a_{41}\sin\theta_4) \end{bmatrix}^{-1} \begin{bmatrix} -a_2\sin\theta_2 \\ +a_2\cos\theta_2 \end{bmatrix}$$

From Equation 3.53, velocity equations for Loop 2 are derived as follows:

$$\begin{bmatrix} \dot{\theta}_5 \\ \dot{\theta}_8 \end{bmatrix} = \begin{bmatrix} j_7 & j_8 & j_9 \\ j_{10} & j_{11} & j_{12} \end{bmatrix} \begin{bmatrix} \dot{\theta}_2 \\ \dot{\theta}_3 \\ \dot{\theta}_9 \end{bmatrix} \tag{3.57}$$

where

$$\begin{bmatrix} j_7 & j_8 & j_9 \\ j_{10} & j_{11} & j_{12} \end{bmatrix}$$
$$= \begin{bmatrix} +a_{51}\sin(\theta_5+\beta_2) & -a_8\sin\theta_8 \\ -a_{51}\cos(\theta_5+\beta_2) & +a_8\cos\theta_8 \end{bmatrix}^{-1} \begin{bmatrix} -a_2\sin\theta_2 & -a_3\sin\theta_3 & +a_9\sin\theta_9 \\ +a_2\cos\theta_2 & +a_3\cos\theta_3 & -a_9\cos\theta_9 \end{bmatrix}$$

From Equation 3.54, velocity equations for Loop 3 are derived as follows:

$$\begin{bmatrix} \dot{\theta}_6 \\ \dot{\theta}_7 \end{bmatrix} = \begin{bmatrix} j_3 & j_4 \\ j_5 & j_6 \end{bmatrix} \begin{bmatrix} \dot{\theta}_4 \\ \dot{\theta}_5 \end{bmatrix} \tag{3.58}$$

where

$$\begin{bmatrix} j_3 & j_4 \\ j_5 & j_6 \end{bmatrix}$$
$$= \begin{bmatrix} +a_6\sin\theta_6 & -(a_{72}\sin\theta_7+a_{71}\cos\theta_7) \\ -a_6\cos\theta_6 & +(a_{72}\cos\theta_7-a_{71}\sin\theta_7) \end{bmatrix}^{-1} \begin{bmatrix} -(a_{41}\cos\theta_4-a_{42}\sin\theta_4) & -a_5\sin\theta_5 \\ -(a_{41}\sin\theta_4+a_{42}\cos\theta_4) & +a_5\cos\theta_5 \end{bmatrix}$$

From Equation 3.55, velocity equations for Loop 4 are derived as follows:

$$\begin{bmatrix} \dot{\theta}_{11} \\ \dot{\theta}_{12} \end{bmatrix} = \begin{bmatrix} j_{13} & j_{14} \\ j_{15} & j_{16} \end{bmatrix} \begin{bmatrix} \dot{\theta}_7 \\ \dot{\theta}_{10} \end{bmatrix} \tag{3.59}$$

where

$$\begin{bmatrix} j_{13} & j_{14} \\ j_{15} & j_{16} \end{bmatrix}$$
$$= \begin{bmatrix} -(b_{42}\sin\theta_{11}+b_{41}\cos\theta_{11}) & +b_3\sin\theta_{12} \\ +(b_{42}\cos\theta_{11}-b_{41}\sin\theta_{11}) & -b_3\cos\theta_{12} \end{bmatrix}^{-1} \begin{bmatrix} -(a_{71}\cos\theta_7-a_{72}\sin\theta_7) & -b_2\sin\theta_{10} \\ -(a_{71}\sin\theta_7+a_{72}\cos\theta_7) & +b_2\cos\theta_{10} \end{bmatrix}$$

The following equations can be derived for future calculations from Equations 3.56, 3.57, 3.58 and 3.59.

$$
\begin{aligned}
\dot{\theta_3} &= j_1\dot{\theta_2} \\
\dot{\theta_4} &= j_2\dot{\theta_2} \\
\dot{\theta_5} &= j_7\dot{\theta_2} + j_8\dot{\theta_3} + j_9\dot{\theta_9} \\
&= (j_7 + j_8j_1)\dot{\theta_2} + j_9\dot{\theta_9} \\
\dot{\theta_8} &= j_{10}\dot{\theta_2} + j_{11}\dot{\theta_3} + j_{12}\dot{\theta_9} \\
&= (j_{10} + j_{11}j_1)\dot{\theta_2} + j_{12}\dot{\theta_9} \\
\dot{\theta_6} &= j_3\dot{\theta_4} + j_4\dot{\theta_5} \\
&= [j_3j_2 + j_4(j_7 + j_8j_1)]\dot{\theta_2} + (j_4j_9)\dot{\theta_9} \\
\dot{\theta_7} &= j_5\dot{\theta_4} + j_6\dot{\theta_5} \\
&= [j_5j_2 + j_6(j_7 + j_8j_1)]\dot{\theta_2} + (j_6j_9)\dot{\theta_9}
\end{aligned}
\tag{3.60}
$$

3.1.3.3 Jacobian Matrix

The relationship in velocities of end effector and motors are related by the Jacobian matrix. In other words, it is the matrix that transmits the end-effector velocity to the required actuator velocities, V_{F_0} and $[\dot{\theta_2}$ and $\dot{\theta_9}]$, respectively.

$$
X_{F_0} = (-a_{11}i + a_{12}) + 2a_{42}e^{i\theta_4} + 2a_{72}e^{i\theta_7} \tag{3.61}
$$

$$
\begin{aligned}
\frac{d(X_{F_0})}{dt} = V_{F_0} &= i2[\dot{\theta_4}a_{42}e^{i\theta_4} + \dot{\theta_7}a_{72}e^{i\theta_7}] \\
&= i2[\dot{\theta_4}a_{42}(\cos\theta_4 + i\sin\theta_4)\dot{\theta_7}a_{72}(\cos\theta_7 + i\sin\theta_7)]
\end{aligned}
\tag{3.62}
$$

The above equation can be written in matrix form as follows:

$$
V_{F_0} = \begin{bmatrix} -2a_{42}\sin\theta_4 & -2a_{72}\sin\theta_7 \\ +2a_{42}\cos\theta_4 & +2a_{72}\cos\theta_7 \end{bmatrix} \begin{bmatrix} \dot{\theta_4} \\ \dot{\theta_7} \end{bmatrix} \tag{3.63}
$$

where; from Equation 3.60;

$$
\begin{bmatrix} \dot{\theta_4} \\ \dot{\theta_7} \end{bmatrix} = \begin{bmatrix} j_2 & 0 \\ j_5j_2 + j_6(j_7 + j_8j_1) & j_6j_9 \end{bmatrix} \begin{bmatrix} \dot{\theta_2} \\ \dot{\theta_9} \end{bmatrix} \tag{3.64}
$$

Then the velocity of the end effector can be written as follows:

$$
V_{F_0} = \begin{bmatrix} -2a_{42}\sin\theta_4 & -2a_{72}\sin\theta_7 \\ +2a_{42}\cos\theta_4 & +2a_{72}\cos\theta_7 \end{bmatrix} \begin{bmatrix} j_2 & 0 \\ j_5j_2 + j_6(j_7 + j_8j_1) & j_6j_9 \end{bmatrix} \begin{bmatrix} \dot{\theta_2} \\ \dot{\theta_9} \end{bmatrix} \tag{3.65}
$$

Then, the Jacobian matrix is written below:

$$J = \begin{bmatrix} -2a_{42}\sin\theta_4 & -2a_{72}\sin\theta_7 \\ +2a_{42}\cos\theta_4 & +2a_{72}\cos\theta_7 \end{bmatrix} \begin{bmatrix} j_2 & 0 \\ j_5 j_2 + j_6(j_7 + j_8 j_1) & j_6 j_9 \end{bmatrix} \tag{3.66}$$

3.1.3.4 Derivation of Motor Torques

Virtual Work Method is used to calculate the required motor torques. By this method, the forces and torques that act on the mechanism are related. The mechanism shown in Figure 3.4 which is considered for the design procedure is updated with the forces and torques acting on the mechanism as in Figure 3.5. In the mechanism, there are motor torques acting at the points A_0 and H_0. Also, there is a pinching force acting on the point F_0. Lastly, passive torques that are produced by the movement of the finger are acting on the points B_0 and E_0.

By the Virtual Theorem method the following equation can be written:

$$\delta W = \delta W_{A_0} + \delta W_{H_0} + \delta W_{MCP} + \delta W_{PIP} + \delta W_{F_{F0}} = 0 \tag{3.67}$$

where

$$\begin{aligned} \delta W_{A_0} &= T_{A0}\,\delta\theta_2 \\ \delta W_{H_0} &= T_{H0}\,\delta\theta_9 \\ \delta W_{MCP} &= T_{MCP}\,\delta\theta_4 \\ \delta W_{PIP} &= T_{PIP}\,\delta\theta_7 \\ \delta W_{F_{F0}} &= \overrightarrow{F_{F0}} \,.\, \overrightarrow{\delta r_{F0}} \end{aligned}$$

In the above Equation 3.67 the variables are defined as follows:

- T_{A0}: The torque value applied by the motor at point A_0.
- T_{H0}: The torque value applied by the motor at point H_0.
- T_{MCP}: The torque value applied by the finger joint MCP at point B_0.
- T_{MCP}: The torque value applied by the finger joint MCP at point B_0.
- F_{F0}: A force acting on the end-effector at point F_0.

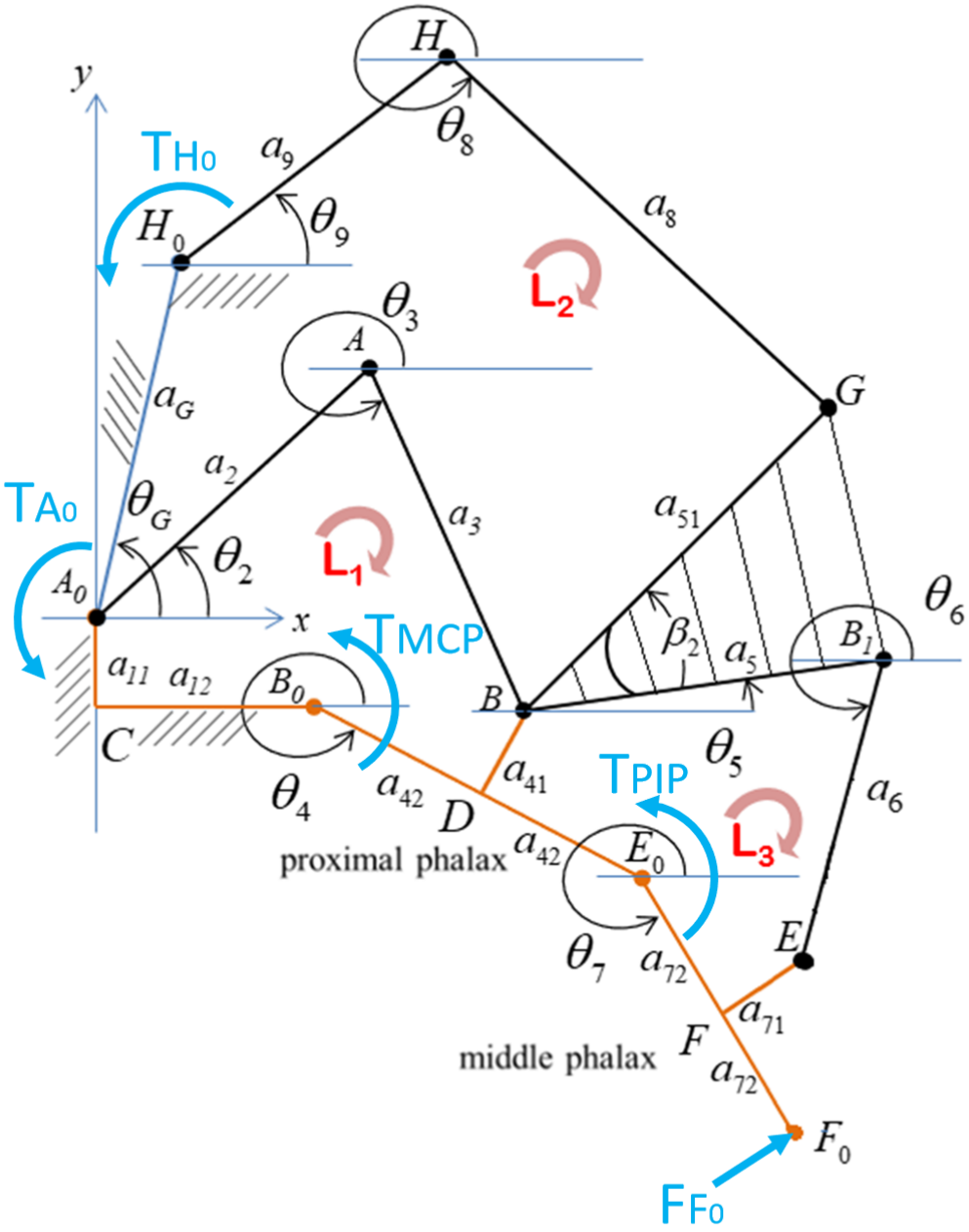

Figure 3.5: Fully actuated index exoskeleton mechanism - with loads

The derivation of the passive torque values is adapted from [11] as follows:

$$\begin{aligned} T_{MCP} &= T_{MCPstatic} - B_{MCP}\dot{\theta}_4 - K_{MCP}\theta_4 \\ T_{PIP} &= T_{PIPstatic} - B_{PIP}(\dot{\theta}_7 - \dot{\theta}_4) - K_{PIP}(\theta_7 - \theta_4) \end{aligned} \tag{3.68}$$

The variables in the Equation 3.68 are detailed in the following Equations 3.69 and 3.70. The spring and damping coefficients are given in the units of [Nm/rad] and [Nms/rad], respectively.

$$\begin{aligned} K_{MCP} &= 1.02(\theta_4)^2 - 0.54\theta_4 + 0.45 \\ K_{PIP} &= 1.06(\theta_7 - \theta_4)^2 - 0.76(\theta_7 - \theta_4) + 0.40 \\ B_{MCP} &= 0.0142 \\ B_{PIP} &= 0.0105 \end{aligned} \tag{3.69}$$

And the static torque values are as follows:

$$\begin{aligned} T_{MCPstatic} &= -0.071(\theta_4)^3 + 0.145(\theta_4)^2 - 0.154(\theta_4) + 0.029 \\ T_{PIPstatic} &= 0.056(\theta_7 - \theta_4)^3 + 0.016(\theta_7 - \theta_4)^2 - 0.132(\theta_7 - \theta_4) + 0.015 \end{aligned} \tag{3.70}$$

Note that the unit for all torque values is [Nm].

The force applying on point F_{F0} is perpendicular. With the knowledge of this information, the following equations for $\overrightarrow{F_{F0}}$ and $\overrightarrow{\delta r_{F0}}$ can be written as follows:

$$\begin{aligned} \overrightarrow{F_{F0}} &= |F_{F0}|e^{i(\theta_7+\pi/2)} \\ \Rightarrow \quad F_{F0,X} &= |F_{F0}|(-\sin\theta_7) \quad \text{and} \quad F_{F0,Y} = |F_{F0}|(\cos\theta_7) \end{aligned} \tag{3.71}$$

$$\begin{aligned} \overrightarrow{r_{F0}} &= (-a_{11}i + a_{12}) + 2a_{42}e^{i\theta_4} + 2a_{72}e^{i\theta_7} \\ \Rightarrow \quad \delta r_{F0,X} &= -2a_{42}\sin(\theta_4)\delta\theta_4 - 2a_{72}\sin(\theta_7)\delta\theta_7 \quad \text{and} \\ \delta r_{F0,Y} &= +2a_{42}\cos(\theta_4)\delta\theta_4 + 2a_{72}\cos(\theta_7)\delta\theta_7 \end{aligned} \tag{3.72}$$

Then, $\delta W_{F_{F0}}$ can be represented by using Equations 3.71 and 3.73 as follows:

$$\begin{aligned} \delta W_{F_{F0}} &= |F_{F_0}|2[a_{42}(\sin(\theta_4)\sin(\theta_7) + \cos(\theta_4)\cos(\theta_7))\delta\theta_7 + a_{72}\delta\theta_7] \\ &= |F_{F_0}|2[a_{42}\cos(\theta_4 - \theta_7)\delta\theta_4 + a_{72}\delta\theta_7] \end{aligned} \tag{3.73}$$

Then, the Equation 3.67 can be updated as follows:

$$\begin{aligned}\delta W =& T_{A0}\,\delta\theta_2 + T_{H0}\,\delta\theta_9 + T_{MCP}\,\delta\theta_4 + T_{PIP}\,\delta\theta_7 \\ &+ |F_{F_0}|2[a_{42}\cos(\theta_4-\theta_7)\delta\theta_4 + a_{72}\delta\theta_7] = 0\end{aligned} \tag{3.74}$$

The Equation 3.74 is given as follow:

$$\begin{aligned}\delta W =& T_{A0}\,\delta\theta_2 + T_{H0}\,\delta\theta_9 \\ &+ [T_{MCP} + 2|F_{F_0}|a_{42}\cos(\theta_4-\theta_7)]\delta\theta_4 \\ &+ [T_{PIP} + 2|F_{F_0}|a_{72}]\delta\theta_7] = 0\end{aligned} \tag{3.75}$$

In order to define $\delta\theta_4$ and $\delta\theta_7$ in terms of $\delta\theta_2$ and $\delta\theta_9$, the 3.60 can be used. Then, the Equation 3.75 becomes as follows:

$$\begin{aligned}\delta W =& T_{A0}\,\delta\theta_2 + T_{H0}\,\delta\theta_9 \\ &+ [T_{MCP} + 2|F_{F_0}|a_{42}\cos(\theta_4-\theta_7)](j_2)\delta\theta_2 \\ &+ [T_{PIP} + 2|F_{F_0}|a_{72}][(j_5j_2 + j_6(j_7 + j_8j_1))\delta\theta_2 + (j_6j_9)\delta\theta_9] = 0\end{aligned} \tag{3.76}$$

Finally, from Equation 3.76, two scalar equalities are obtained as follows:

$$\begin{aligned}&T_{A0} + [T_{MCP} + 2|F_{F_0}|a_{42}\cos(\theta_4-\theta_7)](j_2) \\ &+ [T_{PIP} + 2|F_{F_0}|a_{72}](j_5j_2 + j_6(j_7 + j_8j_1)) = 0\end{aligned} \tag{3.77}$$

and

$$T_{H0} + [T_{PIP} + 2|F_{F_0}|a_{72}](j_6j_9) = 0 \tag{3.78}$$

The Equations 3.77 and 3.78 can be used to estimate motor torque value in the mechanism.

3.1.3.5 Phalanx Sizes and Task Space

Since the mechanism includes a finger, the size of the phalanges affect the motion of the mechanism. The phalanges lengths a_{42}, a_{72} and b_{42} would be used from literature [11] as in the Table 2.1. However the phalanges sizes of the users who are supposed to use the mechanism are different from the literature. In order to obtain a robust mechanism, the updated phalanges sizes are shown in Table 3.2.

Table 3.2: Phalanges Sizes in milimeters

Phalanx Name	Proximal	Middle	Distal
Nominal	40	30	20
Maximum	50	37.5	25
Minimum	32	24	16

Table 3.3: Primary and Secondary Positions

Kinematic Loop	Given	Found
Loop 1	θ_4	θ_2, θ_3
Loop 2	θ_2, θ_3, θ_5	θ_8, θ_9
Loop 3	θ_4, θ_7	θ_5, θ_6
Loop 4	θ_7, θ_{11}	θ_{10}, θ_{12}

Task-Space of the mechanism is constrained by finger joint angles, which are θ_4, θ_7 and θ_{11}. It is necessary to define the task space in order to design the mechanism. The mechanism in the case is where the last loop (Loop 4), namely distal phalange, is ignored. So, only θ_4 and θ_7 constraint the mechanism. Since the mechanism is synthesized via inverse kinematic equations, the phalanx angles(θ_4, θ_7) are needed to be defined. For this purpose, an 8-pointed task space is structured which is a general range of motion of an index finger which includes not only a pinching movement but also many movement that finger is able to make. The analysis is done on those points. The joint angles are given in Table 3.4.

Table 3.4: MCP(θ_4) and PIP(θ_7) joint angles in Task Space

Point Number	θ_4	θ_7
1	$30°$	$20°$
2	$30°$	$-30°$
3	$15°$	$-20°$
4	$0°$	$-15°$
5	$-15°$	$-45°$
6	$-30°$	$-75°$
7	$-45°$	$-90°$
8	$-60°$	$-105°$

3.1.3.6 Defining the Design Metric

The GII(Global Isotropy Index) is defined as the singular value decomposition of the Jacobian [28], as follows:

For each state defined in Table 3.4, the Jacobian is calculated. From the Jacobian, singular value decomposition is generated. Since the size of the matrix is 2 by 2, for a single Jacobian, two singular values are created. For 8 states, it means 16 singular values are obtained. From the overall 16 values, the ratio of the minimum and maximum gives the isotropy value for the whole task space.

3.1.3.7 Design by the Genetic Algorithm

The algorithm basically is used to optimize the design vector by maximizing the GII value for the whole task space. In order to decrease the sensitivity of the human index finger on the mechanism, finger phalanges size is defined as a 3x1 vector and implemented in the code. In each element of the phalange size, the algorithm runs to find optimal values of the design vector. When this procedure is completed for each element, a vector of the fitness function is calculated. The multi-objective optimization problem is solved within the boundaries.

3.2 Transition to Under-actuation: From 4 bar to 5 bar

In order to be able to specify and determine the methodology for the under-actuated mechanism syntheses, a simple example is addressed, which is a 4-bar mechanism. In this case, the first loop of the fully-actuated mechanism in Figure 3.1 is considered. A closer look is given in Figure 3.6.

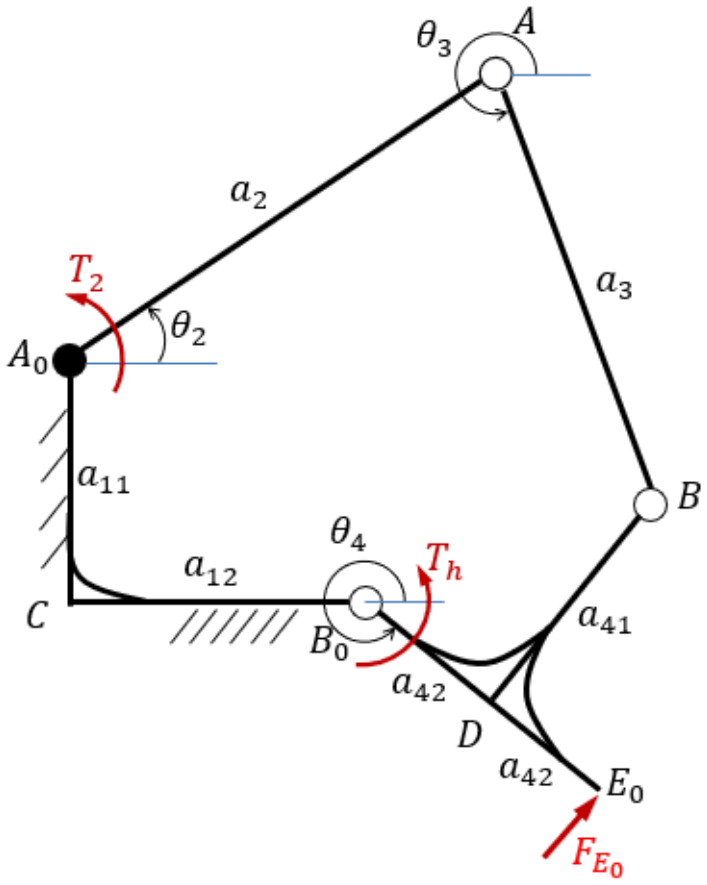

Figure 3.6: First Loop of the Mechanism; A Four Bar Mechanism

The four-bar mechanism can be detailed easily as follows:

For position analysis: Loop Closure Equation:

$$\overrightarrow{A_0AB} = \overrightarrow{A_0CB_0DB} \tag{3.79}$$

$$LCE \Rightarrow a_2 e^{i\theta_2} + a_3 e^{i\theta_3} = (-a_{11}i + a_{12}) + a_{42}e^{i\theta_4} + a_{41}e^{i(\theta_4 + \frac{\pi}{2})} \tag{3.80}$$

The position expression for 3.80 is already derived as it is done for 3.18.

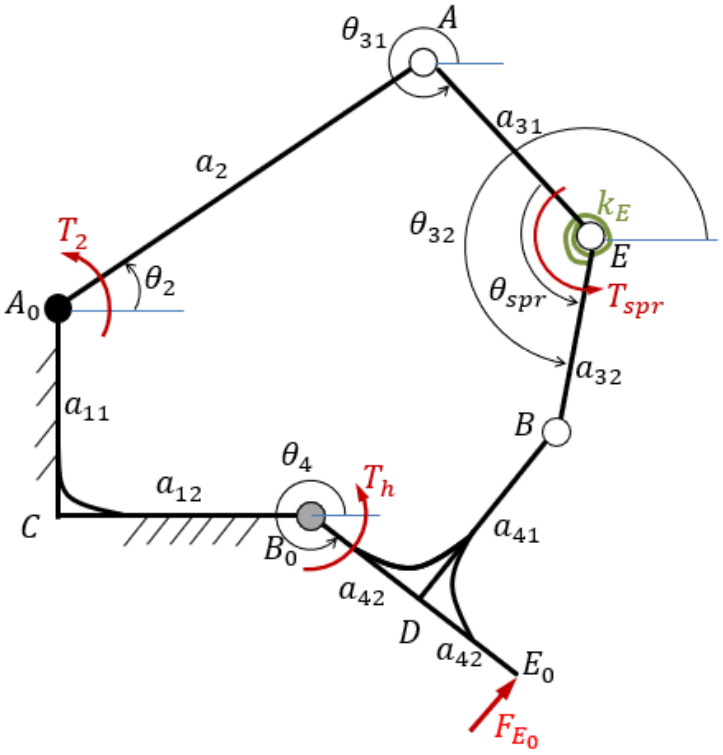

Figure 3.7: First Loop; A Five Bar Mechanism

The five-bar mechanism can be detailed easily as follows:

For position analysis: Loop Closure Equation:

$$\overrightarrow{A_0AEB} = \overrightarrow{A_0CB_0DB} \tag{3.81}$$

$$LCE \Rightarrow a_2e^{i\theta_2} + a_{31}e^{i\theta_{31}} + a_{32}e^{i\theta_{32}} = (-a_{11}i + a_{12}) + a_{42}e^{i\theta_4} + a_{41}e^{i(\theta_4+\frac{\pi}{2})} \tag{3.82}$$

The spring angle θ_{spr} can be defined as follows:

$$\theta_{spr} = \theta_{32} - \theta_{31} + \pi \tag{3.83}$$

Then, angle θ_{32} can be defined as follows:

$$\theta_{32} = \theta_{31} + \theta_{spr} - \pi \tag{3.84}$$

Then, Equation 3.82 becomes as follow:

$$LCE \Rightarrow a_2 e^{i\theta_2} + a_{31} e^{i\theta_{31}} + a_{32} e^{i(\theta_{31}+\theta_{spr}-\pi)} = (-a_{11} i + a_{12}) + a_{42} e^{i\theta_4} + a_{41} e^{i(\theta_4+\frac{\pi}{2})} \tag{3.85}$$

Real and Imaginary parts of the Equation 3.85 are as follows:

$$a_2 \cos\theta_2 + a_{31} \cos\theta_{31} - a_{32} \cos(\theta_{31} + \theta_{spr}) = +a_{12} + a_{42} \cos\theta_4 - a_{41} \sin\theta_4 \tag{3.86}$$

$$a_2 \sin\theta_2 + a_{31} \sin\theta_{31} - a_{32} \sin(\theta_{31} + \theta_{spr}) = -a_{11} + a_{42} \sin\theta_4 + a_{41} \cos\theta_4 \tag{3.87}$$

In the Equations 3.86 and 3.87, there are 3 unknowns; θ_2, θ_{31} and θ_{spr} when θ_4 is given. Since there are two equations with three unknowns, it is not possible to solve the variables analytically. Thus, the methodology is given as follows:

1) Define θ_{spr} symbolically and solve for θ_2 and θ_{31}.
2) Derive velocity equations and obtain Jacobian constants.
3) Use the Virtual Work method and obtain a new equation to use.
4) Find θ_{spr} numerically.
5) Solve everything once again numerically.
6) Obtain performance measure.

Then, by defining θ_{spr} as a symbolic variable, the following equations are derived:

$$\begin{aligned} a_2 \cos\theta_2 &= x_5 - a_{31} \cos\theta_{31} + a_{32} \cos(\theta_{31} + \theta_{spr}) \\ &= x_5 - a_{31} \cos\theta_{31} + a_{32}[\cos(\theta_{31}) \cos(\theta_{spr}) - \sin(\theta_{31}) \sin(\theta_{spr})] \end{aligned} \tag{3.88}$$

$$\begin{aligned} a_2 \sin\theta_2 &= y_5 - a_{31} \sin\theta_{31} + a_{32} \sin(\theta_{31} + \theta_{spr}) \\ &= x_5 - a_{31} \sin\theta_{31} + a_{32}[\sin(\theta_{31}) \cos(\theta_{spr}) + \cos(\theta_{31}) \sin(\theta_{spr})] \end{aligned} \tag{3.89}$$

where

$$x_5 = +a_{12} + a_{42} \cos\theta_4 - a_{41} \sin\theta_4$$

$$y_5 = -a_{11} + a_{42} \sin\theta_4 + a_{41} \cos\theta_4$$

Then, Equations 3.88 and 3.89 become as follows:

$$a_2 \cos\theta_2 = x_5 + \cos\theta_{31} k_1 + \sin\theta_{31} k_2 \tag{3.90}$$

$$a_2 \sin\theta_2 = y_5 + \sin\theta_{31} k_1 + \cos\theta_{31} k_2 \tag{3.91}$$

where

$$k_1 = -a_{31} + a_{32}\cos(\theta_{spr})$$
$$k_2 = -a_{32}\sin(\theta_{spr})$$

Taking squares of the Equations 3.90 and 3.91 and summing them together yields to the following equation:

$$\theta_{31} = 2tan^{-1}(\frac{-B_1 \pm \sqrt{{B_1}^2 - 4A_1C_1}}{2A_1}) \tag{3.92}$$

where

$$K_1 = {x_5}^2 + {y_5}^2 + {k_1}^2 + {k_2}^2 - {a_2}^2$$
$$K_2 = 2(x_5 k_1 - y_5 k_2)$$
$$K_3 = 2(x_5 k_2 + y_5 k_1)$$
$$A_1 = K_1 - K_2$$
$$B_1 = 2K_3$$
$$C_1 = K_1 + K_2$$

With the availability of θ_{31}, Eqs. 3.90 and 3.91, θ_2 can be found without any additional sign variable as follow:

$$\theta_2 = atan_2[(y_5 + \sin\theta_{31} k_1 + \cos\theta_{31} k_2), (x_5 + \cos\theta_{31} k_1 + \sin\theta_{31} k_2)] \tag{3.93}$$

Note that, the position solutions for θ_2 and θ_{31} are functions of θ_{spr}.

3.3 Under-Actuated Mechanism Family

3.3.1 Description of the Mechanism Versions

For the under-actuation, 4 different possible configurations derived from the fully-actuated mechanism are considered. Those are called "Version" from 1 to 4 and given below in the Figures 3.8, 3.9, 3.10, 3.11.

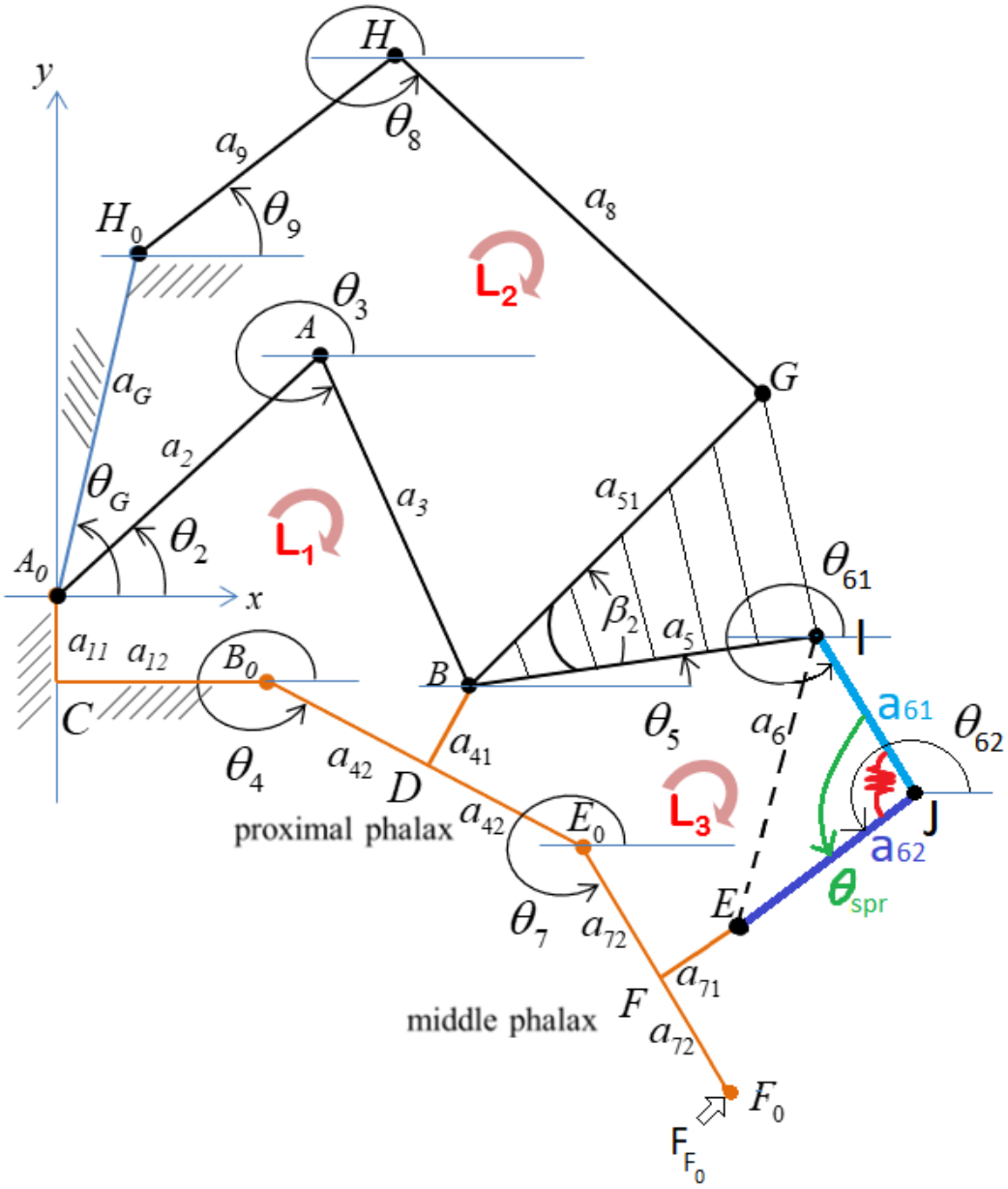

Figure 3.8: Under-actuated Mechanism Version 1

Link a_6 is "broken" to two links a_{61} and a_{62}.

A torsional spring is attached at joint J.

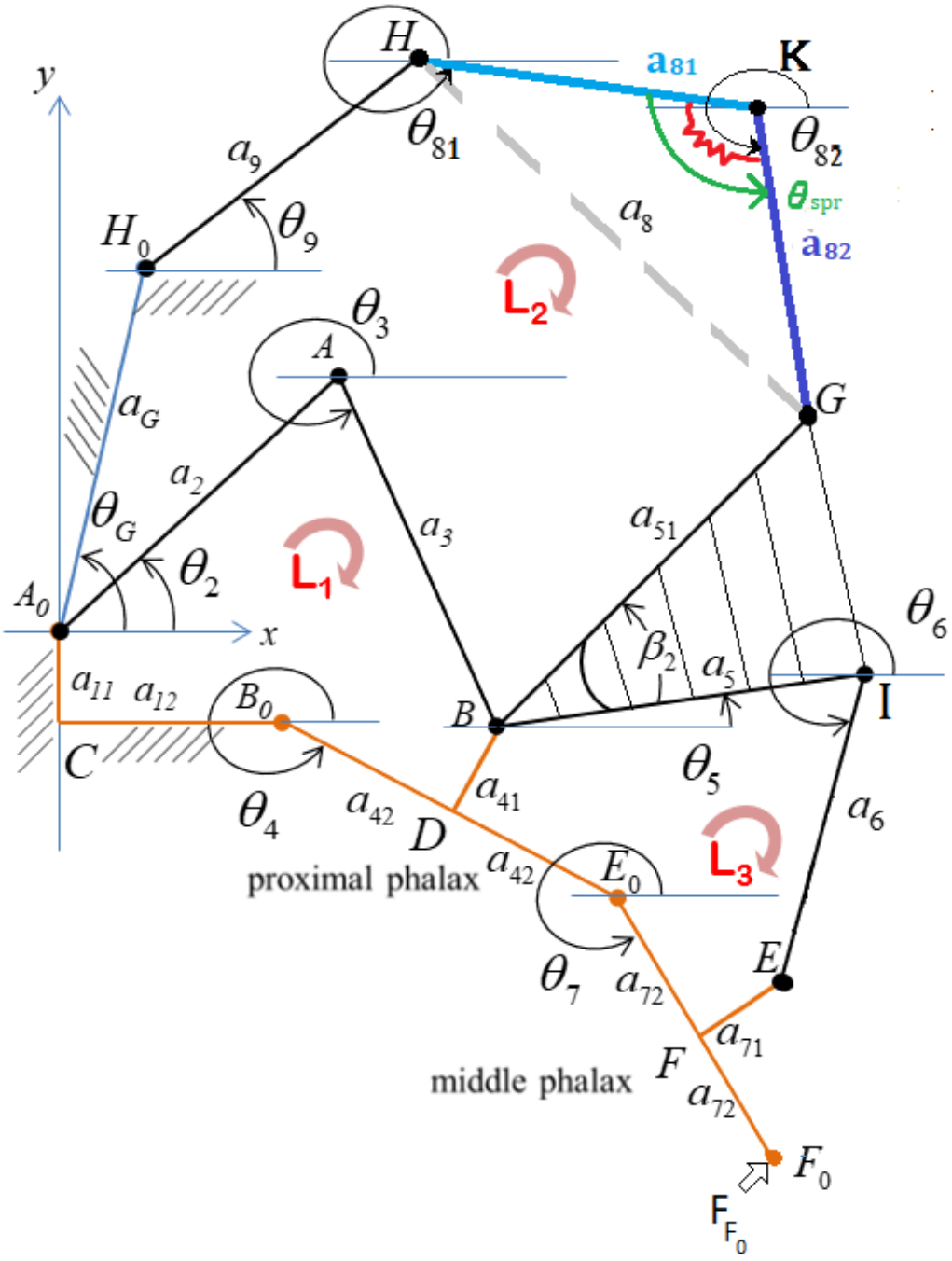

Figure 3.9: Under-actuated Mechanism Version 2

Link a_8 is "broken" to two links a_{81} and a_{82}.

A torsional spring is attached at joint K.

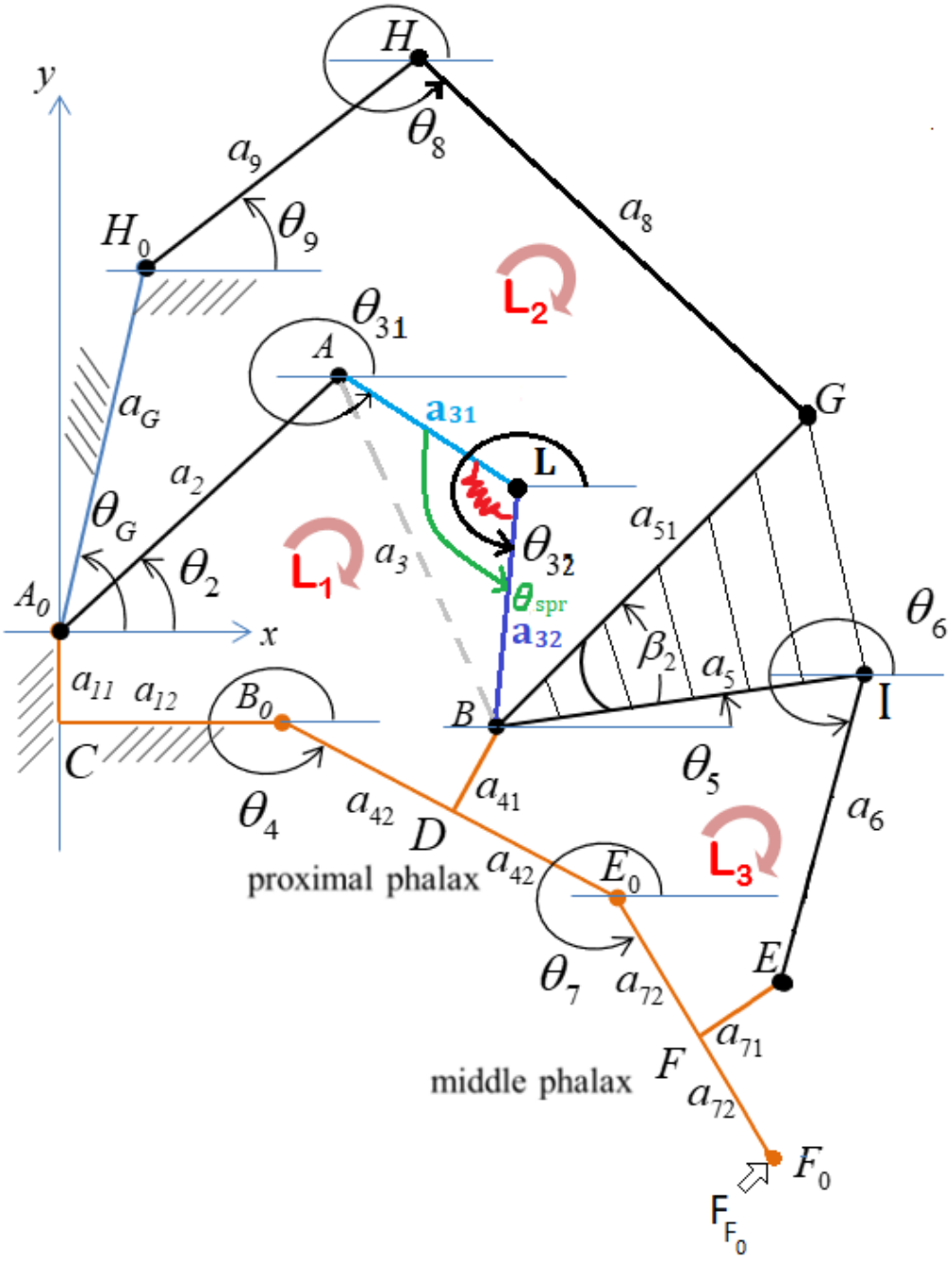

Figure 3.10: Under-actuated Mechanism Version 3

Link a_3 is "broken" to two links a_{31} and a_{32}.

A torsional spring is attached at joint L.

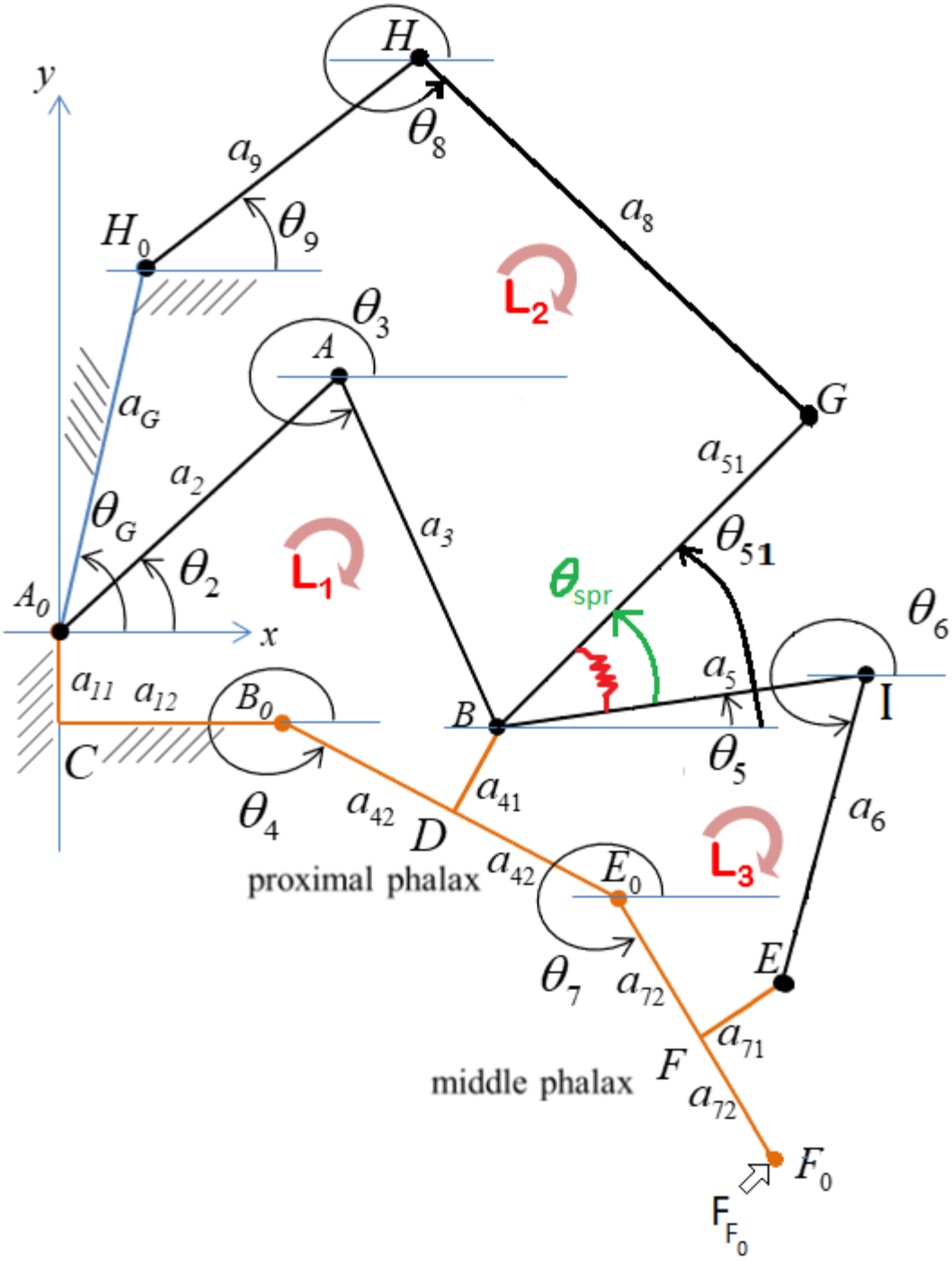

Figure 3.11: Under-actuated Mechanism Version 4

Constant angle β_2 is changed to a variable angle θ_{spr}.

A torsional spring is attached at joint B.

The considered under-actuated mechanism options are given in Figures 3.8, 3.9, 3.10,

3.11. The difference between these under-actuated mechanisms and the fully-actuated mechanism is the addition of a degree of freedom to the mechanism. For versions 1, 2, and 3; there are two new links and a torsional spring added instead of a link. However, a ternary link is broken into two independent inks and a torsion spring is placed between them for version 4. A general summary of the conversion from fully to under-actuation is shown in the list below:

- version 1: . . . . . a_6 $\Rightarrow$ a_{61}, a_{62} and θ_{spr1}
- version 2: . . . . . a_8 $\Rightarrow$ a_{81}, a_{82} and θ_{spr2}
- version 3: . . . . . a_3 $\Rightarrow$ a_{31}, a_{32} and θ_{spr3}
- version 4: . . . ternary link (a_5 and a_{51}) $\Rightarrow$ a_5, a_{51} and θ_{spr4}

The degree of freedom of the under-actuated mechanisms is calculated given the fact that all mechanisms have 10 links and 12 joints.

$$\begin{aligned} N &= 3(l-1) - 2j \\ &= 3(10-1) - (2)(12) = 3 \end{aligned} \tag{3.94}$$

where

l: number of links
j: number of joints.

The number of Loops can be found as:

$$L = j - l + 1 = 12 - 10 + 1 = 3 \tag{3.95}$$

The number of independent variables can be found as:

$$V = 2L + N = (2)(3) + 3 = 9 \tag{3.96}$$

In these mechanisms, the *doa* is 2, which are at the points A_0 and H_0 while the *dof* is 3. So, in order to be able to control the mechanism, there is a torsional spring added at points J, K, L, and B for each version, respectively.

The position variables of the defined mechanism in Figures 3.8, 3.9, 3.10 and 3.11 can be shown as follows:

$$V_1 = [\theta_2, \theta_3, \theta_4, \theta_5, \theta_{61}, \theta_{62}, \theta_7, \theta_8, \theta_9] \tag{3.97}$$

$$V_2 = [\theta_2, \theta_3, \theta_4, \theta_5, \theta_6, \theta_7, \theta_{81}, \theta_{82}, \theta_9] \tag{3.98}$$

$$V_3 = [\theta_2, \theta_{31}, \theta_{32}, \theta_4, \theta_5, \theta_6, \theta_7, \theta_8, \theta_9] \tag{3.99}$$

$$V_4 = [\theta_2, \theta_3, \theta_4, \theta_5, \theta_{51}, \theta_6, \theta_7, \theta_8, \theta_9] \tag{3.100}$$

Also, the design vector for each version can be shown as follows:

$$S_1 = [a_{11}, a_{12}, a_G, a_2, a_3, a_{41}, a_{42}, a_5, a_{51}, a_{61}, a_{62}, a_{71}, a_{72}, a_8, a_9, \beta_2, \theta_G, \theta_{spr1_{free}}, K_1] \tag{3.101}$$

$$S_2 = [a_{11}, a_{12}, a_G, a_2, a_3, a_{41}, a_{42}, a_5, a_{51}, a_6, a_{71}, a_{72}, a_{81}, a_{82}, a_9, \beta_2, \theta_G, \theta_{spr2_{free}}, K_2] \tag{3.102}$$

$$S_3 = [a_{11}, a_{12}, a_G, a_2, a_{31}, a_{32}, a_{41}, a_{42}, a_5, a_{51}, a_6, a_{71}, a_{72}, a_8, a_9, \beta_2, \theta_G, \theta_{spr3_{free}}, K_3] \tag{3.103}$$

$$S_4 = [a_{11}, a_{12}, a_G, a_2, a_3, a_{41}, a_{42}, a_5, a_{51}, a_6, a_{71}, a_{72}, a_8, a_9, \theta_G, \theta_{spr4_{free}}, K_4] \tag{3.104}$$

The consequent primary variables are the same as in the fully-actuated model.

3.3.2 Design Methodology

In the design of an under-actuated mechanism, as in the fully-actuated one, the structure parameters are optimized, which are given in Equations 3.101, 3.102, 3.103 and 3.104. A basic flowchart, a pseudo-code of the design procedure for the under-actuation design procedure is represented in Figure 3.12. In the flow chart, obtaining an analytical solution can not be achieved before including force equations. Therefore, all position analysis and force equations are obtained in terms of θ_{spr}. Then

an equation is obtained which is only a function of θ_{spr} as in the Equations 3.190, 3.195, 3.200 and 3.205. The solution of that equation gives the numerical value of θ_{spr}. Then everything is calculated once again so that the GII value is obtained. In brief, the force equations are used in order to extract the necessary equation to solve the variable θ_{spr}.

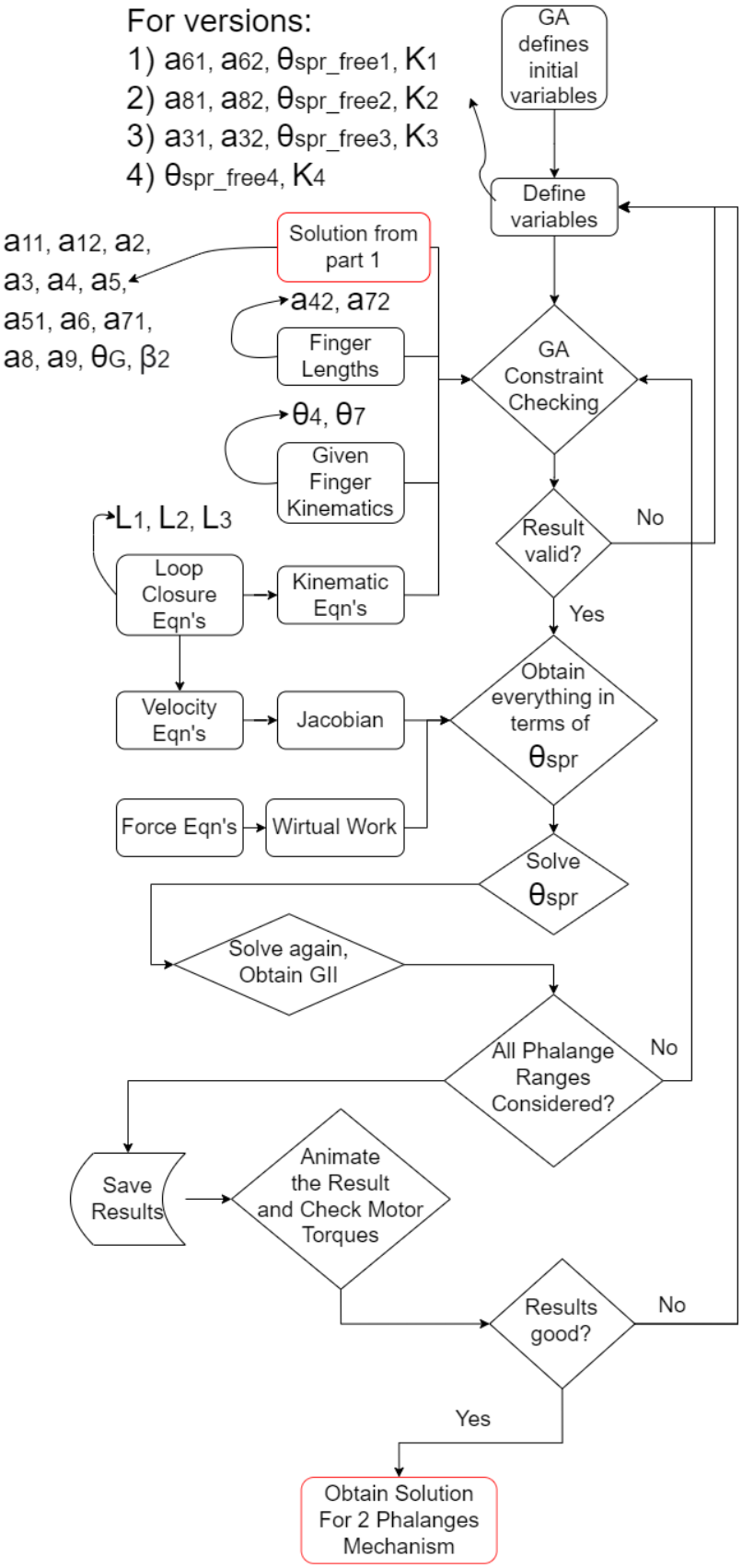

Figure 3.12: Under-actuated Design Flow Chart

3.3.3 Mechanism Synthesis

3.3.3.1 Position Analysis

Loop Closure Equations

For the position analysis of each under-actuated mechanism version, the Loop Closure Equations (LCE's) are written in Equations 3.105, 3.106, 3.107, 3.108.

Version 1:

$$\begin{aligned} L1 &\Rightarrow \overrightarrow{A_0AB} = \overrightarrow{A_0CB_0DB} \\ L2 &\Rightarrow \overrightarrow{A_0H_0HG} = \overrightarrow{A_0ABG} \\ L3 &\Rightarrow \overrightarrow{DBIJE} = \overrightarrow{DE_0FE} \end{aligned} \tag{3.105}$$

Version 2:

$$\begin{aligned} L1 &\Rightarrow \overrightarrow{A_0AB} = \overrightarrow{A_0CB_0DB} \\ L2 &\Rightarrow \overrightarrow{A_0H_0HKG} = \overrightarrow{A_0ABG} \\ L3 &\Rightarrow \overrightarrow{DBIJE} = \overrightarrow{DE_0FE} \end{aligned} \tag{3.106}$$

Version 3:

$$\begin{aligned} L1 &\Rightarrow \overrightarrow{A_0ALB} = \overrightarrow{A_0CB_0DB} \\ L2 &\Rightarrow \overrightarrow{A_0H_0HG} = \overrightarrow{A_0ABG} \\ L3 &\Rightarrow \overrightarrow{DBIJE} = \overrightarrow{DE_0FE} \end{aligned} \tag{3.107}$$

Version 4:

$$\begin{aligned} L1 &\Rightarrow \overrightarrow{A_0AB} = \overrightarrow{A_0CB_0DB} \\ L2 &\Rightarrow \overrightarrow{A_0H_0HG} = \overrightarrow{A_0ABG} \\ L3 &\Rightarrow \overrightarrow{DBIE} = \overrightarrow{DE_0FE} \end{aligned} \tag{3.108}$$

Note that, the differences between the fully-actuated mechanism LCE's and the under-actuated mechanism LCE's is on the loops in which the addition of the degree of freedom is occured. For version 1; it is at Loop 3. For version 2; it is at Loop 2. For version 3; it is at Loops 1 and 2. However, in the final version, there is no change in LCE's but the structure parameter β_2 is now became a variable with a new representation as θ_{spr4}. So, the detailed expressions are given for each version as follows:

For version 1:

$$L3 \Rightarrow a_{41}e^{i(\theta_4+\frac{\pi}{2})} + a_5e^{i\theta_5} + a_{61}e^{i\theta_{61}} + a_{62}e^{i\theta_{62}} = a_{42}e^{i\theta_4} + a_{72}e^{i\theta_7} + a_{71}e^{i(\theta_7+\frac{\pi}{2})} \tag{3.109}$$

For version 2:

$$L2 \Rightarrow a_Ge^{i\theta_G} + a_9e^{i\theta_9} + a_{81}e^{i\theta_{81}} + a_{82}e^{i\theta_{82}} = a_2e^{i\theta_2} + a_3e^{i\theta_3} + a_{51}e^{i(\theta_5+\beta_2)} \tag{3.110}$$

For version 3:

$$L1 \Rightarrow a_2e^{i\theta_2} + a_{31}e^{i\theta_{31}} + a_{32}e^{i\theta_{32}} = (-a_{11}i + a_{12}) + a_{42}e^{i\theta_4} + a_{41}e^{i(\theta_4+\frac{\pi}{2})} \tag{3.111}$$

$$L2 \Rightarrow a_Ge^{i\theta_G} + a_9e^{i\theta_9} + a_8e^{i\theta_8} = a_2e^{i\theta_2} + a_{31}e^{i\theta_{31}} + a_{32}e^{i\theta_{32}} + a_{51}e^{i(\theta_5+\beta_2)} \tag{3.112}$$

For version 4:

$$L2 \Rightarrow a_Ge^{i\theta_G} + a_9e^{i\theta_9} + a_8e^{i\theta_8} = a_2e^{i\theta_2} + a_3e^{i\theta_3} + a_{51}e^{i(\theta_5+\theta_{spr4})} \tag{3.113}$$

The position of the end-effector is the same as in the fully-actuated mechanism as it was given in the Equation 3.24. The expression is given once again below:

$$\underline{P} = \begin{bmatrix} p_1 \\ p_2 \end{bmatrix} = \begin{bmatrix} +a_{12} + 2a_{42}\cos(\theta_4) + 2a_{72}\cos(\theta_7) \\ -a_{11} + 2a_{42}\sin(\theta_4) + 2a_{72}\sin(\theta_7) \end{bmatrix}$$

For version 1, from Equation 3.109, real and imaginary parts can be written as follows:

$$\begin{aligned} -a_{41}\sin\theta_4 + a_5\cos\theta_5 + a_{61}\cos\theta_{61} + a_{62}\cos\theta_{62} = a_{42}\cos\theta_4 + a_{72}\cos\theta_7 \\ - a_{71}\sin\theta_7 \end{aligned} \tag{3.114}$$

$$+a_{41}\cos\theta_4 + a_5\sin\theta_5 + a_{61}\sin\theta_{61} + a_{62}\cos\theta_{62} = a_{42}\sin\theta_4 + a_{72}\sin\theta_7 + a_{71}\cos\theta_7 \tag{3.115}$$

The spring angle θ_{spr1} can be defined as follows:

$$\theta_{spr1} = \theta_{62} - \theta_{61} + \pi \tag{3.116}$$

Then, angle θ_{62} can be defined as follows:

$$\theta_{62} = \theta_{61} + \theta_{spr1} - \pi \tag{3.117}$$

Then, the following equations are derived:

$$\begin{aligned} a_5\cos\theta_5 &= x_6 - a_{61}\cos\theta_{61} + a_{62}\cos(\theta_{61}+\theta_{spr1}) \\ &= x_6 - a_{61}\cos\theta_{61} + a_{62}[\cos(\theta_{61})\cos(\theta_{spr1}) - \sin(\theta_{61})\sin(\theta_{spr1})] \end{aligned} \tag{3.118}$$

$$\begin{aligned} a_5\sin\theta_5 &= y_6 - a_{61}\sin\theta_{61} + a_{62}\sin(\theta_{61}+\theta_{spr1}) \\ &= y_6 - a_{61}\sin\theta_{61} + a_{62}[\sin(\theta_{61})\cos(\theta_{spr1}) + \cos(\theta_{61})\sin(\theta_{spr1})] \end{aligned} \tag{3.119}$$

where

$$x_6 = +a_{42}\cos\theta_4 + a_{41}\sin\theta_4 + a_{72}\cos\theta_7 - a_{71}\sin\theta_7$$

$$y_6 = +a_{42}\sin\theta_4 - a_{41}\cos\theta_4 + a_{72}\sin\theta_7 + a_{71}\cos\theta_7$$

Then, Equations 3.118 and 3.119 become as follows:

$$a_5\cos\theta_5 = x_6 + \cos\theta_{61}k_3 + \sin\theta_{61}k_4 \tag{3.120}$$

$$a_5\sin\theta_5 = y_6 + \sin\theta_{61}k_3 + \cos\theta_{61}k_4 \tag{3.121}$$

where

$$k_3 = -a_{61} + a_{62}\cos(\theta_{spr1})$$

$$k_4 = -a_{62}\sin(\theta_{spr1})$$

Taking squares of the Equations 3.120 and 3.121 and summing them together yields to the following equation:

$$\theta_{61} = 2tan^{-1}\left(\frac{-B_2 \pm \sqrt{{B_2}^2 - 4A_2C_2}}{2A_2}\right) \tag{3.122}$$

where

$$K_4 = {x_6}^2 + {y_6}^2 + {k_3}^2 + {k_4}^2 - {a_5}^2$$

$$K_5 = 2(x_6 k_3 - y_6 k_4)$$

$$K_6 = 2(x_6 k_4 + y_6 k_3)$$

$$A_2 = K_4 - K_5$$

$$B_2 = 2K_6$$

$$C_2 = K_4 + K_5$$

With the availability of θ_{61}, Equations 3.120 and 3.121, θ_5 can be found without any additional sign variable as follow:

$$\theta_5 = atan_2[(y_6 + \sin\theta_{61} k_3 + \cos\theta_{61} k_4), (x_6 + \cos\theta_{61} k_3 + \sin\theta_{61} k_4)] \tag{3.123}$$

Note that, the position solutions for θ_5 and θ_{61} are functions of θ_{spr1}.

For version 2, from Equation 3.112, real and imaginary parts can be written as follows:

$$a_G \cos\theta_G + a_9 \cos\theta_9 + a_{81} \cos\theta_{81} + a_{82} \cos\theta_{82} = +a_2 \cos\theta_2 + a_3 \cos\theta_3 + a_{51} \cos(\theta_5 + \beta_2) \tag{3.124}$$

$$a_G \sin\theta_G + a_9 \sin\theta_9 + a_{81} \sin\theta_{81} + a_{82} \sin\theta_{82} = +a_2 \sin\theta_2 + a_3 \sin\theta_3 + a_{51} \sin(\theta_5 + \beta_2) \tag{3.125}$$

The spring angle θ_{spr2} can be defined as follows:

$$\theta_{spr2} = \theta_{82} - \theta_{81} + \pi \tag{3.126}$$

Then, angle θ_{82} can be defined as follows:

$$\theta_{82} = \theta_{81} + \theta_{spr2} - \pi \tag{3.127}$$

Then, the following equations are derived:

$$\begin{aligned} a_9 \cos\theta_9 &= x_7 - a_{81} \cos\theta_{81} + a_{82} \cos(\theta_{81} + \theta_{spr2}) \\ &= x_7 - a_{81} \cos\theta_{81} + a_{82}[\cos(\theta_{81}) \cos(\theta_{spr2}) - \sin(\theta_{81}) \sin(\theta_{spr2})] \end{aligned} \tag{3.128}$$

$$a_9 \sin\theta_9 = y_7 - a_{81}\sin\theta_{81} + a_{82}\sin(\theta_{81}+\theta_{spr2})$$
$$= y_7 - a_{81}\sin\theta_{81} + a_{82}[\sin(\theta_{81})\cos(\theta_{spr2}) + \cos(\theta_{81})\sin(\theta_{spr2})] \quad (3.129)$$

where

$$x_7 = +a_2\cos\theta_2 + a_3\cos\theta_3 + a_{51}\cos(\theta_5+\beta_2) - a_G\cos\theta_G$$
$$y_7 = +a_2\sin\theta_2 + a_3\sin\theta_3 + a_{51}\sin(\theta_5+\beta_2) - a_G\sin\theta_G$$

Then, Equations 3.128 and 3.129 become as follows:

$$a_9\cos\theta_9 = x_7 + \cos\theta_{81}k_5 + \sin\theta_{81}k_6 \quad (3.130)$$

$$a_9\sin\theta_9 = y_7 + \sin\theta_{81}k_5 + \cos\theta_{81}k_6 \quad (3.131)$$

where

$$k_5 = -a_{81} + a_{82}\cos(\theta_{spr2})$$
$$k_6 = -a_{82}\sin(\theta_{spr2})$$

Taking squares of the Equations 3.130 and 3.131 and summing them together yields the following equation:

$$\theta_{81} = 2tan^{-1}(\frac{-B_3 \pm \sqrt{{B_3}^2 - 4A_3C_3}}{2A_3}) \quad (3.132)$$

where

$$K_7 = {x_7}^2 + {y_7}^2 + {k_5}^2 + {k_6}^2 - {a_9}^2$$
$$K_8 = 2(x_7k_5 - y_7k_6)$$
$$K_9 = 2(x_7k_6 + y_7k_5)$$
$$A_3 = K_7 - K_8$$
$$B_3 = 2K_9$$
$$C_3 = K_7 + K_8$$

With the availability of θ_{81}, Equations 3.130 and 3.131, θ_9 can be found without any additional sign variable as follow:

$$\theta_9 = atan_2[(y_7 + \sin\theta_{81}k_5 + \cos\theta_{81}k_6), (x_7 + \cos\theta_{81}k_5 + \sin\theta_{81}k_6)] \quad (3.133)$$

Note that, the position solutions for θ_9 and θ_{81} are functions of θ_{spr2}.

For version 3, from Equation 3.111, real and imaginary parts can be written as follows:

$$a_2\cos\theta_2 + a_{31}\cos\theta_{31} + a_{32}\cos(\theta_{32}) = +a_{12} + a_{42}\cos\theta_4 - a_{41}\sin\theta_4 \quad (3.134)$$

$$a_2 \sin\theta_2 + a_{31} \sin\theta_{31} + a_{32} \sin(\theta_{32}) = -a_{11} + a_{42} \sin\theta_4 + a_{41} \cos\theta_4 \tag{3.135}$$

The spring angle θ_{spr3} can be defined as follows:

$$\theta_{spr3} = \theta_{32} - \theta_{31} + \pi \tag{3.136}$$

Then, angle θ_{32} can be defined as follows:

$$\theta_{32} = \theta_{31} + \theta_{spr3} - \pi \tag{3.137}$$

Then, the following equations are derived:

$$\begin{aligned} a_2 \cos\theta_2 &= x_8 - a_{31} \cos\theta_{31} + a_{32} \cos(\theta_{31} + \theta_{spr3}) \\ &= x_8 - a_{31} \cos\theta_{31} + a_{32}[\cos(\theta_{31}) \cos(\theta_{spr3}) - \sin(\theta_{31}) \sin(\theta_{spr3})] \end{aligned} \tag{3.138}$$

$$\begin{aligned} a_2 \sin\theta_2 &= y_8 - a_{31} \sin\theta_{31} + a_{32} \sin(\theta_{31} + \theta_{spr3}) \\ &= y_8 - a_{31} \sin\theta_{31} + a_{32}[\sin(\theta_{31}) \cos(\theta_{spr3}) + \cos(\theta_{31}) \sin(\theta_{spr3})] \end{aligned} \tag{3.139}$$

where

$$x_8 = +a_{12} + a_{42} \cos\theta_4 - a_{41} \sin\theta_4$$

$$y_8 = -a_{11} + a_{42} \sin\theta_4 + a_{41} \cos\theta_4$$

Then, Equations 3.138 and 3.139 become as follows:

$$a_2 \cos\theta_2 = x_8 + \cos\theta_{31} k_7 + \sin\theta_{31} k_8 \tag{3.140}$$

$$a_2 \sin\theta_2 = y_8 + \sin\theta_{31} k_7 + \cos\theta_{31} k_8 \tag{3.141}$$

where

$$k_7 = -a_{31} + a_{32} \cos(\theta_{spr3})$$

$$k_8 = -a_{32} \sin(\theta_{spr3})$$

Taking squares of the Equations 3.140 and 3.141 and summing them together yields the following equation:

$$\theta_{31} = 2tan^{-1}\left(\frac{-B_4 \pm \sqrt{{B_4}^2 - 4A_4C_4}}{2A_4}\right) \tag{3.142}$$

where

$$K_{10} = {x_8}^2 + {y_8}^2 + {k_7}^2 + {k_8}^2 - {a_2}^2$$
$$K_{11} = 2(x_8 k_7 - y_7 k_8)$$
$$K_{12} = 2(x_8 k_8 + y_7 k_7)$$
$$A_4 = K_{10} - K_{11}$$
$$B_4 = 2K_{12}$$
$$C_4 = K_{10} + K_{11}$$

With the availability of θ_{31}, Equations 3.140 and 3.141, θ_2 can be found without any additional sign variable as follow:

$$\theta_2 = atan_2[(y_8 + \sin\theta_{31} k_7 + \cos\theta_{31} k_8), (x_8 + \cos\theta_{31} k_7 + \sin\theta_{31} k_8)] \tag{3.143}$$

Note that, the position solutions for θ_2 and θ_{31} are functions of θ_{spr3}.

For version 4, from Equation 3.113, real and imaginary parts can be written as follows:

$$a_G \cos\theta_G + a_9 \cos\theta_9 + a_8 \cos\theta_8 = +a_2 \cos\theta_2 + a_3 \cos\theta_3 + a_{51} \cos\theta_{51} \tag{3.144}$$

$$a_G \sin\theta_G + a_9 \sin\theta_9 + a_8 \sin\theta_8 = +a_2 \sin\theta_2 + a_3 \sin\theta_3 + a_{51} \sin\theta_{51} \tag{3.145}$$

The spring angle θ_{spr4} can be defined as follows:

$$\theta_{spr4} = \theta_{51} - \theta_5 \tag{3.146}$$

Then, angle θ_{51} can be defined as follows:

$$\theta_{51} = \theta_5 + \theta_{spr4} \tag{3.147}$$

So, the Equations 3.144 and 3.145 becomes as follows:

$$a_G \cos\theta_G + a_9 \cos\theta_9 + a_8 \cos\theta_8 = +a_2 \cos\theta_2 + a_3 \cos\theta_3 + a_{51} \cos(\theta_5 + \theta_{spr4}) \tag{3.148}$$

$$a_G \sin\theta_G + a_9 \sin\theta_9 + a_8 \sin\theta_8 = +a_2 \sin\theta_2 + a_3 \sin\theta_3 + a_{51} \sin(\theta_5 + \theta_{spr4}) \tag{3.149}$$

Then, the following equations are derived:

$$a_9 \cos\theta_9 = x_9 - a_8 \cos\theta_8 \tag{3.150}$$

$$a_9 \sin\theta_9 = y_9 - a_8 \sin\theta_8 \tag{3.151}$$

where

$$x_9 = +a_2 \cos\theta_2 + a_3 \cos\theta_3 + a_{51} \cos(\theta_5 + \theta_{spr4}) - a_G \cos\theta_G$$

$$y_9 = +a_2 \sin\theta_2 + a_3 \sin\theta_3 + a_{51} \sin(\theta_5 + \theta_{spr4}) - a_G \sin\theta_G$$

Then, θ_8 is derived as follows:

$$\theta_8 = \Psi_5 + \sigma_5 \gamma_5 \tag{3.152}$$

where

$$\Psi_5 = atan_2(y_9, x_9)$$

$$f_5 = ({x_9}^2 + {y_9}^2 + {a_8}^2 - {a_9}^2)/(2a_8)$$

$$g_5 = \sqrt{{x_9}^2 + {y_9}^2 - {f_5}^2}$$

$$\gamma_5 = atan_2(g_5, f_5)$$

$$\sigma_5 = \pm 1$$

With the availability of θ_8, Equations 3.150 and 3.151, θ_9 can be found without any additional sign variable as follow:

$$\theta_9 = atan_2[(y_9 - a_8 \sin\theta_8), (x_9 - a_8 \cos\theta_8)] \tag{3.153}$$

Note that, the position solutions for θ_9 and θ_8 are functions of θ_{spr4}.

3.3.3.2 Velocity Analysis

The velocity equations are obtained by taking the derivative of position equations with respect to time. In this mechanism, end-effector velocity is the same as in the fully-actuated mechanism as in Equation 3.62. The expression is given once again as follows:

$$\frac{d(X_{F_0})}{dt} = V_{F_0} = i2[\dot{\theta}_4 a_{42} e^{i\theta_4} + \dot{\theta}_7 a_{72} e^{i\theta_7}]$$

$$= i2[\dot{\theta}_4 a_{42}(\cos\theta_4 + i\sin\theta_4)\dot{\theta}_7 a_{72}(\cos\theta_7 + i\sin\theta_7)]$$

Velocity equation for version 1 (Loop 3)

$$\begin{bmatrix} -a_{61}\sin\theta_{61} + a_{62}\sin(\theta_{61}+\theta_{spr1}) & +(a_{72}\sin\theta_7 + a_{71}\cos\theta_7) \\ +a_{61}\cos\theta_{61} - a_{62}\cos(\theta_{61}+\theta_{spr1}) & -(a_{72}\cos\theta_7 - a_{71}\sin\theta_7) \end{bmatrix} \begin{bmatrix} \dot{\theta}_{61} \\ \dot{\theta}_7 \end{bmatrix}$$
$$= \begin{bmatrix} +(a_{41}\cos\theta_4 - a_{42}\sin\theta_4) & +a_5\sin\theta_5 & -a_{62}\sin(\theta_{61}+\theta_{spr1}) \\ +(a_{41}\sin\theta_4 + a_{42}\cos\theta_4) & -a_5\cos\theta_5 & +a_{62}\cos(\theta_{61}+\theta_{spr1}) \end{bmatrix} \begin{bmatrix} \dot{\theta}_4 \\ \dot{\theta}_5 \\ \dot{\theta}_{spr1} \end{bmatrix} \tag{3.154}$$

Velocity equation for version 2 (Loop 2)

$$\begin{bmatrix} +a_{51}\sin(\theta_5+\beta_2) & -a_{81}\sin\theta_{81} + a_{82}\sin(\theta_{81}+\theta_{spr2}) \\ -a_{51}\cos(\theta_5+\beta_2) & +a_{81}\cos\theta_{81} - a_{82}\cos(\theta_{81}+\theta_{spr2}) \end{bmatrix} \begin{bmatrix} \dot{\theta}_5 \\ \dot{\theta}_{81} \end{bmatrix}$$
$$= \begin{bmatrix} -a_2\sin\theta_2 & -a_3\sin\theta_3 & +a_9\sin\theta_9 & +a_{82}\sin(\theta_{81}+\theta_{spr2}) \\ +a_2\cos\theta_2 & +a_3\cos\theta_3 & -a_9\cos\theta_9 & -a_{82}\cos(\theta_{81}+\theta_{spr2}) \end{bmatrix} \begin{bmatrix} \dot{\theta}_2 \\ \dot{\theta}_3 \\ \dot{\theta}_9 \\ \dot{\theta}_{spr2} \end{bmatrix} \tag{3.155}$$

Velocity equations for version 3 (Loop 1 and Loop 2)

Velocity equation for Loop 1 is expressed in the Equation 3.156.

$$\begin{bmatrix} +a_{31}\sin\theta_{31} - a_{32}\sin(\theta_{31}+\theta_{spr3}) & -(a_{42}\sin\theta_4 + a_{41}\cos\theta_4) \\ -a_{31}\cos\theta_{31} + a_{32}\cos(\theta_{31}+\theta_{spr3}) & +(a_{42}\cos\theta_4 - a_{41}\sin\theta_4) \end{bmatrix} \begin{bmatrix} \dot{\theta}_{31} \\ \dot{\theta}_4 \end{bmatrix}$$
$$= \begin{bmatrix} -a_2\sin\theta_2 & -a_{32}\sin(\theta_{31}+\theta_{spr3}) \\ +a_2\cos\theta_2 & +a_{32}\cos(\theta_{31}+\theta_{spr3}) \end{bmatrix} \begin{bmatrix} \dot{\theta}_2 \\ \dot{\theta}_{spr3} \end{bmatrix} \tag{3.156}$$

Velocity equation for Loop 2 is expressed in the Equation 3.157.

$$\begin{bmatrix} +a_{51}\sin(\theta_5+\beta_2) & -a_8\sin\theta_8 \\ -a_{51}\cos(\theta_5+\beta_2) & +a_8\cos\theta_8 \end{bmatrix} \begin{bmatrix} \dot{\theta}_5 \\ \dot{\theta}_8 \end{bmatrix}$$

$$= \begin{bmatrix} -a_2\sin\theta_2 & -a_{31}\sin\theta_{31} + a_{32}\sin(\theta_{31}+\theta_{spr3}) & +a_9\sin\theta_9 & +a_{32}\sin(\theta_{31}+\theta_{spr3}) \\ +a_2\cos\theta_2 & +a_{31}\cos\theta_{31} - a_{32}\cos(\theta_{31}+\theta_{spr3}) & -a_9\cos\theta_9 & -a_{32}\cos(\theta_{31}+\theta_{spr3}) \end{bmatrix} \begin{bmatrix} \dot{\theta}_2 \\ \dot{\theta}_{31} \\ \dot{\theta}_9 \\ \dot{\theta}_{spr3} \end{bmatrix} \quad (3.157)$$

Velocity equation for version 4 (Loop 2)

$$\begin{bmatrix} +a_{51}\sin(\theta_5+\theta_{spr4}) & -a_8\sin\theta_8 \\ -a_{51}\cos(\theta_5+\theta_{spr4}) & +a_8\cos\theta_8 \end{bmatrix} \begin{bmatrix} \dot{\theta}_5 \\ \dot{\theta}_8 \end{bmatrix}$$

$$= \begin{bmatrix} -a_2\sin\theta_2 & -a_3\sin\theta_3 & +a_9\sin\theta_9 & -a_{51}\sin(\theta_5+\theta_{spr4}) \\ +a_2\cos\theta_2 & +a_3\cos\theta_3 & -a_9\cos\theta_9 & +a_{51}\cos(\theta_5+\theta_{spr4}) \end{bmatrix} \begin{bmatrix} \dot{\theta}_2 \\ \dot{\theta}_3 \\ \dot{\theta}_9 \\ \dot{\theta}_{spr4} \end{bmatrix} \quad (3.158)$$

From Equations 3.154, 3.155, 3.156, 3.157 and 3.158; velocity derivations in order to calculate Jacobian matrix for each version are shown in the Equations 3.159, 3.161, 3.163, 3.166 and 3.168:

For the first version, the only difference is at Loop 3. So, only Loop 3's derivation is expressed in the Equation 3.159.

$$\begin{bmatrix} \dot{\theta}_{61} \\ \dot{\theta}_7 \end{bmatrix} = \begin{bmatrix} j_{17} & j_{18} & j_{19} \\ j_{20} & j_{21} & j_{22} \end{bmatrix} \begin{bmatrix} \dot{\theta}_4 \\ \dot{\theta}_5 \\ \dot{\theta}_{spr1} \end{bmatrix} \quad (3.159)$$

where

$$\begin{bmatrix} j_{17} & j_{18} & j_{19} \\ j_{20} & j_{21} & j_{22} \end{bmatrix} = \begin{bmatrix} -a_{61}\sin\theta_{61} + a_{62}\sin(\theta_{61}+\theta_{spr}) & +(a_{72}\sin\theta_7 + a_{71}\cos\theta_7) \\ +a_{61}\cos\theta_{61} - a_{62}\cos(\theta_{61}+\theta_{spr}) & -(a_{72}\cos\theta_7 - a_{71}\sin\theta_7) \end{bmatrix}^{-1} \begin{bmatrix} +(a_{41}\cos\theta_4 - a_{42}\sin\theta_4) & +a_5\sin\theta_5 & -a_{62}\sin(\theta_{61}+\theta_{spr}) \\ +(a_{41}\sin\theta_4 + a_{42}\cos\theta_4) & -a_5\cos\theta_5 & +a_{62}\cos(\theta_{61}+\theta_{spr}) \end{bmatrix}$$

The following equations can be derived for future calculations from Equations 3.56, 3.57, and 3.159.

$$\begin{aligned} \dot{\theta_3} &= j_1\dot{\theta_2} \\ \dot{\theta_4} &= j_2\dot{\theta_2} \\ \dot{\theta_5} &= j_7\dot{\theta_2} + j_8\dot{\theta_3} + j_9\dot{\theta_9} \\ &= (j_7 + j_8j_1)\dot{\theta_2} + j_9\dot{\theta_9} \\ \dot{\theta_8} &= j_{10}\dot{\theta_2} + j_{11}\dot{\theta_3} + j_{12}\dot{\theta_9} \\ &= (j_{10} + j_{11}j_1)\dot{\theta_2} + j_{12}\dot{\theta_9} \\ \dot{\theta}_{61} &= j_{17}\dot{\theta_4} + j_{18}\dot{\theta_5} + j_{19}\dot{\theta}_{spr1} \\ &= [j_{17}j_2 + j_{18}(j_7 + j_8j_1)]\dot{\theta_2} + (j_{18}j_9)\dot{\theta_9} + j_{19}\dot{\theta}_{spr1} \\ \dot{\theta_7} &= j_{20}\dot{\theta_4} + j_{21}\dot{\theta_5} + j_{22}\dot{\theta}_{spr1} \\ &= [j_{20}j_2 + j_{21}(j_7 + j_8j_1)]\dot{\theta_2} + (j_{21}j_9)\dot{\theta_9} + j_{22}\dot{\theta}_{spr1} \end{aligned} \tag{3.160}$$

For the second version, the only difference is at Loop 2. So, only Loop 2's derivation is expressed in the Equation 3.161.

$$\begin{bmatrix} \dot{\theta_5} \\ \dot{\theta}_{81} \end{bmatrix} = \begin{bmatrix} j_{23} & j_{24} & j_{25} & j_{26} \\ j_{27} & j_{28} & j_{29} & j_{30} \end{bmatrix} \begin{bmatrix} \dot{\theta_2} \\ \dot{\theta_3} \\ \dot{\theta_9} \\ \dot{\theta}_{spr2} \end{bmatrix} \tag{3.161}$$

where

$$\begin{bmatrix} j_{23} & j_{24} & j_{25} & j_{26} \\ j_{27} & j_{28} & j_{29} & j_{30} \end{bmatrix} = \begin{bmatrix} +a_{51}\sin(\theta_5+\beta_2) & -a_{81}\sin\theta_{81} \\ -a_{51}\cos(\theta_5+\beta_2) & +a_{81}\cos\theta_{81} \end{bmatrix}^{-1} \begin{bmatrix} -a_2\sin\theta_2 & -a_3\sin\theta_3 & +a_9\sin\theta_9 & +a_{82}\sin(\theta_{81}+\theta_{spr2}) \\ +a_2\cos\theta_2 & +a_3\cos\theta_3 & -a_9\cos\theta_9 & -a_{82}\cos(\theta_{81}+\theta_{spr2}) \end{bmatrix}$$

The following equations can be derived for future calculations from Equations 3.56, 3.161, and 3.58.

$$\begin{aligned} \dot{\theta}_3 &= j_1\dot{\theta}_2 \\ \dot{\theta}_4 &= j_2\dot{\theta}_2 \\ \dot{\theta}_5 &= j_{23}\dot{\theta}_2 + j_{24}\dot{\theta}_3 + j_{25}\dot{\theta}_9 + j_{26}\dot{\theta}_{spr2} \\ &= (j_{23}+j_{24}j_1)\dot{\theta}_2 + j_{25}\dot{\theta}_9 + j_{26}\dot{\theta}_{spr2} \\ \dot{\theta}_{81} &= j_{27}\dot{\theta}_2 + j_{28}\dot{\theta}_3 + j_{29}\dot{\theta}_9 + j_{30}\dot{\theta}_{spr2} \\ &= (j_{27}+j_{28}j_1)\dot{\theta}_2 + j_{29}\dot{\theta}_9 + j_{30}\dot{\theta}_{spr2} \\ \dot{\theta}_6 &= j_3\dot{\theta}_4 + j_4\dot{\theta}_5 \\ &= [j_3j_2 + j_4(j_{23}+j_{24}j_1)]\dot{\theta}_2 + (j_4j_{25})\dot{\theta}_9 + (j_4j_{26})\dot{\theta}_{spr2} \\ \dot{\theta}_7 &= j_5\dot{\theta}_4 + j_6\dot{\theta}_5 \\ &= [j_5j_2 + j_6(j_{23}+j_{24}j_1)]\dot{\theta}_2 + (j_6j_{25})\dot{\theta}_9 + (j_6j_{26})\dot{\theta}_{spr2} \end{aligned} \tag{3.162}$$

Then, for the third version, the derivation is expressed as follows:

$$\begin{bmatrix} \dot{\theta}_{31} \\ \dot{\theta}_4 \end{bmatrix} = \begin{bmatrix} j_{31} & j_{32} \\ j_{33} & j_{34} \end{bmatrix} \begin{bmatrix} \dot{\theta}_2 \\ \dot{\theta}_{spr3} \end{bmatrix} \tag{3.163}$$

and

$$\begin{bmatrix} \dot{\theta}_5 \\ \dot{\theta}_8 \end{bmatrix} = \begin{bmatrix} j_{35} & j_{36} & j_{37} & j_{38} \\ j_{39} & j_{40} & j_{41} & j_{42} \end{bmatrix} \begin{bmatrix} \dot{\theta}_2 \\ \dot{\theta}_{31} \\ \dot{\theta}_9 \\ \dot{\theta}_{spr3} \end{bmatrix} \tag{3.164}$$

where

$$\begin{bmatrix} j_{31} & j_{32} \\ j_{33} & j_{34} \end{bmatrix} = \begin{bmatrix} +a_{31}\sin\theta_{31} & -(a_{42}\sin\theta_4 + a_{41}\cos\theta_4) \\ -a_{31}\cos\theta_{31} & +(a_{42}\cos\theta_4 - a_{41}\sin\theta_4) \end{bmatrix}^{-1} \begin{bmatrix} -a_2\sin\theta_2 & -a_{32}\sin(\theta_{31}+\theta_{spr3}) \\ +a_2\cos\theta_2 & +a_{32}\cos(\theta_{31}+\theta_{spr3}) \end{bmatrix}$$

and

$$\begin{bmatrix} j_{35} & j_{36} & j_{37} & j_{38} \\ j_{39} & j_{40} & j_{41} & j_{42} \end{bmatrix} = \begin{bmatrix} +a_{51}\sin(\theta_5+\beta_2) & -a_8\sin\theta_8 \\ -a_{51}\cos(\theta_5+\beta_2) & +a_8\cos\theta_8 \end{bmatrix}^{-1} \begin{bmatrix} -a_2\sin\theta_2 & -a_{31}\sin\theta_{31} + a_{32}\sin(\theta_{31}+\theta_{spr3}) & +a_9\sin\theta_9 & +a_{32}\sin(\theta_{31}+\theta_{spr3}) \\ +a_2\cos\theta_2 & +a_{31}\cos\theta_{31} - a_{32}\cos(\theta_{31}+\theta_{spr3}) & -a_9\cos\theta_9 & -a_{32}\cos(\theta_{31}+\theta_{spr3}) \end{bmatrix}$$

The following equations can be derived for future calculations from Equations 3.163, 3.164 and 3.58.

$$\begin{aligned} \dot{\theta}_{31} &= j_{31}\dot{\theta}_2 + j_{32}\dot{\theta}_{spr3} \\ \dot{\theta}_4 &= j_{33}\dot{\theta}_2 + j_{34}\dot{\theta}_{spr3} \\ \dot{\theta}_5 &= j_{35}\dot{\theta}_2 + j_{36}\dot{\theta}_{31} + j_{37}\dot{\theta}_9 + j_{38}\dot{\theta}_{spr3} \\ &= (j_{35} + j_{36}j_{31})\dot{\theta}_2 + j_{37}\dot{\theta}_9 + j_{38}\dot{\theta}_{spr3} \\ \dot{\theta}_8 &= j_{39}\dot{\theta}_2 + j_{40}\dot{\theta}_{31} + j_{41}\dot{\theta}_9 + j_{42}\dot{\theta}_{spr3} \\ &= (j_{39} + j_{40}j_{31})\dot{\theta}_2 + j_{41}\dot{\theta}_9 + j_{42}\dot{\theta}_{spr3} \\ \dot{\theta}_6 &= j_3\dot{\theta}_4 + j_4\dot{\theta}_5 \\ &= [j_3j_{33} + (j_4)(j_{35} + j_{36}j_{31})]\dot{\theta}_2 + (j_4j_{37})\dot{\theta}_9 + (j_3j_{34} + j_4j_{38})\dot{\theta}_{spr3} \\ \dot{\theta}_7 &= j_5\dot{\theta}_4 + j_6\dot{\theta}_5 \\ &= [j_5j_{33} + (j_6)(j_{35} + j_{36}j_{31})]\dot{\theta}_2 + (j_6j_{37})\dot{\theta}_9 + (j_5j_{34} + j_6j_{38})\dot{\theta}_{spr3} \end{aligned} \tag{3.165}$$

The above equation can be simplified by redefining Equation 3.164 as follows:

$$\begin{bmatrix} \dot{\theta}_5 \\ \dot{\theta}_8 \end{bmatrix} = \begin{bmatrix} j_{51} & j_{52} \\ j_{53} & j_{54} \end{bmatrix} \begin{bmatrix} \dot{\theta}_4 \\ \dot{\theta}_9 \end{bmatrix} \tag{3.166}$$

$$\begin{bmatrix} j_{51} & j_{52} \\ j_{53} & j_{54} \end{bmatrix} = \begin{bmatrix} +a_{51}\sin(\theta_5+\beta_2) & -a_8\sin\theta_8 \\ -a_{51}\cos(\theta_5+\beta_2) & +a_8\cos\theta_8 \end{bmatrix}^{-1} \begin{bmatrix} -(a_{42}\sin\theta_4 + a_{41}\sin(\theta_4+\frac{\pi}{2})) & +a_9\sin\theta_9 \\ +(a_{42}\cos\theta_4 + a_{41}\cos(\theta_4+\frac{\pi}{2})) & -a_9\cos\theta_9 \end{bmatrix}$$

Then, the following set of solutions are obtained as follows:

$$
\begin{aligned}
\dot{\theta}_{31} &= j_{31}\dot{\theta}_2 + j_{32}\dot{\theta}_{spr3} \\
\dot{\theta}_4 &= j_{33}\dot{\theta}_2 + j_{34}\dot{\theta}_{spr3} \\
\dot{\theta}_5 &= j_{51}\dot{\theta}_4 + j_{52}\dot{\theta}_9 \\
&= (j_{51}j_{33})\dot{\theta}_2 + j_{52}\dot{\theta}_9 + (j_{51}j_{34})\dot{\theta}_{spr3} \\
\dot{\theta}_8 &= j_{53}\dot{\theta}_4 + j_{54}\dot{\theta}_9 \\
&= (j_{53}j_{33})\dot{\theta}_2 + j_{54}\dot{\theta}_9 + (j_{53}j_{34})\dot{\theta}_{spr3} \\
\dot{\theta}_6 &= j_3\dot{\theta}_4 + j_4\dot{\theta}_5 \\
&= [j_3j_{33} + (j_4)(j_{51}j_{33})]\dot{\theta}_2 + (j_4j_{52})\dot{\theta}_9 + (j_3j_{34} + j_4(j_{51}j_{34}))\dot{\theta}_{spr3} \\
\dot{\theta}_7 &= j_5\dot{\theta}_4 + j_6\dot{\theta}_5 \\
&= [j_5j_{33} + (j_6)(j_{51}j_{33})]\dot{\theta}_2 + (j_6j_{52})\dot{\theta}_9 + (j_5j_{34} + j_6(j_{51}j_{34}))\dot{\theta}_{spr3}
\end{aligned}
\tag{3.167}
$$

Finally, for the last version, the derivation is expressed as follows:

$$
\begin{bmatrix} \dot{\theta}_5 \\ \dot{\theta}_8 \end{bmatrix} = \begin{bmatrix} j_{43} & j_{44} & j_{45} & j_{46} \\ j_{47} & j_{48} & j_{49} & j_{50} \end{bmatrix} \begin{bmatrix} \dot{\theta}_2 \\ \dot{\theta}_3 \\ \dot{\theta}_9 \\ \dot{\theta}_{spr4} \end{bmatrix} \tag{3.168}
$$

where

$$
\begin{bmatrix} j_{43} & j_{44} & j_{45} & j_{46} \\ j_{47} & j_{48} & j_{49} & j_{50} \end{bmatrix} = \begin{bmatrix} +a_{51}\sin(\theta_5 + \theta_{spr4}) & -a_8\sin\theta_8 \\ -a_{51}\cos(\theta_5 + \theta_{spr4}) & +a_8\cos\theta_8 \end{bmatrix}^{-1} \begin{bmatrix} -a_2\sin\theta_2 & -a_3\sin\theta_3 & +a_9\sin\theta_9 & -a_{51}\sin(\theta_5 + \theta_{spr4}) \\ +a_2\cos\theta_2 & +a_3\cos\theta_3 & -a_9\cos\theta_9 & +a_{51}\cos(\theta_5 + \theta_{spr4}) \end{bmatrix}
$$

The following equations can be derived for future calculations from Equations 3.56, 3.168, and 3.58.

$$
\begin{aligned}
\dot{\theta}_3 &= j_1\dot{\theta}_2 \\
\dot{\theta}_4 &= j_2\dot{\theta}_2 \\
\dot{\theta}_5 &= j_{43}\dot{\theta}_2 + j_{44}\dot{\theta}_3 + j_{45}\dot{\theta}_9 + j_{46}\dot{\theta}_{spr4} \\
&= (j_{43} + j_{44}j_1)\dot{\theta}_2 + j_{45}\dot{\theta}_9 + j_{46}\dot{\theta}_{spr4} \\
\dot{\theta}_8 &= j_{47}\dot{\theta}_2 + j_{48}\dot{\theta}_3 + j_{49}\dot{\theta}_9 + j_{50}\dot{\theta}_{spr4} \\
&= (j_{47} + j_{48}j_1)\dot{\theta}_2 + j_{49}\dot{\theta}_9 + j_{50}\dot{\theta}_{spr4} \\
\dot{\theta}_6 &= j_3\dot{\theta}_4 + j_4\dot{\theta}_5 \\
&= [j_3j_2 + j_4(j_{43} + j_{44}j_1)]\dot{\theta}_2 + (j_4j_{45})\dot{\theta}_9 + (j_4j_{46})\dot{\theta}_{spr4} \\
\dot{\theta}_7 &= j_5\dot{\theta}_4 + j_6\dot{\theta}_5 \\
&= [j_5j_2 + j_6(j_{43} + j_{44}j_1)]\dot{\theta}_2 + (j_6j_{45})\dot{\theta}_9 + (j_6j_{46})\dot{\theta}_{spr4}
\end{aligned}
\tag{3.169}
$$

3.3.3.3 Jacobian Matrix

The end-effector position in matrix form was defined in Equation 3.63 as follows:

$$
V_{F_0} = \begin{bmatrix} -2a_{42}\sin\theta_4 & -2a_{72}\sin\theta_7 \\ +2a_{42}\cos\theta_4 & +2a_{72}\cos\theta_7 \end{bmatrix} \begin{bmatrix} \dot{\theta}_4 \\ \dot{\theta}_7 \end{bmatrix} \tag{3.170}
$$

From Equations 3.160, 3.162, 3.165 and 3.169; calculation of Jacobian matrices for each version are derived as follows:

Version 1

From Equation 3.160;

$$
\begin{bmatrix} \dot{\theta}_4 \\ \dot{\theta}_7 \end{bmatrix} = \begin{bmatrix} j_2 & 0 & 0 \\ j_{20}j_2 + j_{21}(j_7 + j_8j_1) & (j_{21}j_9) & j_{22} \end{bmatrix} \begin{bmatrix} \dot{\theta}_2 \\ \dot{\theta}_9 \\ \dot{\theta}_{spr1} \end{bmatrix} \tag{3.171}
$$

Then the velocity of the end effector can be written as follows:

$$
V_{F_0} = \begin{bmatrix} -2a_{42}\sin\theta_4 & -2a_{72}\sin\theta_7 \\ +2a_{42}\cos\theta_4 & +2a_{72}\cos\theta_7 \end{bmatrix} \begin{bmatrix} j_2 & 0 & 0 \\ j_{20}j_2 + j_{21}(j_7 + j_8j_1) & (j_{21}j_9) & j_{22} \end{bmatrix} \begin{bmatrix} \dot{\theta}_2 \\ \dot{\theta}_9 \\ \dot{\theta}_{spr1} \end{bmatrix} \tag{3.172}
$$

Then, the Jacobian matrix is written below:

$$J_1 = \begin{bmatrix} -2a_{42}\sin\theta_4 & -2a_{72}\sin\theta_7 \\ +2a_{42}\cos\theta_4 & +2a_{72}\cos\theta_7 \end{bmatrix} \begin{bmatrix} j_2 & 0 & 0 \\ j_{20}j_2 + j_{21}(j_7 + j_8 j_1) & (j_{21}j_9) & j_{22} \end{bmatrix} \tag{3.173}$$

Version 2

From Equation 3.162;

$$\begin{bmatrix} \dot{\theta}_4 \\ \dot{\theta}_7 \end{bmatrix} = \begin{bmatrix} j_2 & 0 & 0 \\ j_5 j_2 + j_6(j_{23} + j_{24}j_1) & (j_6 j_{25}) & (j_6 j_{26}) \end{bmatrix} \begin{bmatrix} \dot{\theta}_2 \\ \dot{\theta}_9 \\ \dot{\theta}_{spr2} \end{bmatrix} \tag{3.174}$$

Then the velocity of the end effector can be written as follows:

$$V_{F_0} = \begin{bmatrix} -2a_{42}\sin\theta_4 & -2a_{72}\sin\theta_7 \\ +2a_{42}\cos\theta_4 & +2a_{72}\cos\theta_7 \end{bmatrix} \begin{bmatrix} j_2 & 0 & 0 \\ j_5 j_2 + j_6(j_{23} + j_{24}j_1) & (j_6 j_{25}) & (j_6 j_{26}) \end{bmatrix} \begin{bmatrix} \dot{\theta}_2 \\ \dot{\theta}_9 \\ \dot{\theta}_{spr2} \end{bmatrix} \tag{3.175}$$

Then, the Jacobian matrix is written below:

$$J_2 = \begin{bmatrix} -2a_{42}\sin\theta_4 & -2a_{72}\sin\theta_7 \\ +2a_{42}\cos\theta_4 & +2a_{72}\cos\theta_7 \end{bmatrix} \begin{bmatrix} j_2 & 0 & 0 \\ j_5 j_2 + j_6(j_{23} + j_{24}j_1) & (j_6 j_{25}) & (j_6 j_{26}) \end{bmatrix} \tag{3.176}$$

Version 3

From Equation 3.167;

$$\begin{bmatrix} \dot{\theta}_4 \\ \dot{\theta}_7 \end{bmatrix} = \begin{bmatrix} j_{33} & 0 & j_{34} \\ j_5 j_{33} + (j_6)(j_{51}j_{33}) & (j_6 j_{52}) & (j_5 j_{34} + j_6 j_{51} j_{34}) \end{bmatrix} \begin{bmatrix} \dot{\theta}_2 \\ \dot{\theta}_9 \\ \dot{\theta}_{spr3} \end{bmatrix} \tag{3.177}$$

Then the velocity of the end effector can be written as follows:

$$V_{F_0} = \begin{bmatrix} -2a_{42}\sin\theta_4 & -2a_{72}\sin\theta_7 \\ +2a_{42}\cos\theta_4 & +2a_{72}\cos\theta_7 \end{bmatrix} \begin{bmatrix} j_{33} & 0 & j_{34} \\ j_5 j_{33} + (j_6)(j_{51} j_{33}) & (j_6 j_{52}) & (j_5 j_{34} + j_6 j_{51} j_{34}) \end{bmatrix} \begin{bmatrix} \dot{\theta}_2 \\ \dot{\theta}_9 \\ \dot{\theta}_{spr3} \end{bmatrix} \tag{3.178}$$

Then, the Jacobian matrix is written below:

$$J_3 = \begin{bmatrix} -2a_{42}\sin\theta_4 & -2a_{72}\sin\theta_7 \\ +2a_{42}\cos\theta_4 & +2a_{72}\cos\theta_7 \end{bmatrix} \begin{bmatrix} j_{33} & 0 & j_{34} \\ j_5 j_{33} + (j_6)(j_{51} j_{33}) & (j_6 j_{52}) & (j_5 j_{34} + j_6 j_{51} j_{34}) \end{bmatrix} \tag{3.179}$$

Version 4

From Equation 3.169;

$$\begin{bmatrix} \dot{\theta}_4 \\ \dot{\theta}_7 \end{bmatrix} = \begin{bmatrix} j_2 & 0 & 0 \\ j_5 j_2 + j_6(j_{43} + j_{44} j_1) & (j_6 j_{45}) & (j_6 j_{46}) \end{bmatrix} \begin{bmatrix} \dot{\theta}_2 \\ \dot{\theta}_9 \\ \dot{\theta}_{spr4} \end{bmatrix} \tag{3.180}$$

Then the velocity of the end effector can be written as follows:

$$V_{F_0} = \begin{bmatrix} -2a_{42}\sin\theta_4 & -2a_{72}\sin\theta_7 \\ +2a_{42}\cos\theta_4 & +2a_{72}\cos\theta_7 \end{bmatrix} \begin{bmatrix} j_2 & 0 & 0 \\ j_5 j_2 + j_6(j_{43} + j_{44} j_1) & (j_6 j_{45}) & (j_6 j_{46}) \end{bmatrix} \begin{bmatrix} \dot{\theta}_2 \\ \dot{\theta}_9 \\ \dot{\theta}_{spr4} \end{bmatrix} \tag{3.181}$$

Then, the Jacobian matrix is written below:

$$J_4 = \begin{bmatrix} -2a_{42}\sin\theta_4 & -2a_{72}\sin\theta_7 \\ +2a_{42}\cos\theta_4 & +2a_{72}\cos\theta_7 \end{bmatrix} \begin{bmatrix} j_2 & 0 & 0 \\ j_5 j_2 + j_6(j_{43} + j_{44} j_1) & (j_6 j_{45}) & (j_6 j_{46}) \end{bmatrix} \tag{3.182}$$

3.3.3.4 Force Analysis

By the Virtual Theorem method the following equation can be written:

$$\begin{aligned} &\textit{for} \quad i = 1, 2, 3, 4 \quad \textit{(Each version)} \\ &\delta W_i = \delta W_{A_0} + \delta W_{H_0} + \delta W_{MCP} + \delta W_{PIP} + \delta W_{F_{F0}} + \delta W_{T_{spr,i}} = 0 \end{aligned} \tag{3.183}$$

where δW_{A_0}, δW_{H_0}, δW_{MCP}, δW_{PIP} and $\delta W_{F_{F0}}$ are defined in fully-actuated mechanism. $\delta W_{T_{spr,i}}$ can be defined as follows for each under-actuated mechanism version:

$$\delta W_{T_{spr,i}} = T_{spr,i}\ \delta\theta_{spr,i} \tag{3.184}$$

where

$$T_{spr,i} = -K_i(\theta_{spr} - \theta_{spr,i_{free}})$$

In the above Equation 3.183 the variables are defined as follows:

- T_{A0}: The torque value applied by the motor at point A_0.
- T_{H0}: The torque value applied by the motor at point H_0.
- T_{MCP}: The torque value applied by the finger joint MCP at point B_0.
- T_{PIP}: The torque value applied by the finger joint PIP at point E_0.
- F_{F0}: A force acting on the end-effector at point F_0.
- $T_{spr,i}$: The torque acting by the spring on the point J, K, L and B for each version, sequentially.

With the addition of $\delta W_{T_{spr,i}}$ in the Virtual Work theorem, the equation becomes as follow:

$$\begin{aligned} \delta W_i = &T_{A0}\ \delta\theta_2 + T_{H0}\ \delta\theta_9 \\ &+ [T_{MCP} + 2|F_{F_0}|a42\cos(\theta_4 - \theta_7)]\delta\theta_4 \\ &+ [T_{PIP} + 2|F_{F_0}|a72]\delta\theta_7] + T_{spr,i}\ \delta\theta_{spr,i} = 0 \end{aligned} \tag{3.185}$$

In order to define $\delta\theta_4$ and $\delta\theta_7$ in terms of $\delta\theta_2$, $\delta\theta_9$ and $\delta\theta_{spr,i}$ the Equations 3.160, 3.162, 3.165 and 3.169 can be used. Then, the Equation 3.185 becomes for each version as follows:

Version 1

$$\begin{aligned}\delta W_1 =& T_{A0}\,\delta\theta_2 + T_{H0}\,\delta\theta_9 \\ &+ [T_{MCP} + 2|F_{F_0}|a42\cos(\theta_4 - \theta_7)](j_2)\delta\theta_2 \\ &+ [T_{PIP} + 2|F_{F_0}|a72][[j_{20}j_2 + j_{21}(j_7 + j_8 j_1)]\dot{\theta}_2 + (j_{21}j_9)\dot{\theta}_9 + j_{22}\dot{\theta}_{spr1}] \\ &+ T_{spr1}\delta\theta_{spr1} = 0\end{aligned} \tag{3.186}$$

Then, from Equation 3.186, three scalar equalities are obtained as follows:

$$\begin{aligned}&T_{A0} + [T_{MCP} + 2|F_{F_0}|a42\cos(\theta_4 - \theta_7)](j_2) \\ &+ [T_{PIP} + 2|F_{F_0}|a72]([j_{20}j_2 + j_{21}(j_7 + j_8 j_1)) = 0\end{aligned} \tag{3.187}$$

,

$$T_{H0} + [T_{PIP} + 2|F_{F_0}|a72](j_{21}j_9) = 0 \tag{3.188}$$

and

$$T_{spr1} + [T_{PIP} + 2|F_{F_0}|a72](j_{22}) = 0 \tag{3.189}$$

The Equations 3.187 and 3.188 can be used to estimate motor torque values in the first version of the under-actuated mechanism. The Equation 3.189 can be used to find θ_{spr1} numerically as follows:

$$-K_1(\theta_{spr1} - \theta_{spr1_{free}}) + (T_{PIP} + 2|F_{F_0}|a72)j_{22} = 0$$

$$\Rightarrow \theta_{spr1} = \frac{(T_{PIP} + 2|F_{F_0}|a72)j_{22}}{K_1} + \theta_{spr1_{free}} \tag{3.190}$$

Version 2

$$\begin{aligned}\delta W_2 =& T_{A0}\,\delta\theta_2 + T_{H0}\,\delta\theta_9 \\ &+ [T_{MCP} + 2|F_{F_0}|a42\cos(\theta_4 - \theta_7)](j_2)\delta\theta_2 \\ &+ [T_{PIP} + 2|F_{F_0}|a72][[j_5 j_2 + j_6(j_{23} + j_{24}j_1)]\dot{\theta}_2 + (j_6 j_{25})\dot{\theta}_9 + (j_6 j_{26})\dot{\theta}_{spr2}] \\ &+ T_{spr2}\delta\theta_{spr2} = 0\end{aligned} \tag{3.191}$$

Then, from Equation 3.191, three scalar equalities are obtained as follows:

$$\begin{aligned} &T_{A0} + [T_{MCP} + 2|F_{F_0}|a42\cos(\theta_4 - \theta_7)](j_2) \\ &+ [T_{PIP} + 2|F_{F_0}|a72]([j_5 j_2 + j_6(j_{23} + j_{24} j_1)) = 0 \end{aligned} \tag{3.192}$$

,

$$T_{H0} + [T_{PIP} + 2|F_{F_0}|a72](j_6 j_{25}) = 0 \tag{3.193}$$

and

$$T_{spr2} + [T_{PIP} + 2|F_{F_0}|a72](j_6 j_{26}) = 0 \tag{3.194}$$

The Equations 3.192 and 3.193 can be used to estimate motor torque values in the second version of the under-actuated mechanism. The Equation 3.194 can be used to find θ_{spr2} numerically as follows:

$$-K_2(\theta_{spr2} - \theta_{spr2_{free}}) + (T_{PIP} + 2|F_{F_0}|a72)(j_6 j_{26}) = 0$$

$$\Rightarrow \theta_{spr2} = \frac{(T_{PIP} + 2|F_{F_0}|a72)(j_6 j_{26})}{K_2} + \theta_{spr2_{free}} \tag{3.195}$$

Version 3

$$\begin{aligned} \delta W_3 =& T_{A0}\,\delta\theta_2 + T_{H0}\,\delta\theta_9 \\ &+ [T_{MCP} + 2|F_{F_0}|a42\cos(\theta_4 - \theta_7)](j_{33}\delta\theta_2 + j_{34}\delta\theta_{spr3}) \\ &+ [T_{PIP} + 2|F_{F_0}|a72] \\ &\quad [[j_5 j_{33} + (j_6)(j_{51} j_{33})]\delta\theta_2 + (j_6 j_{52})\delta\theta_9 + (j_5 j_{34} + j_6(j_{51} j_{34}))\delta\theta_{spr3}] \\ &+ T_{spr3}\delta\theta_{spr3} = 0 \end{aligned} \tag{3.196}$$

Then, from Equation 3.196, three scalar equalities are obtained as follows:

$$\begin{aligned} &T_{A0} + [T_{MCP} + 2|F_{F_0}|a42\cos(\theta_4 - \theta_7)](j_{33}) \\ &+ [T_{PIP} + 2|F_{F_0}|a72][j_5 j_{33} + (j_6)(j_{51} j_{33})] = 0 \end{aligned} \tag{3.197}$$

,

$$T_{H0} + [T_{PIP} + 2|F_{F_0}|a72](j_6 j_{52}) = 0 \tag{3.198}$$

and

$$\begin{aligned} T_{spr3} + [T_{MCP} + 2|F_{F_0}|a42\cos(\theta_4 - \theta_7)](j_{34}) \\ + [T_{PIP} + 2|F_{F_0}|a72](j_5 j_{34} + j_6(j_{51} j_{34})) = 0 \end{aligned} \tag{3.199}$$

The Equations 3.197 and 3.198 can be used to estimate motor torque values in the third version of the under-actuated mechanism. The Equation 3.199 can be used to find θ_{spr3} numerically as follows:

$$\begin{aligned} -K_3(\theta_{spr3} - \theta_{spr3_{free}}) + [T_{MCP} + 2|F_{F_0}|a42\cos(\theta_4 - \theta_7)](j_{34}) \\ + [T_{PIP} + 2|F_{F_0}|a72](j_5 j_{34} + j_6(j_{51} j_{34})) = 0 \end{aligned}$$

$$\begin{aligned} \Rightarrow \theta_{spr3} = & \frac{[T_{MCP} + 2|F_{F_0}|a42\cos(\theta_4 - \theta_7)](j_{34})}{K_3} \\ & + \frac{[T_{PIP} + 2|F_{F_0}|a72](j_5 j_{34} + j_6(j_{51} j_{34}))}{K_3} \\ & + \theta_{spr3_{free}} \end{aligned} \tag{3.200}$$

Version 4

$$\begin{aligned} \delta W_4 = & T_{A0}\,\delta\theta_2 + T_{H0}\,\delta\theta_9 \\ & + [T_{MCP} + 2|F_{F_0}|a42\cos(\theta_4 - \theta_7)](j_2)\delta\theta_2 \\ & + [T_{PIP} + 2|F_{F_0}|a72][[j_5 j_2 + j_6(j_{43} + j_{44} j_1)]\dot{\theta}_2 + (j_6 j_{45})\dot{\theta}_9 + (j_6 j_{46})\dot{\theta}_{spr4}] \\ & + T_{spr4}\delta\theta_{spr4} = 0 \end{aligned} \tag{3.201}$$

Then, from Equation 3.201, three scalar equalities are obtained as follows:

$$\begin{aligned} T_{A0} + [T_{MCP} + 2|F_{F_0}|a42\cos(\theta_4 - \theta_7)](j_2) \\ + [T_{PIP} + 2|F_{F_0}|a72]([j_5 j_2 + j_6(j_{43} + j_{44} j_1)) = 0 \end{aligned} \tag{3.202}$$

,

$$T_{H0} + [T_{PIP} + 2|F_{F_0}|a72](j_6 j_{45}) = 0 \tag{3.203}$$

and

$$T_{spr4} + [T_{PIP} + 2|F_{F_0}|a72](j_6 j_{46}) = 0 \tag{3.204}$$

The Equations 3.202 and 3.203 can be used to estimate motor torque values in the fourth version of the under-actuated mechanism. The Equation 3.204 can be used to find θ_{spr4} numerically as follows:

$$-K_4(\theta_{spr4} - \theta_{spr4_{free}}) + (T_{PIP} + 2|F_{F_0}|a72)(j_6 j_{46}) = 0$$

$$\Rightarrow \theta_{spr4} = \frac{(T_{PIP} + 2|F_{F_0}|a72)(j_6 j_{46})}{K_4} + \theta_{spr4_{free}} \tag{3.205}$$

Note that right sides of the Equations 3.190, 3.195, 3.200 and 3.205 are the functions of $\theta_{spr,i}$. So, the solutions of the Equations 3.190, 3.195, 3.200 and 3.205 give the $\theta_{spr,i}$ values numerically. After a $\theta_{spr,i}$ value is found numerically, the whole procedure can be applied once again to find all the results numerically.

After finding θ_{spr} numerically, the system solution becomes just like in the fully-actuated one.

CHAPTER 4

GENETIC ALGORITHM RESULTS

In this chapter, there are 3 sections. Firstly, a fully-actuated mechanism optimization is carried out. Secondly, a methodology is invented for the under-actuated mechanism synthesis by solving a symbolical equation. For this purpose, the most straightforward possible problem is defined which is a transition problem from 4 bar to 5 bar mechanism. Finally, under-actuated mechanisms are optimized using the proposed method. There are 4 versions in the under-actuated mechanism family. Each version is conducted and a selection is performed between those alternatives.

The GII value is desired to be maximized for each state in the task space. The optimization algorithm worked for minimizing, thus the fitness function is defined as "1-GII", where the best solution is GII being equal to 1, gives the result of 0. Therefore, the algorithm is used to find the value of 0, where the GII is the value of 1. In the algorithm, finger segment length and fingertip positions (task space) are used as inputs which are shown in the Tables 3.2 and 3.4, respectively.

4.1 Fully-Actuated Mechanism

There are four parts in this section. In the first part, a single-optimization problem is conducted without including the sensitivity metric, only mean values of phalanges are used. Then, in the second part, a single-optimization problem including sensitivity is presented which means a set of finger sizes is considered. In the third part, a multi-objective problem is conducted in order to explicit the result obtained in the single-optimization with sensitivity. Finally, a selection is carried out from the alternatives. The lower and upper boundaries for each structure parameter are defined in the Table

4.1.

Table 4.1: Lower and Upper Boundaries of the Design Vector

Parameter	Lower Boundary	Upper Boundary	Unit
a_{11}	15	30	mm
a_{12}	20	45	mm
a_2	20	60	mm
a_3	30	70	mm
a_{41}	15	35	mm
a_G	30	40	mm
a_5	30	70	mm
a_{51}	20	60	mm
a_6	30	70	mm
a_{71}	15	35	mm
a_8	30	70	mm
a_9	20	55	mm
θ_G	0	45	deg
β_2	0	90	deg

4.1.1 Single Objective Optimization - Without Sensitivity

For this purpose, a fixed phalange length value is selected, which is the mean value in Table 3.2. The values are given in the below expression:

$$a_{42} = 40/2 = 20 \quad mm \quad \text{and} \quad a_{72} = 30/2 = 15 \quad mm \tag{4.1}$$

Genetic algorithm search is given in Figure 4.1. There are 300 generations completed with a high population size of 750 samples. An integer searching is implemented in order to speed up the optimization process. The results are given in the Table 4.2.

The mechanism is animated for each state. Only one state is shown in Figure 4.2. The estimated actuator torques, finger joint passive torques, actuator angles(θ_2 and θ_9), and transmission angles are depicted in Figure 4.3.

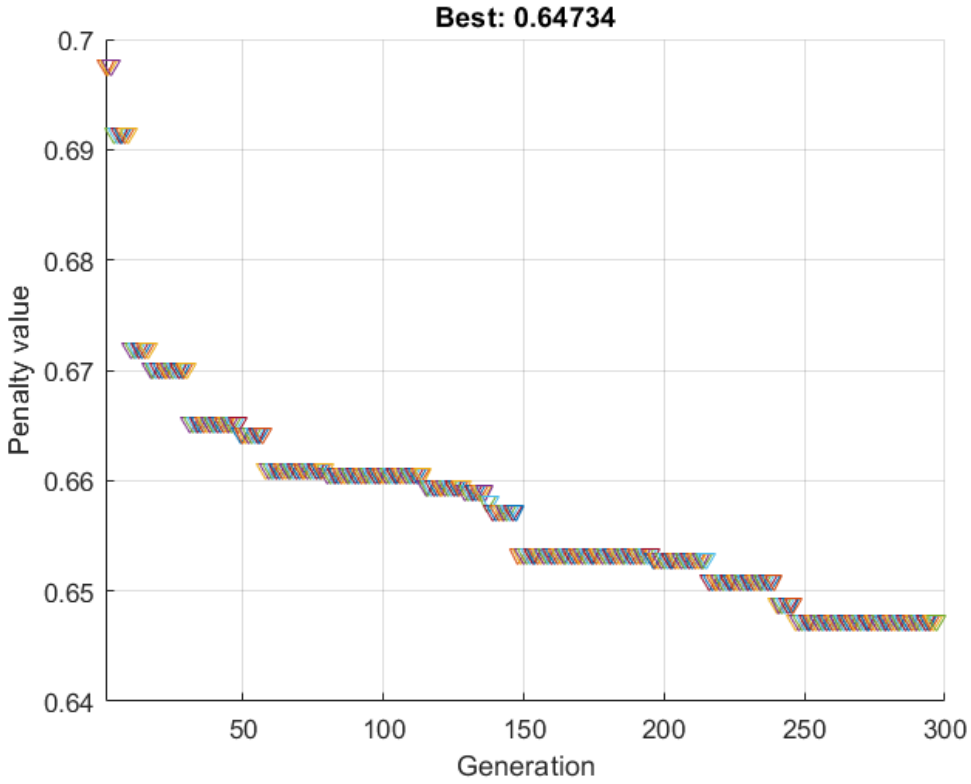

Figure 4.1: Single Optimization GA

Table 4.2: Fully-Actuated, Single-Optimization Without Sensitivity, Structure Parameter Results

Parameter	Result	Unit
a_{11}	15	mm
a_{12}	31	mm
a_2	60	mm
a_3	40	mm
a_{41}	15	mm
a_G	30	mm
a_5	57	mm
a_{51}	51	mm
a_6	32	mm
a_{71}	32	mm
a_8	43	mm
a_9	52	mm
θ_G	31	deg
β_2	36	deg
GII	0.35	-

All of the graphs look within the desired ranges in Figure 4.3. The optimized mechanism is feasible for the given finger sizes. However, a robust mechanism is desired. The mechanism is supposed to be suitable for different phalanges sizes. Unfortunately, when the mechanism is checked if it is convenient for the minimum and maximum finger sizes defined in Table 3.2, it is detected that the mechanism is not applicable since the mechanism is very sensitive to the variation of the phalanges size. Then, it is decided to define another single-objective problem in which the sensitivity is considered.

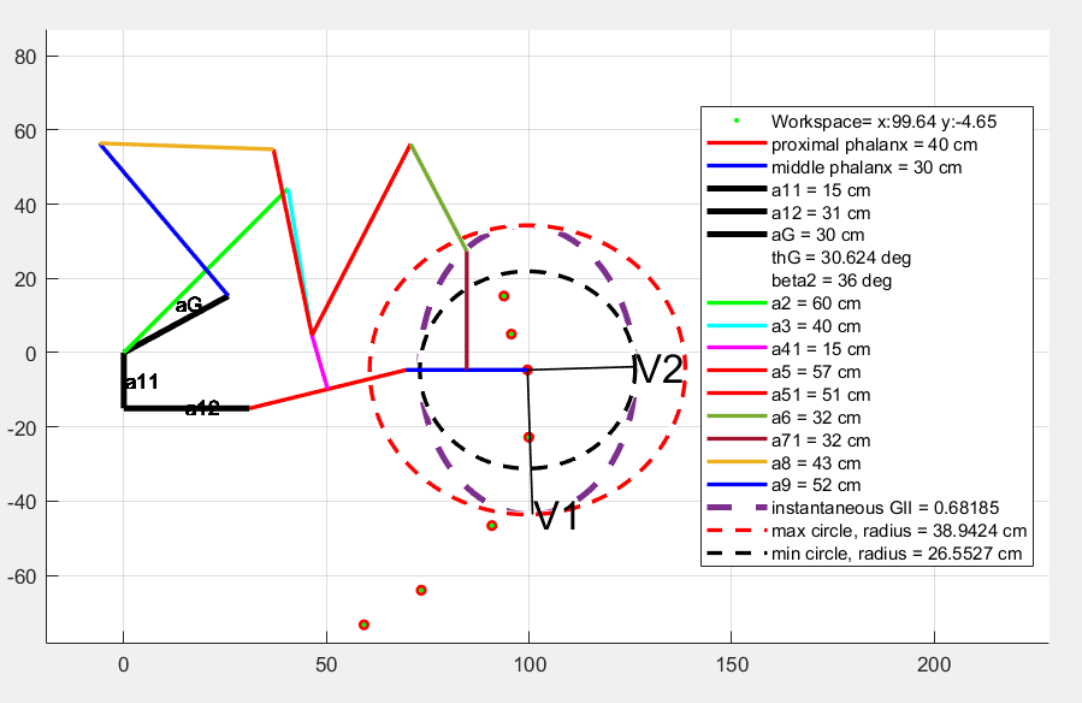

Figure 4.2: Single Optimization Animation - Without Sensitivity

4.1.2 Single Objective Optimization - With Sensitivity

A single-objective fitness function is defined such that 3 different phalanges sizes are considered. All 3 possibilities on the finger size are checked and the worst one from those 3 is wanted to be maximized. The one with the worst GII result is always wanted to be maximized in the design algorithm.

Genetic algorithm search is given in Figure 4.4. There are 300 generations to be completed with a high population size of 750 samples. However, the algorithm finds an optimal result before reaching the generation number of 300. An integer search is implemented in order to speed up the optimization process as in the without sensitivity part. The results are given in Table 4.3.

Even though it looks like the GII value is less than the single-optimization result, the GII value is almost the same when the finger phalange sizes vary. Therefore, the mechanism is not sensitive to phalanges length. The mechanism is animated for each state. Only one state is shown in Figures 4.5 and 4.6.

Table 4.3: Fully-Actuated, Single-Optimization With Sensitivity, Structure Parameter Results

Parameter	Result	Unit
a_{11}	37	mm
a_{12}	39	mm
a_2	46	mm
a_3	56	mm
a_{41}	29	mm
a_G	39	mm
a_5	42	mm
a_{51}	38	mm
a_6	31	mm
a_{71}	35	mm
a_8	46	mm
a_9	55	mm
θ_G	15	deg
β_2	32	deg
GII	0.19	-

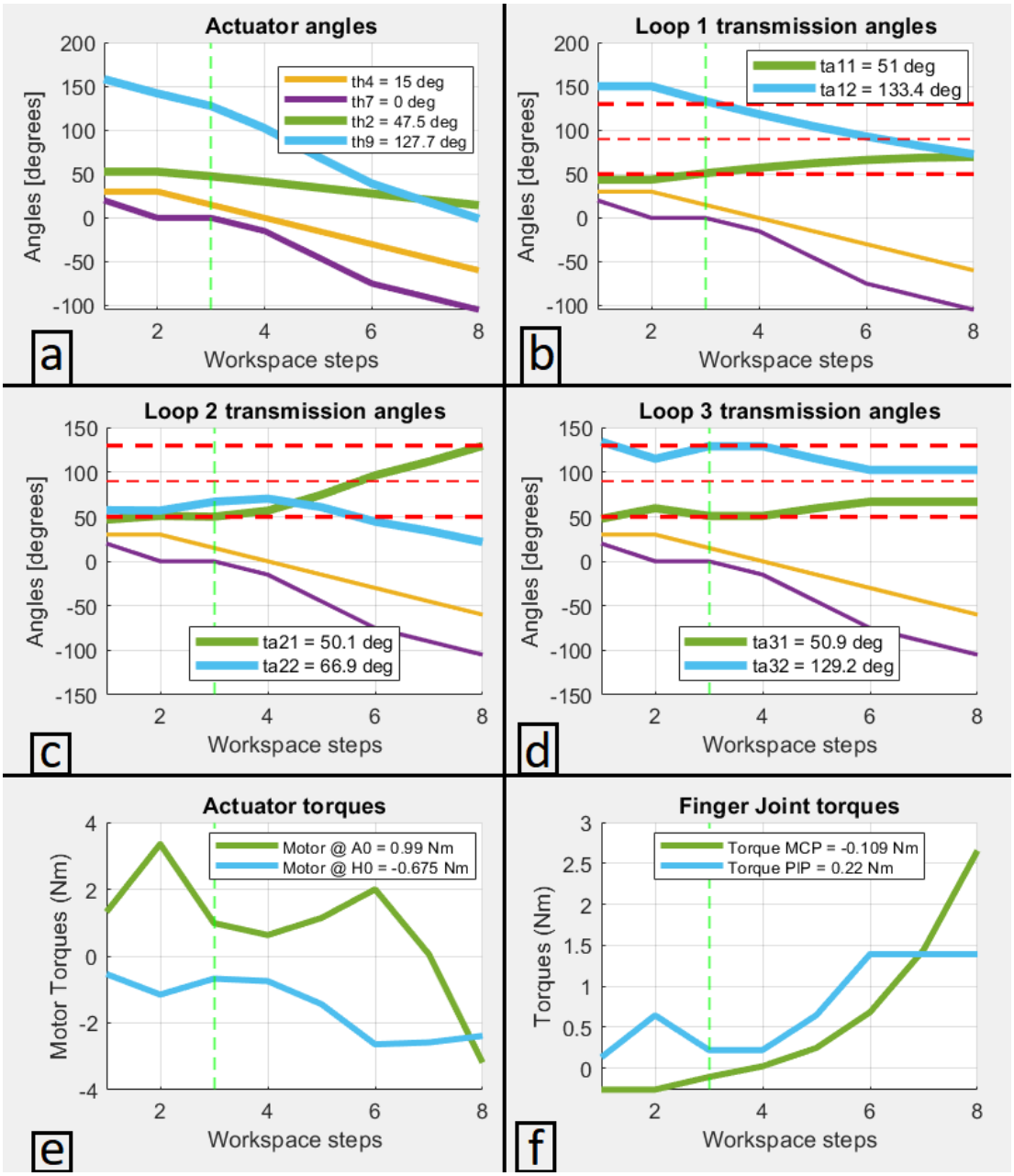

Figure 4.3: Single Optimization Animation - Without Sensitivity, Angles and Torques

Finger angles and motor angles for the 8 states are given in the part a. Forward and backward transmission angles are represented for the each loop in the part b,c and d. The area between the horizontal dashed red lines show the desired transmission angle range in parts b,c and d. In the part e, calculated motor torque values are given for the each state. In the part f, calculated finger joint torque values are shown.

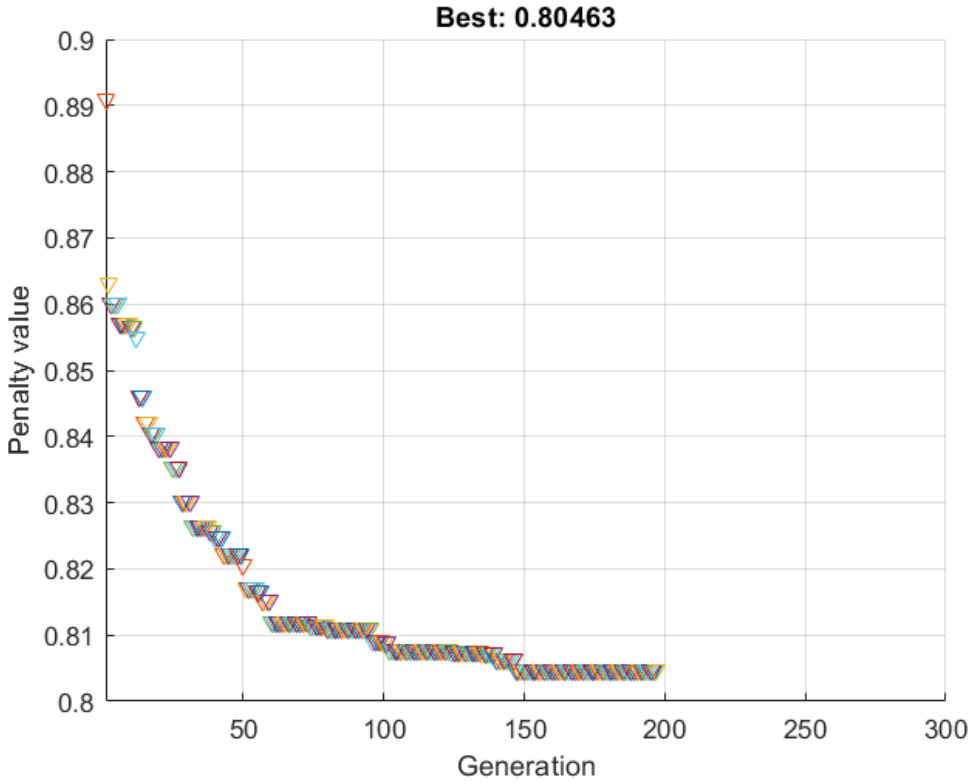

Figure 4.4: Single Optimization GA with Sensitivity

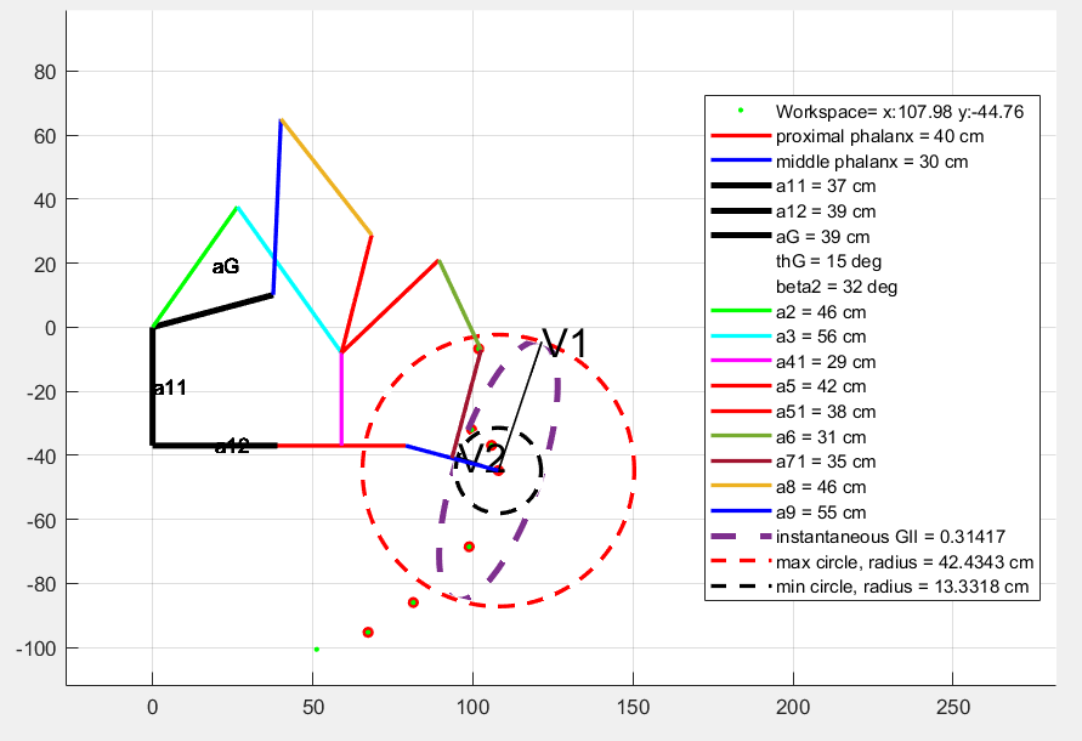

Figure 4.5: Single Optimization Animation - With Sensitivity

The change of the GII value with the variation of phalanges sizes is given in Figure 4.7. A zoomed version of this Figure is given in 4.8. The overall change in the GII is very small with a value of 0.006.

4.1.3 Multi Objective Optimization

A multi-objective fitness function is defined such that the GII value is maximized for 3 different phalanges sizes as in Table 3.2. The upper and lower boundaries of the structure parameters are the same as the single-objective optimization problem as in Table 4.1. The results are given below. An integer search is desired, unfortunately, MATLAB does not allow to use of integer search in multi-objective problems.

The Pareto-front solution is given in Figure 4.9. An optimal solution is selected from the solution set. Selected results are in Table 4.4.

The mechanism is animated for each state. Only one state is shown in Figures 4.10, 4.11.

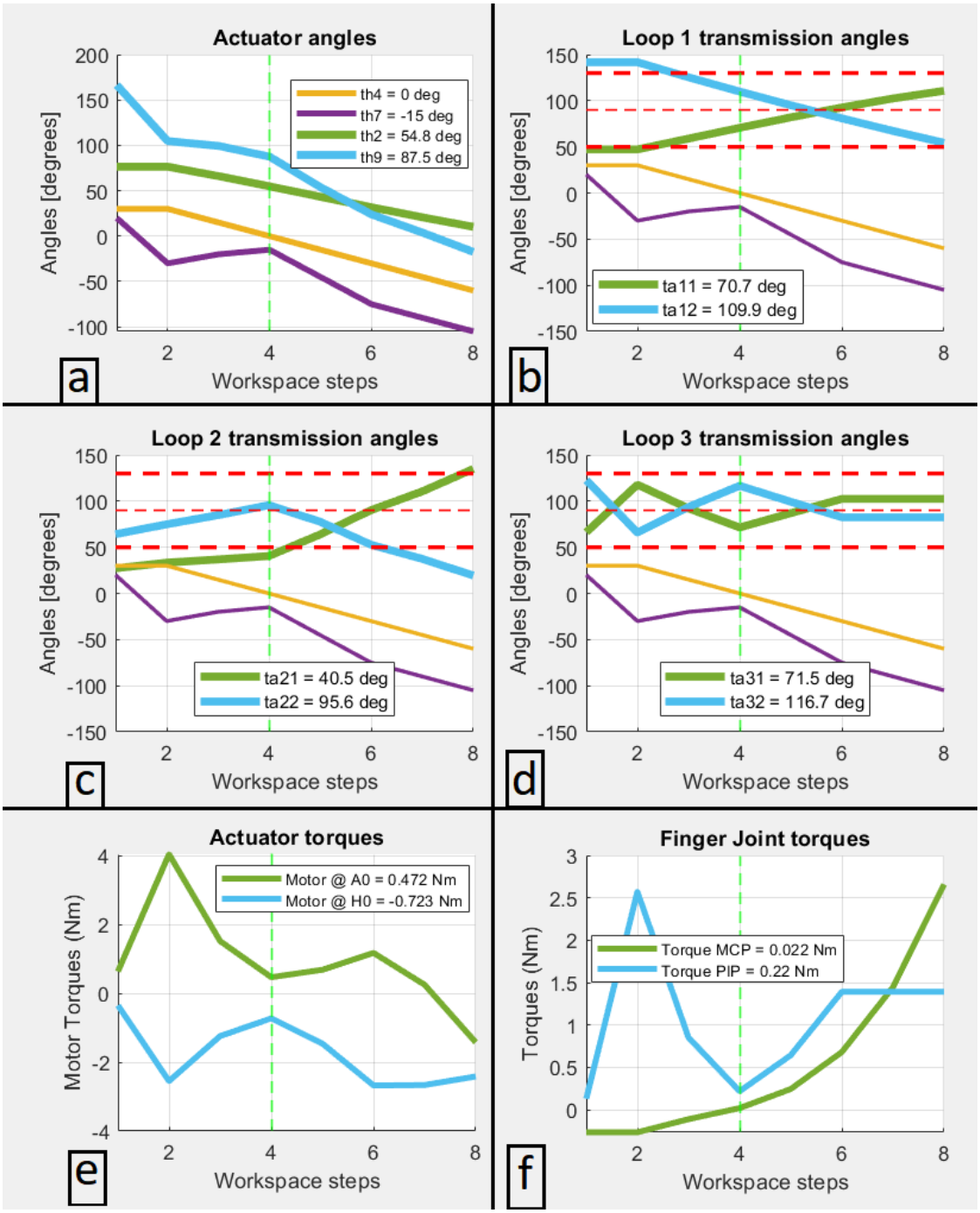

Figure 4.6: Single Optimization Animation - With Sensitivity, Angles and Torques

Finger angles and motor angles for the 8 states are given in the part a. Forward and backward transmission angles are represented for the each loop in the part b,c and d. The area between the horizontal dashed red lines show the desired transmission angle range in parts b,c and d. In the part e, calculated motor torque values are given for the each state. In the part f, calculated finger joint torque values are shown.

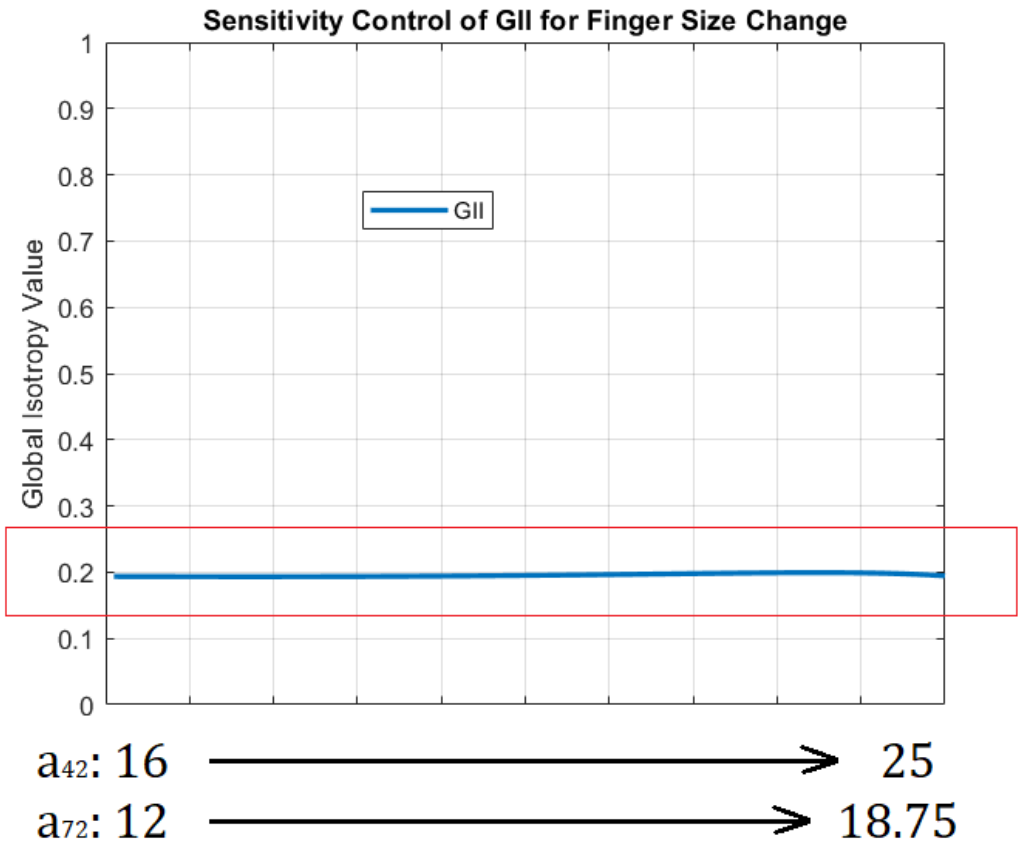

Figure 4.7: Sensitivity Check for phalanges sizes with respect to GII

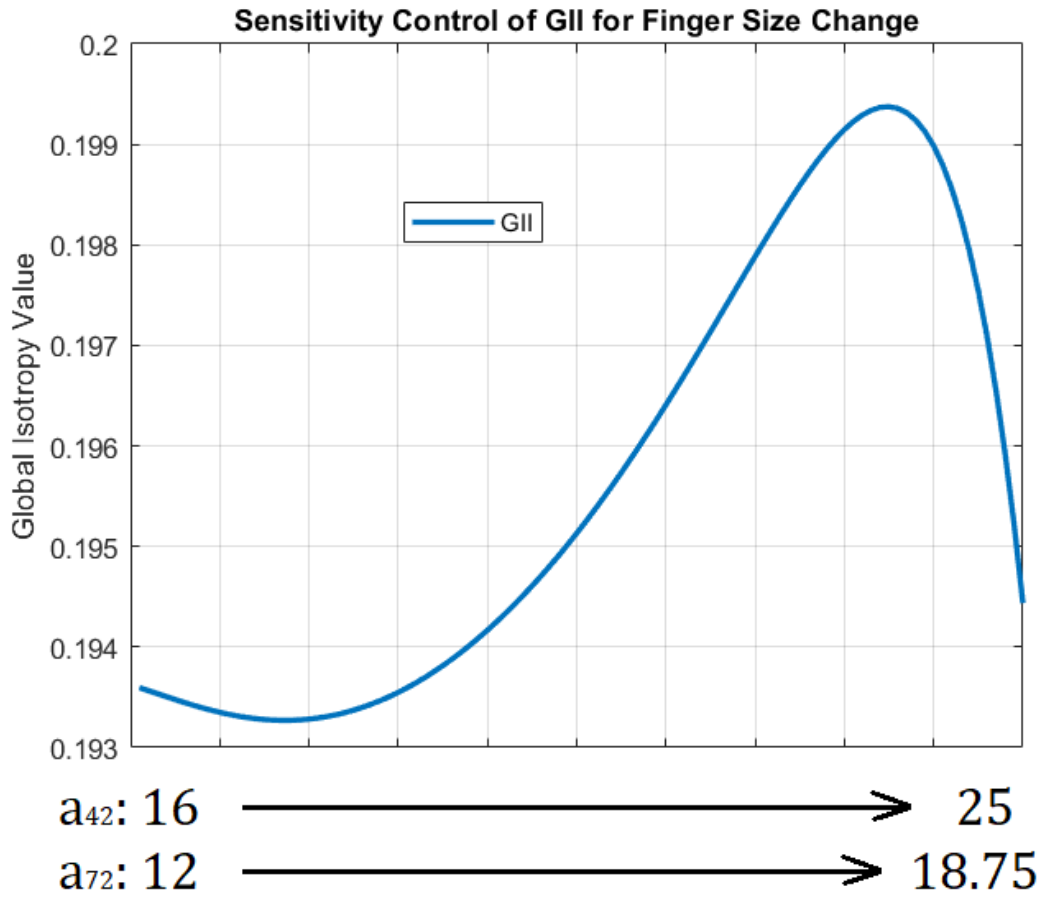

Figure 4.8: Sensitivity Check for phalanges sizes with respect to GII, zoomed

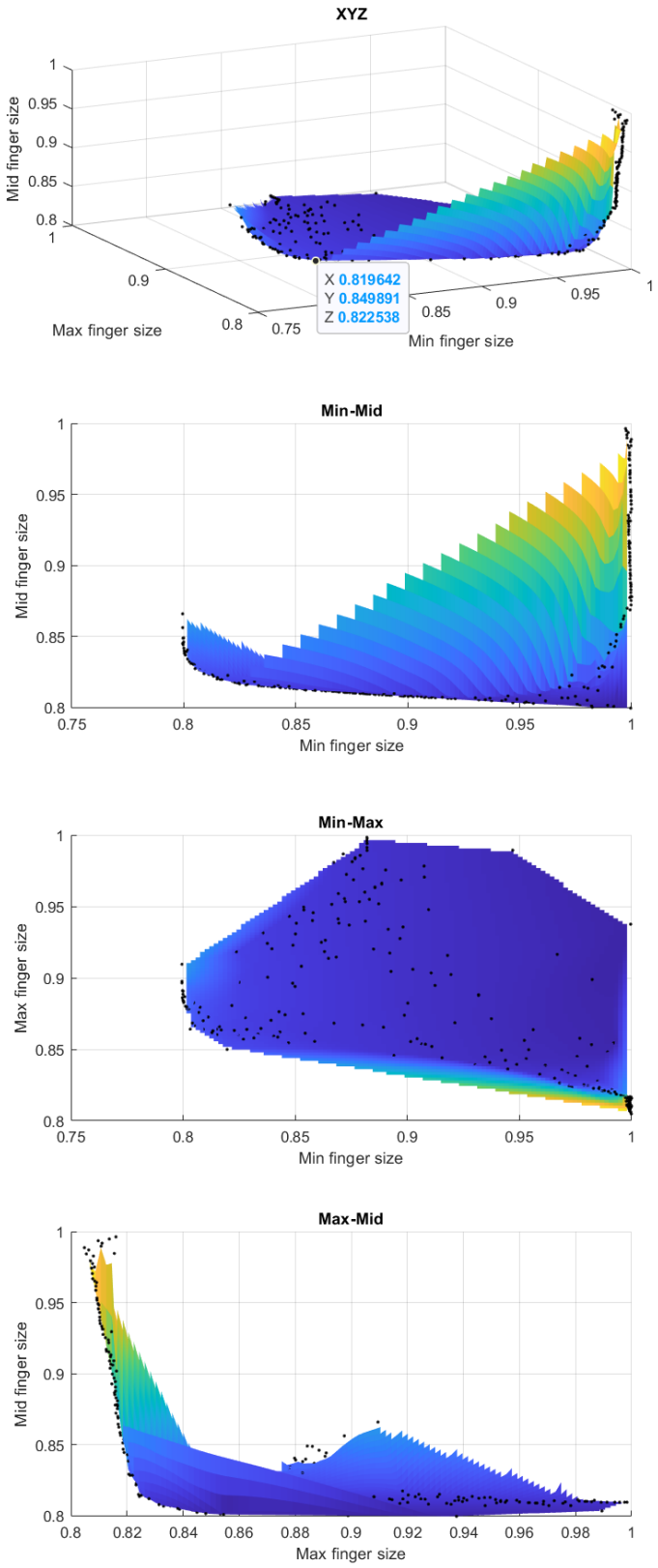

Figure 4.9: Multi Optimization 3D Plot

Table 4.4: Fully-Actuated, Multi-Optimization, Structure Parameter Results

Parameter	Result	Unit
a_{11}	23.7	mm
a_{12}	40.4	mm
a_2	51.4	mm
a_3	50.1	mm
a_{41}	24.8	mm
a_G	34.9	mm
a_5	64.2	mm
a_{51}	54.3	mm
a_6	42.6	mm
a_{71}	33.4	mm
a_8	37.3	mm
a_9	45.5	mm
θ_G	2	deg
β_2	88.5	deg
GII	[0.18, 0.15, 0.18]	-

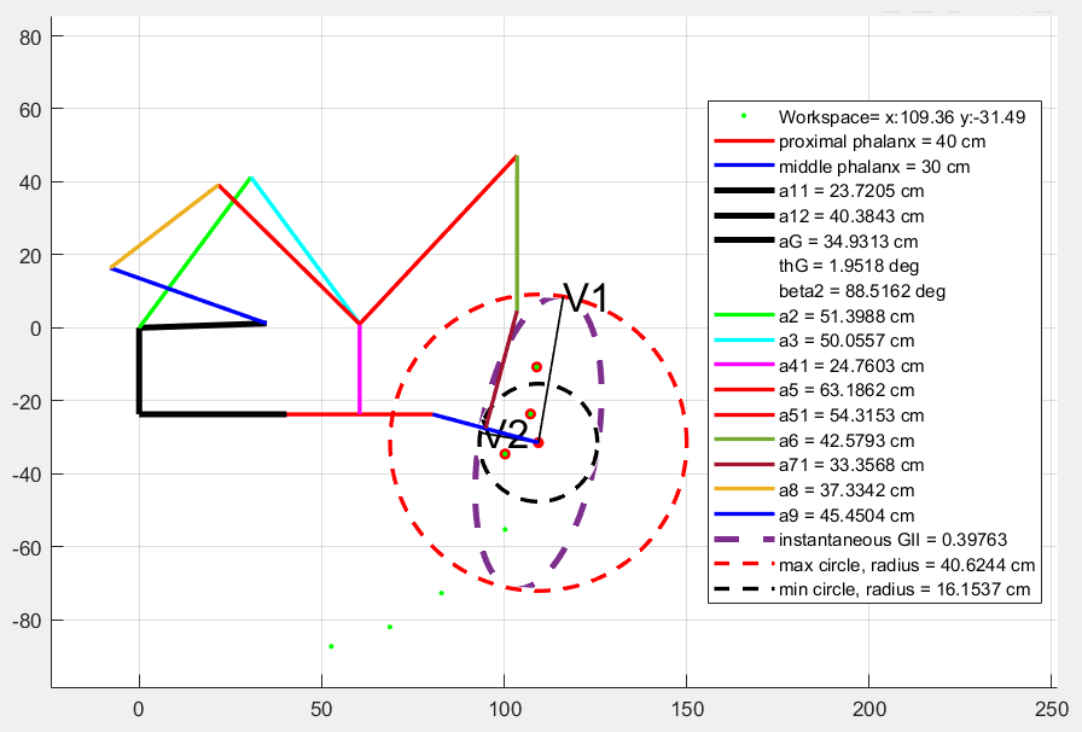

Figure 4.10: Multi Objective Optimization Animation

4.2 Transition from 4bar to 5 bar

In this section θ_{spr} is found numerically. As it was detailed in Chapter 3, in order to synthesize the mechanism, θ_{spr} is needed to be defined as a symbolic variable. Then, everything is calculated as a function of this value. At the end of the Virtual Work method, a function of θ_{spr} is obtained which is given as:

$$-K(\theta_{spr} - \theta_{spr_{free}}) = -(T_{PIP} + 2|F_{F_0}|a72)j_{22} \tag{4.2}$$

The equation is needed to be solved so that θ_{spr} gets obtained its numerical value. For this purpose, Matlab's "vpasolve" function is used. It is an equation solver in order to find a numerical solution. The θ_{spr} values are found as it is shown in the below Figure 4.12.

From the Figure 4.12, there is a intersection between the left and right side of the Equation in 4.2 for each state in the task-space. That intersection point is the θ_{spr} for that state.

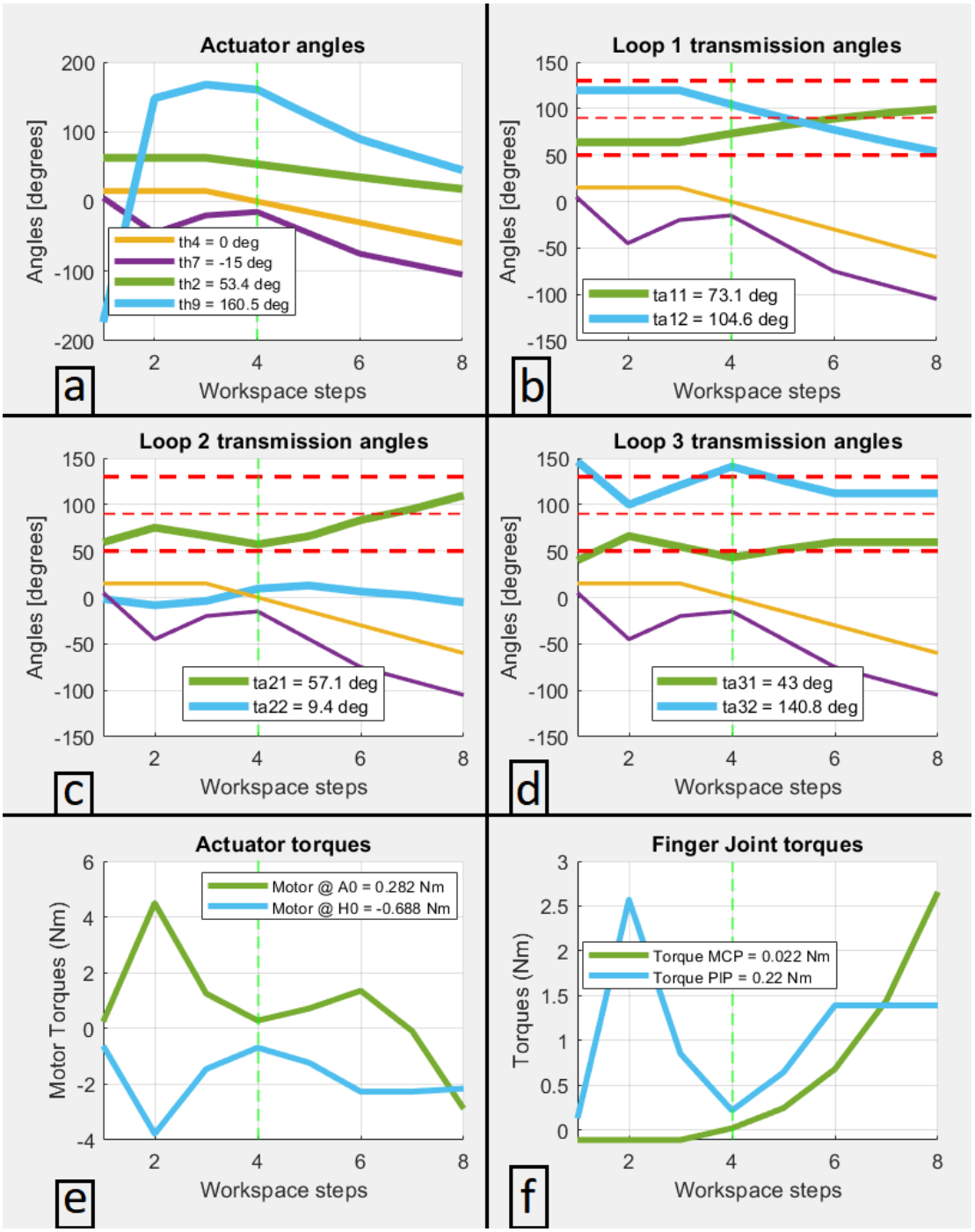

Figure 4.11: Multi Objective Optimization Animation, Angles and Torques

Finger angles and motor angles for the 8 states are given in the part a. Forward and backward transmission angles are represented for the each loop in the part b,c and d. The area between the horizontal dashed red lines show the desired transmission angle range in parts b,c and d. In the part e, calculated motor torque values are given for the each state. In the part f, calculated finger joint torque values are shown.

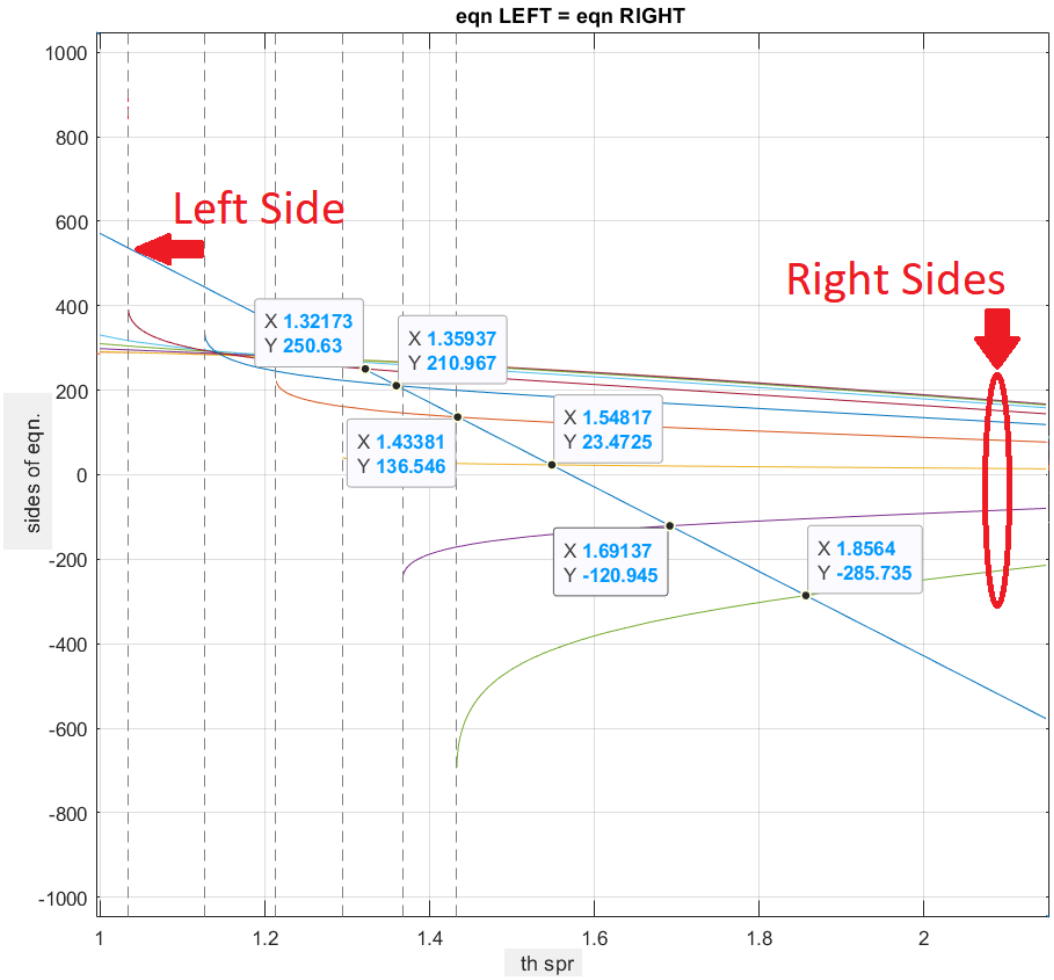

Figure 4.12: Finding θ_{spr} numerically

4.3 Under-Actuated Mechanism

For the under-actuated mechanism optimization, the fully-actuated mechanism outputs are used which are shown in the Table 4.3. There are 4 versions for the under-actuated mechanisms. They are given as follows.

4.3.1 Version 1

At loop 3, the link a_6 is broken to two as a_{61} and a_{62} with a torsional spring between these new links with a coefficient of K_1 and a free spring angle $\theta_{spr1_{free}}$. The boundaries for the new search parameters are given as:

Table 4.5: Lower and Upper Boundaries of the Structure Parameters of Under-Actuated Mechanism

Parameter	Lower Boundary	Upper Boundary	Unit
a_{61}	15	45	mm
a_{62}	15	45	mm
$th_{spr1_{free}}$	30	150	deg
K_1	$6/\pi \approx 1.9$	$60/\pi \approx 19.1$	Nm/rad

The genetic algorithm search is given in Figure 4.13. The solution set is in the Table 4.6. Animation of the mechanism is represented in Figure 4.14.

Table 4.6: Under-Actuated Mechanism Version 1 Results

Parameter	Result	Unit
a_{61}	25	mm
a_{62}	48	mm
$th_{spr1_{free}}$	60	deg
K_1	5.1	Nm/rad
GII	0.2038	-

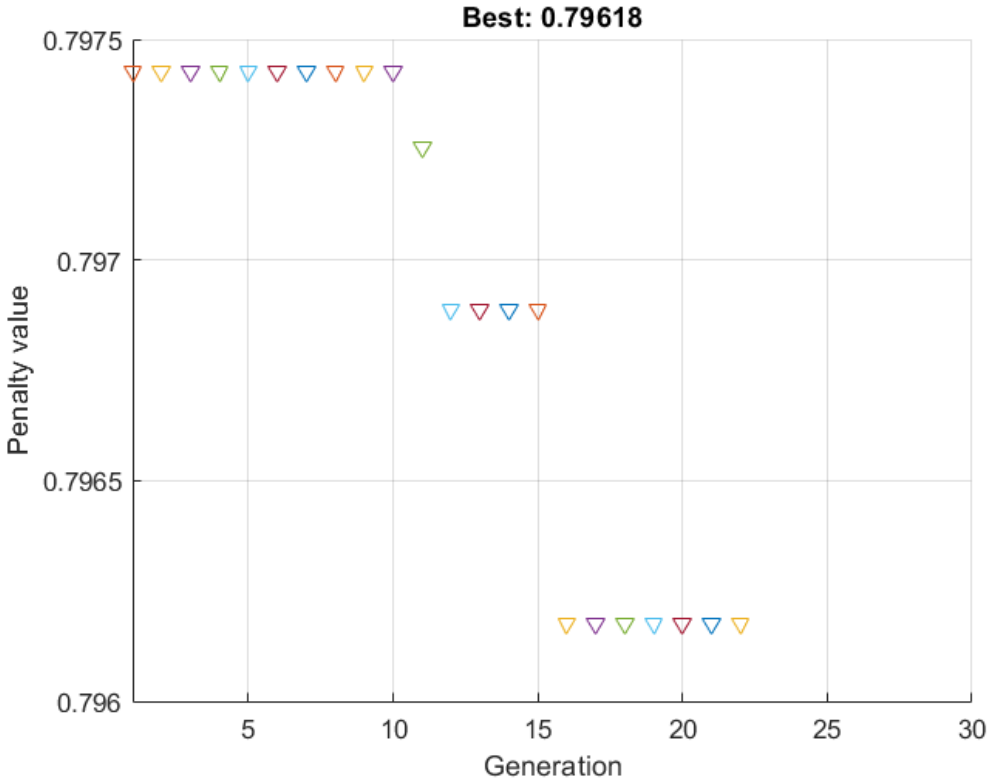

Figure 4.13: Under-Actuated Version 1 Genetic Algorithm

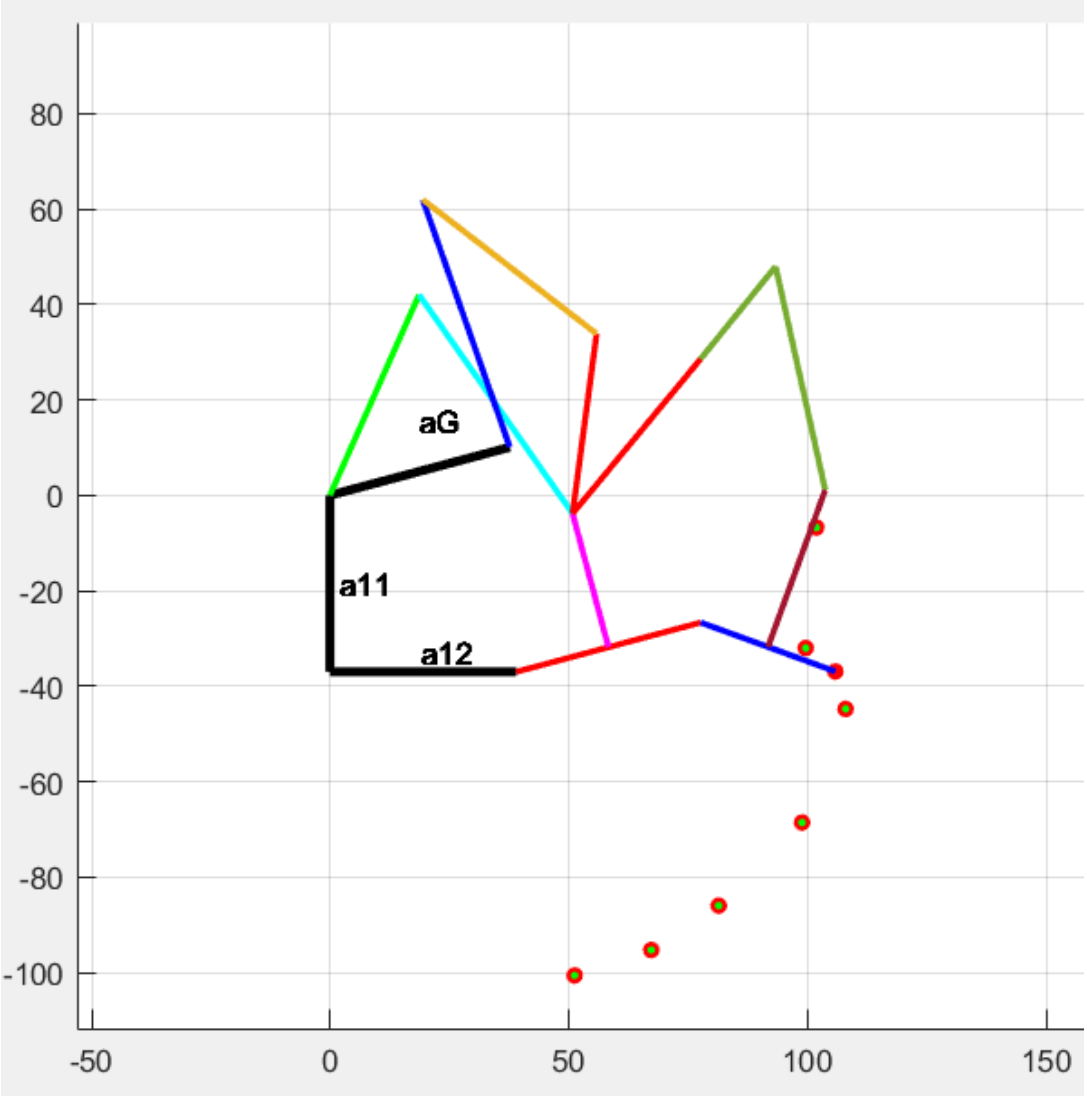

Figure 4.14: Under-Actuated Version 1 Animation, A State

4.3.2 Version 2

At loop 2, the link a_8 is broken into two as a_{81} and a_{82} with a torsional spring between these new links with a coefficient of K_2 and a free spring angle $\theta_{spr2_{free}}$. The boundaries for the new search parameters are given in Table 4.9.

The genetic algorithm search is given in Figure 4.15. The solution set is in the Table 4.8. A particular state of the mechanism is represented in Figure 4.16.

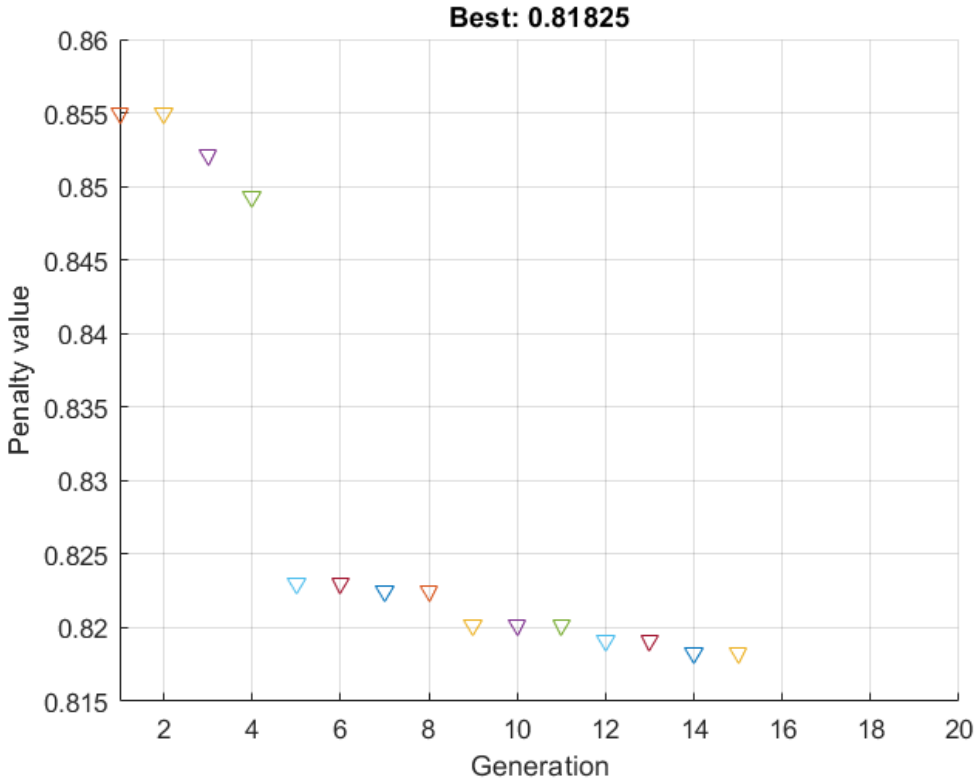

Figure 4.15: Under-Actuated Version 2 Genetic Algorithm

Table 4.7: Lower and Upper Boundaries of the Structure Parameters of Under-Actuated Mechanism

Parameter	Lower Boundary	Upper Boundary	Unit
a_{81}	40	65	mm
a_{82}	20	50	mm
$th_{spr2_{free}}$	30	150	deg
K_2	$6/\pi \approx 1.9$	$60/\pi \approx 19.1$	Nm/rad

Table 4.8: Under-Actuated Mechanism Version 2 Results

Parameter	Result	Unit
a_{61}	64	mm
a_{62}	20	mm
$th_{spr2_{free}}$	30	deg
K_2	17.8	Nm/rad
GII	0.1985	-

4.3.3 Version 3

At loop 1, the link a_3 is broken into two as a_{31} and a_{32} with a torsional spring between these new links with a coefficient of K_3 and a free spring angle $\theta_{spr3_{free}}$. The boundaries for the new search parameters are given below:

The genetic algorithm search is given in Figure 4.17. The solution set is in the Table 4.10. A particular state of the mechanism is represented in Figure 4.18.

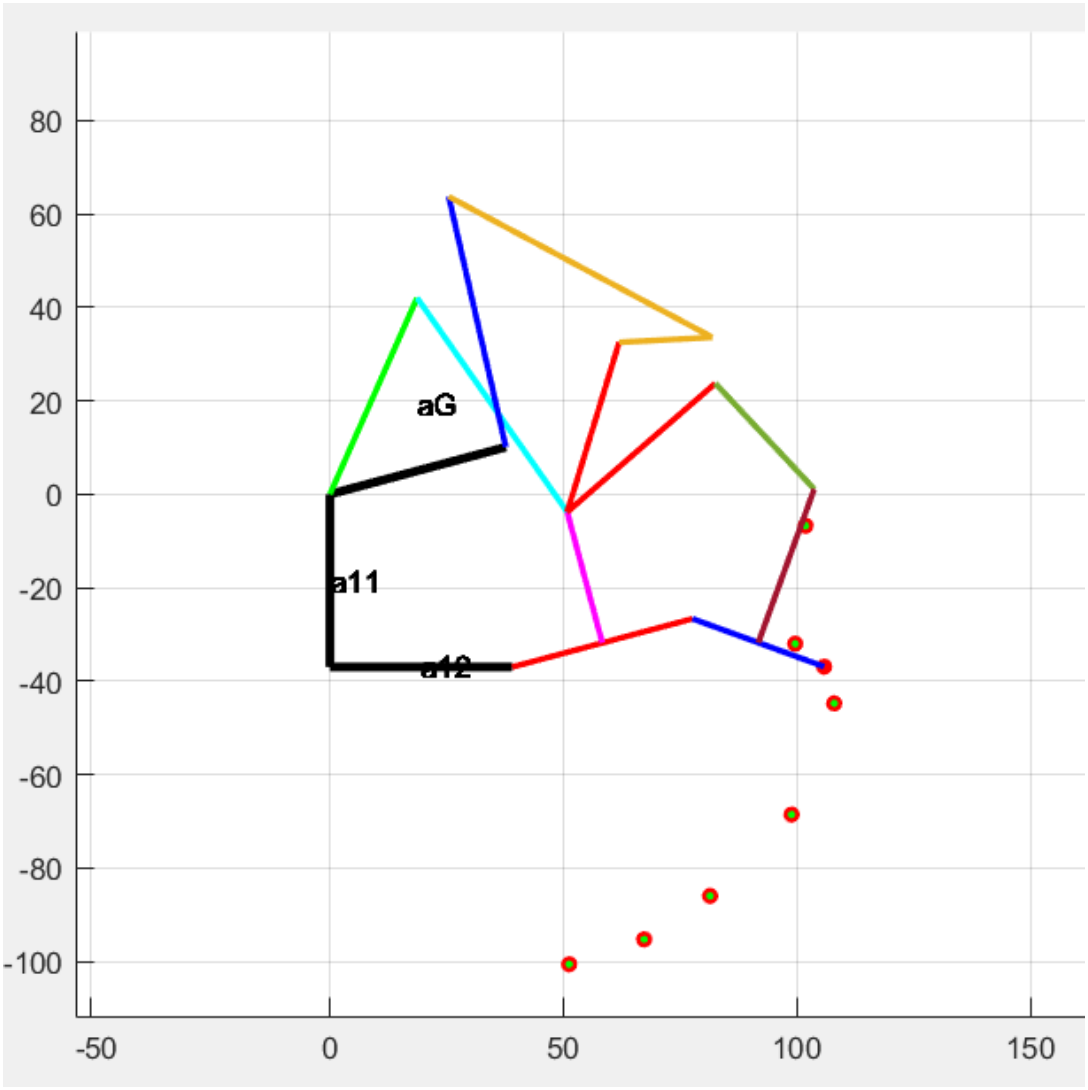

Figure 4.16: Under-Actuated Version 2 Animation, A State

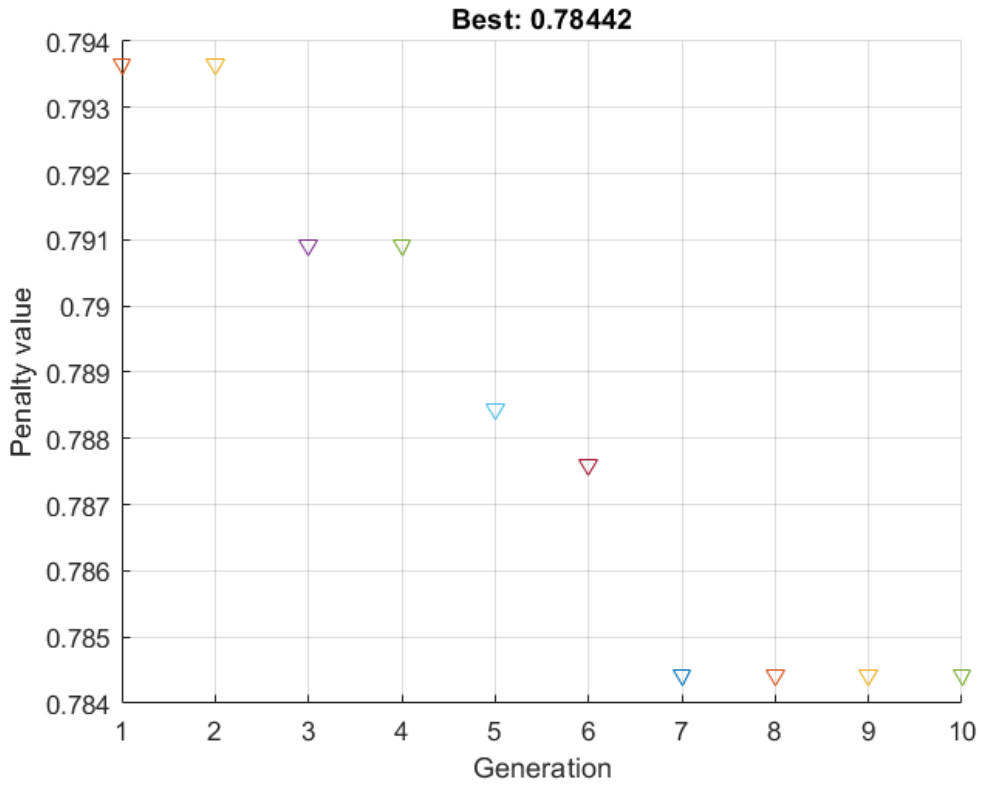

Figure 4.17: Under-Actuated Version 3 Genetic Algorithm

Table 4.9: Lower and Upper Boundaries of the Structure Parameters of Under-Actuated Mechanism

Parameter	Lower Boundary	Upper Boundary	Unit
a_{31}	25	65	mm
a_{32}	25	65	mm
$th_{spr3_{free}}$	30	150	deg
K_3	6/$\pi \approx 1.9$	60/$\pi \approx 19.1$	Nm/rad

Table 4.10: Under-Actuated Mechanism Version 3 Results

Parameter	Result	Unit
a_{31}	35	mm
a_{32}	26	mm
$th_{spr3_{free}}$	135	deg
K_3	10.4	Nm/rad
GII	0.2156	-

4.3.4 Version 4

In this version, the ternary link is broken into two links by defining a constant angle β_2 as a variable. So, a torsional spring is added between the links a_{51} and a_5 with a coefficient of K_4 and a free spring angle $\theta_{spr4_{free}}$. The boundaries for the new search parameters are given below:

Table 4.11: Lower and Upper Boundaries of the Structure Parameters of Under-Actuated Mechanism

Parameter	Lower Boundary	Upper Boundary	Unit
$th_{spr4_{free}}$	30	150	deg
K_4	6/$\pi \approx 1.9$	60/$\pi \approx 19.1$	Nm/rad

The genetic algorithm search is given in Figure 4.19. The solution set is in the Table 4.12. A particular state of the mechanism is represented in Figure 4.13.

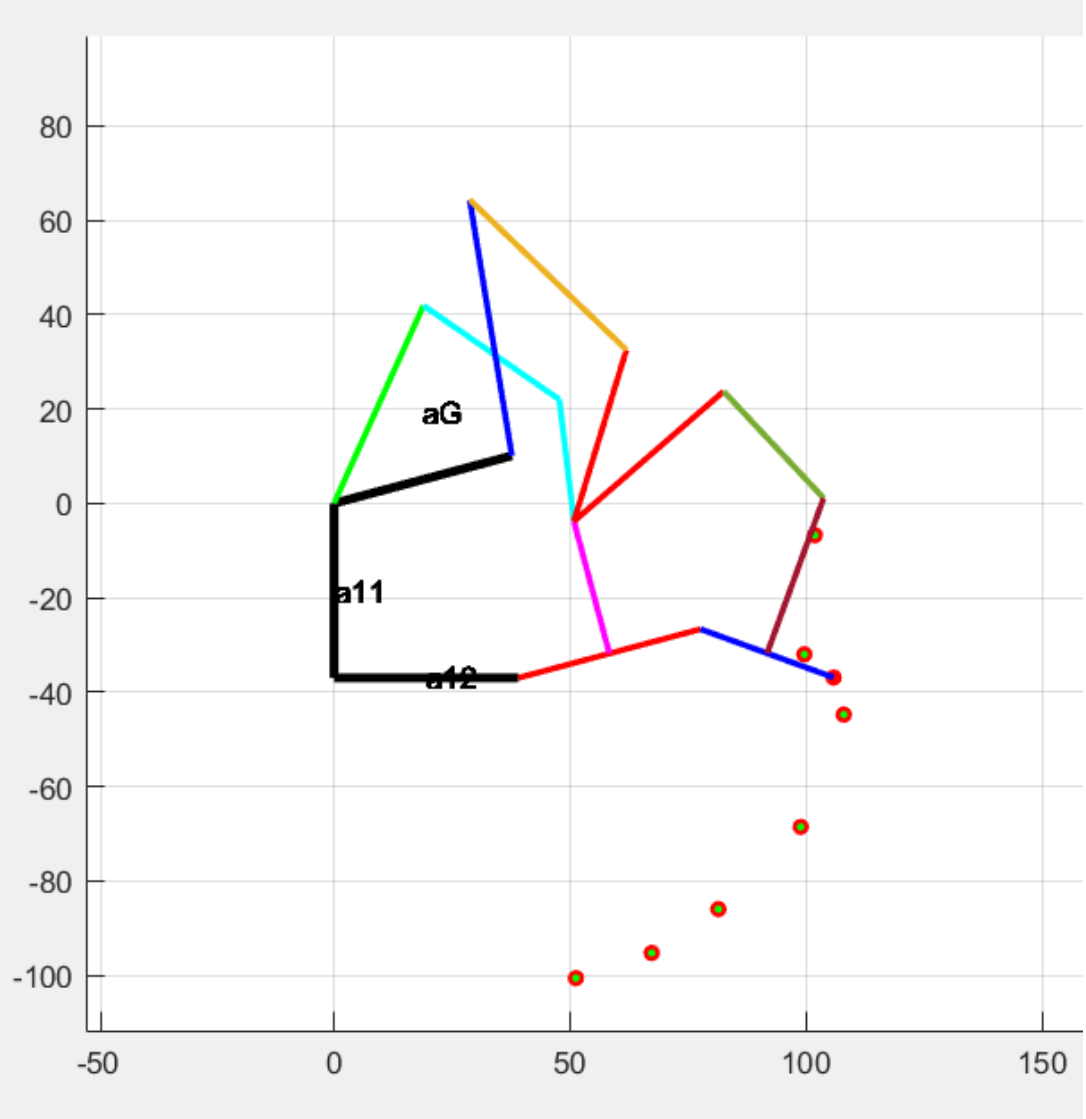

Figure 4.18: Under-Actuated Version 3 Animation, A State

Table 4.12: Under-Actuated Mechanism Version 4 Results

Parameter	Result	Unit
$th_{spr4_{free}}$	45	deg
K_4	12.2	Nm/rad
GII	0.1927	-

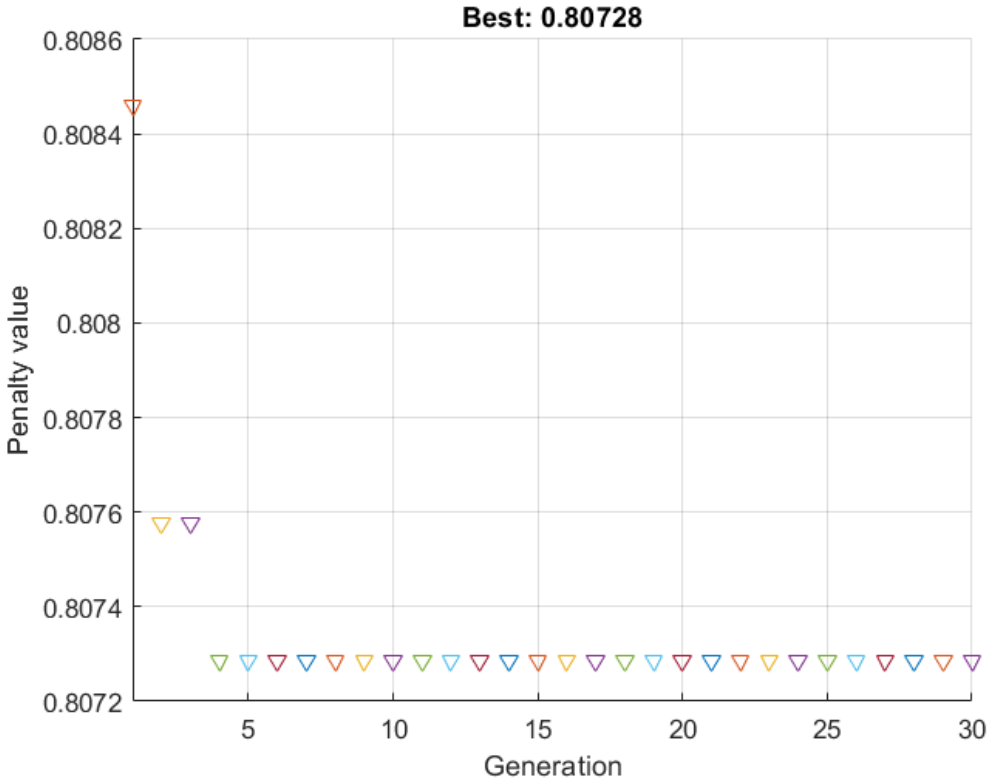

Figure 4.19: Under-Actuated Version 4 Genetic Algorithm

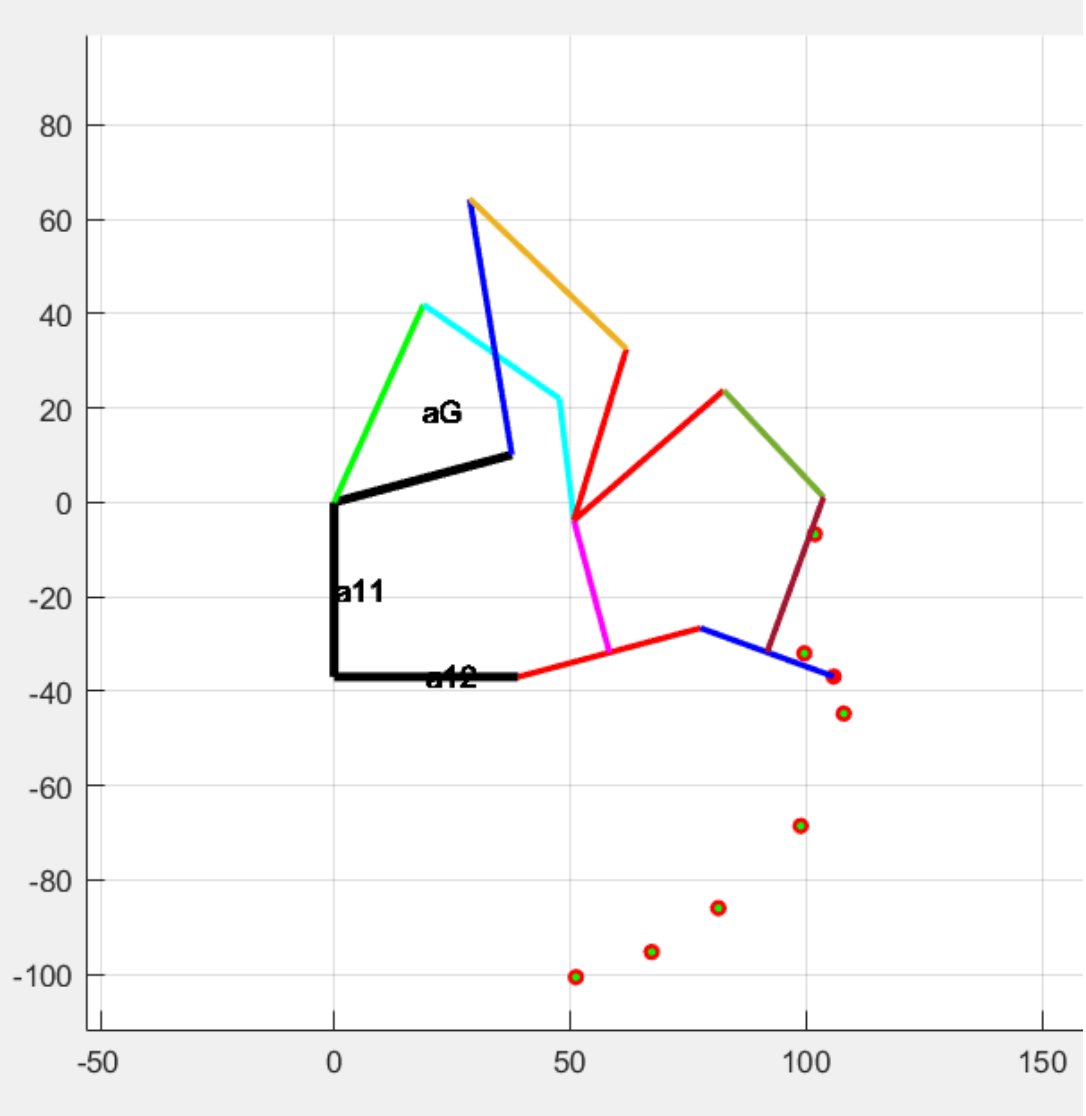

Figure 4.20: Under-Actuated Version 4 Animation, A State

4.3.5 Overview

An overview of the fully-actuated and under-actuated results is given in Table 4.13. For the under-actuated mechanism family, four solutions are constructed as thoroughly illustrated in Table 4.13. From these versions, the one with the best result in terms of the highest GII value difference occurrence is selected, which is version 3.

Table 4.13: Results of Mechanism Optimization, GII values

Phalange Size	Fully v0	Under v1	Under v2	Under v3	Under v4
Minimum	0.1936	0.2038	0.1985	0.2156	0.1927
Nominal	0.1946	0.2381	0.2377	0.2484	0.2260
Maximum	0.1944	0.2357	0.2622	0.2163	0.2300
Worst Case	0.1936	0.2038	0.1985	0.2156	0.1927

CHAPTER 5

MECHANISM REALIZATION AND PRODUCTION

The AutoDesk Fusion 360 CAD program is used for mechanical engineering. Ball bearings are used for revolute joint connections. The mechanism is manufactured using a 3D printer.

5.1 Fully-actuated Mechanism

There are two parts in this section. At first, a prototype is manufactured. While this process is going, some challenges are encountered, such as the collusion of the links and the connection method between the user's finger and the mechanism. Those are overcome early in the development of the first prototype. Then, a second prototype is manufactured with coupled motors, which is presented in the second part of this section.

5.1.1 Prototype 1

For prototype purposes, rapid manufacturing is conducted without the addition of motors. The structure parameters are selected from the multi-optimization problem as in Table 4.4. The mechanism is shown in Figures 5.1, 5.2 and 5.3.

Results have been tested with a large range of phalanges sizes from $a_{42} = 25$ and $a_{72} = 16$. Singularity has not been observed within the defined task space. The pictures are presented in Figures 5.4 and 5.5.

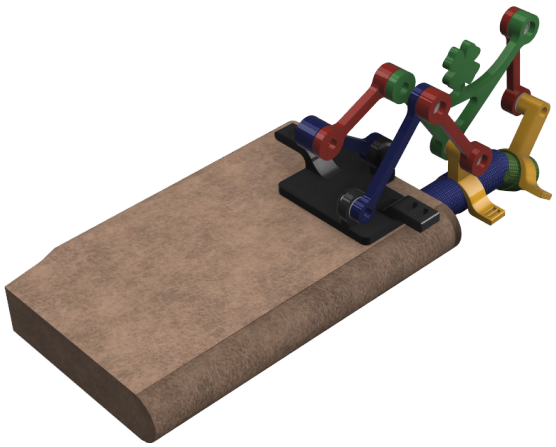

Figure 5.1: Fully-Actuated Prototype 1 Isometric View 1

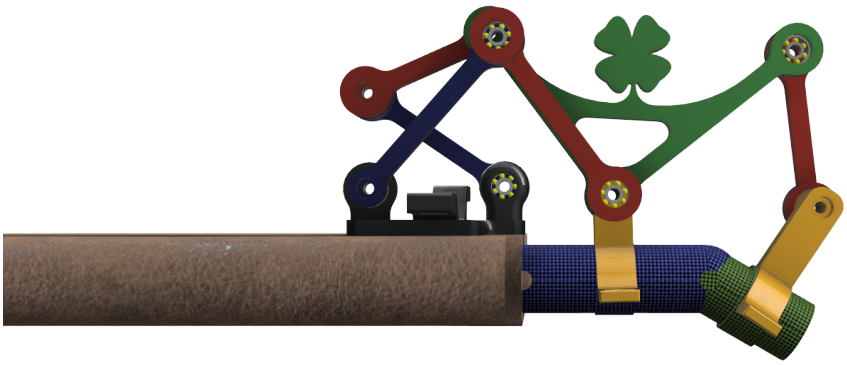

Figure 5.2: Fully-Actuated Prototype 1 Front View

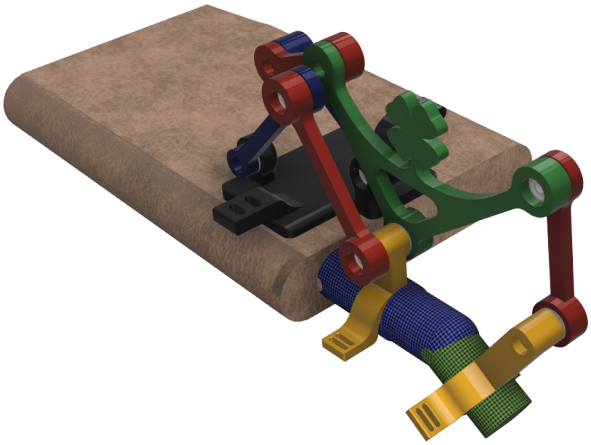

Figure 5.3: Fully-Actuated Prototype 1 Isometric View 2

Figure 5.4: Manufactured Fully-Actuated Prototype 1 View 1

Figure 5.5: Manufactured Fully-Actuated Prototype 1 View 2

5.1.2 Prototype 2

For the final fully-actuated prototype, the addition of motors is performed. In this case, the solution set from the single-optimization with sensitivity problem with a better GII value is carried out. The results in Table 4.3 are used for this prototype. The mechanism is shown in Figures 5.6, 5.7, 5.8. and 5.9.

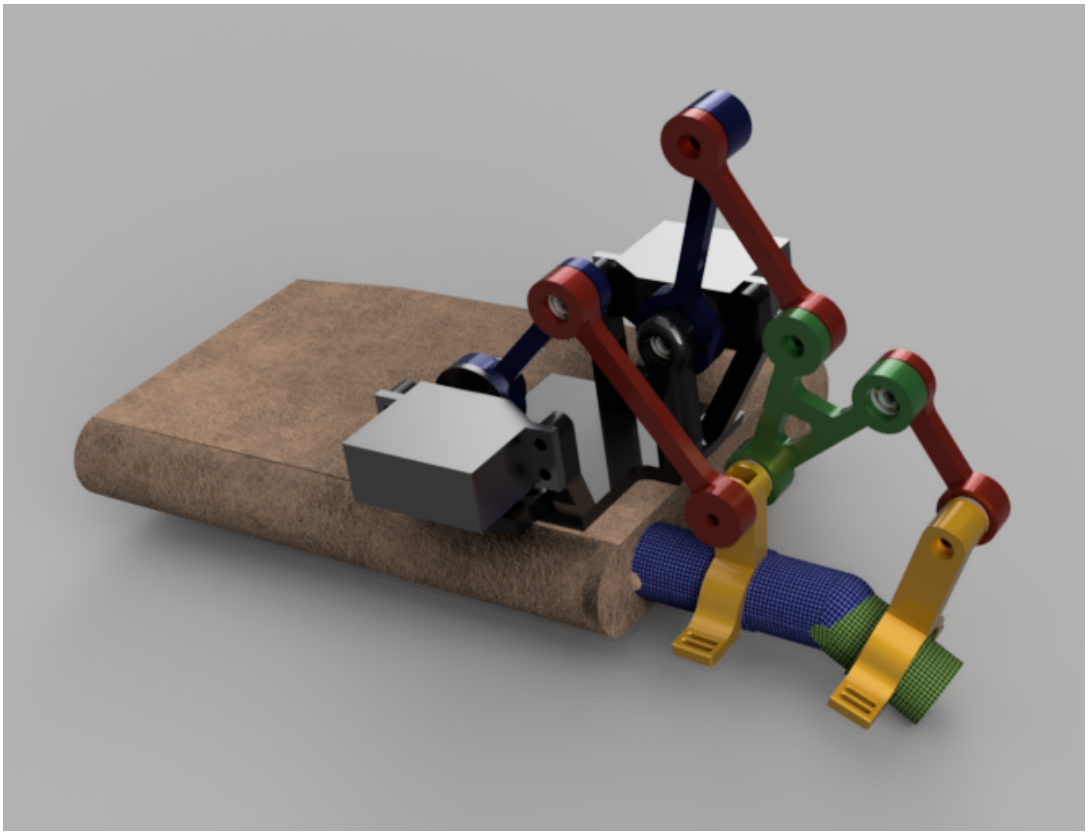

Figure 5.6: Fully-Actuated Prototype 2 View 1

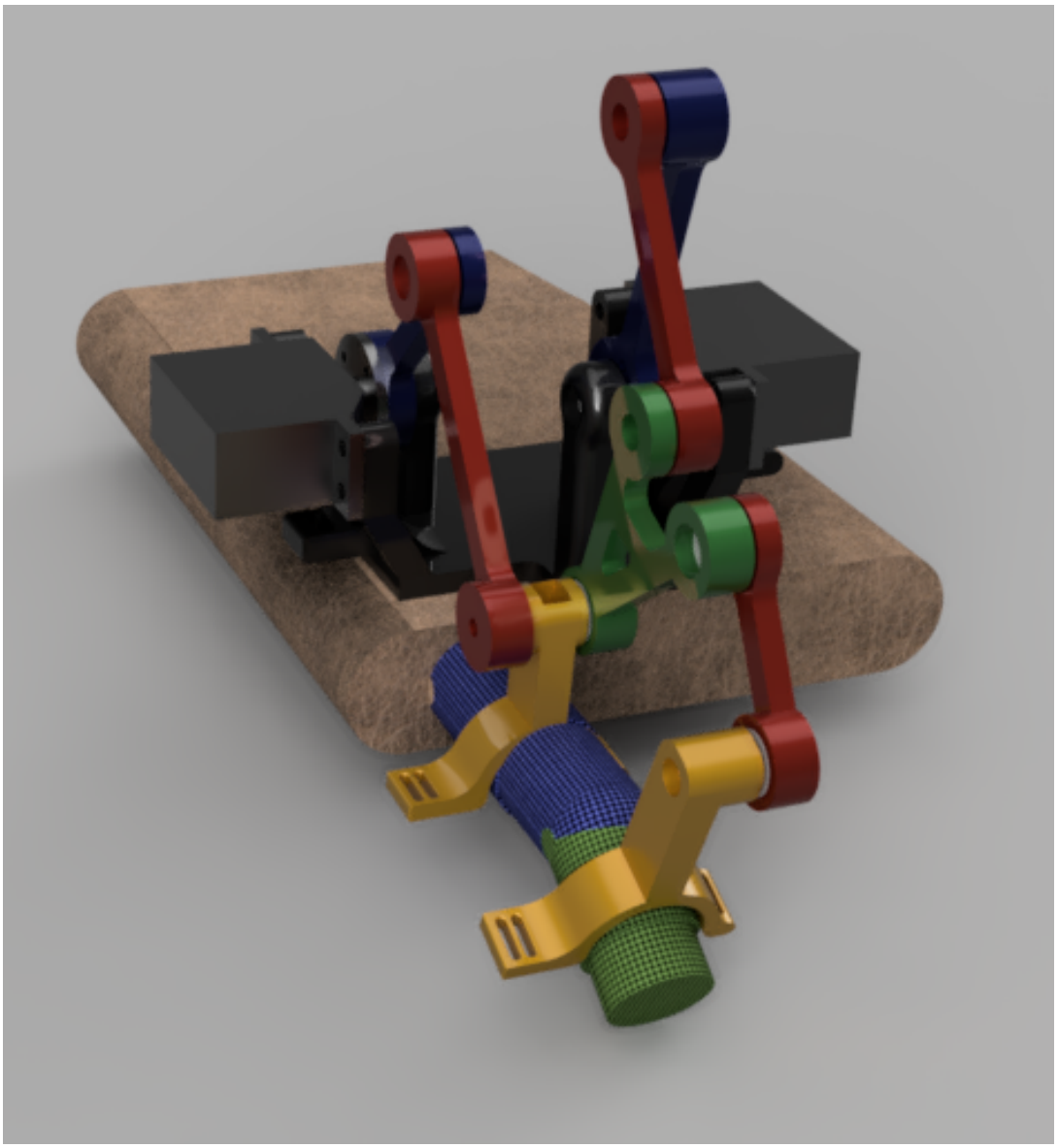

Figure 5.7: Fully-Actuated Prototype 2 View 2

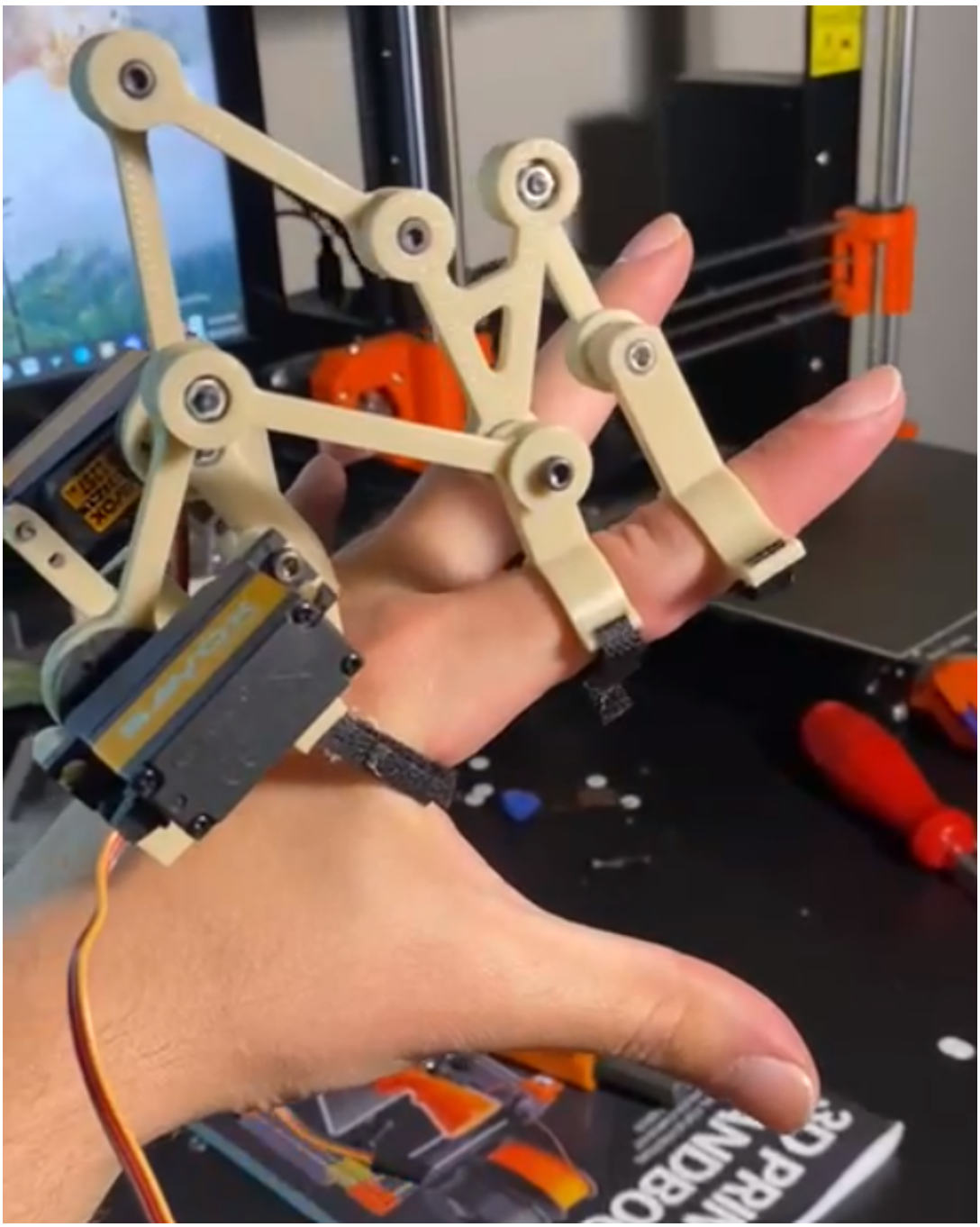

Figure 5.8: Manufactured Fully-Actuated Prototype 2 View 1

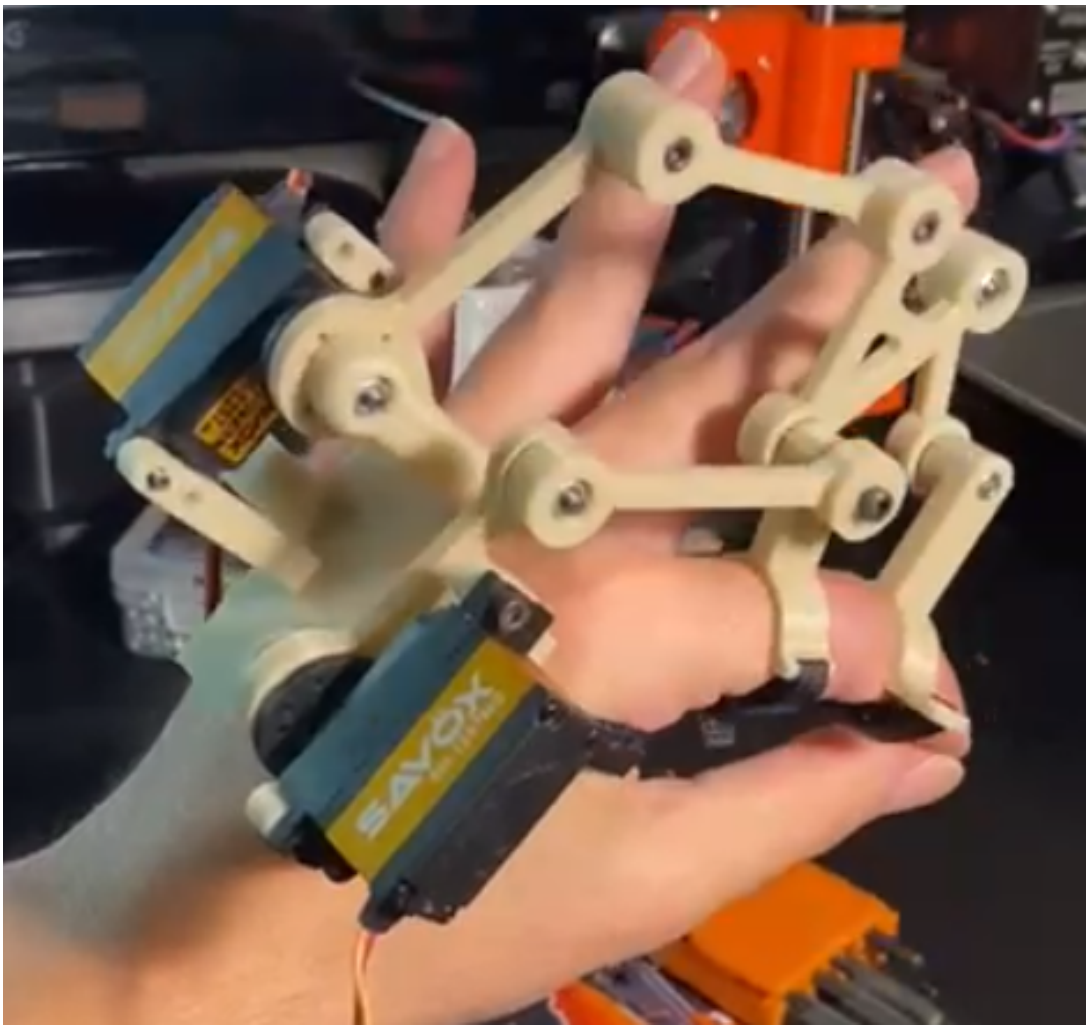

Figure 5.9: Manufactured Fully-Actuated Prototype 2 View 2

5.2 Under-actuated Mechanism

The under-actuated mechanism is derived from the fully-actuated one. Version 3 from the under-actuated mechanism family is selected for the final product. A torsion spring is used in order to be able to control the mechanism. Also, a potentiometer is needed in the under-actuated mechanism so that the kinematics of the mechanism can be studied. The potentiometer that is desired to be used is given in Figure 5.10.

Figure 5.10: Potentiometer

Installation of the potentiometer results as a new adaptor named an "Under-actuated Adaptor". The adaptor is shown in Figures 5.11 and 5.12. The design of the torsion spring is dependent on the potentiometer's size. In this case, the outer diameter of the rod is 13.4 mm. So, the inner diameter of the spring is good to be 15.5 mm, which is $\%115$ larger than the rod size. Four different torsion springs with wire diameters of

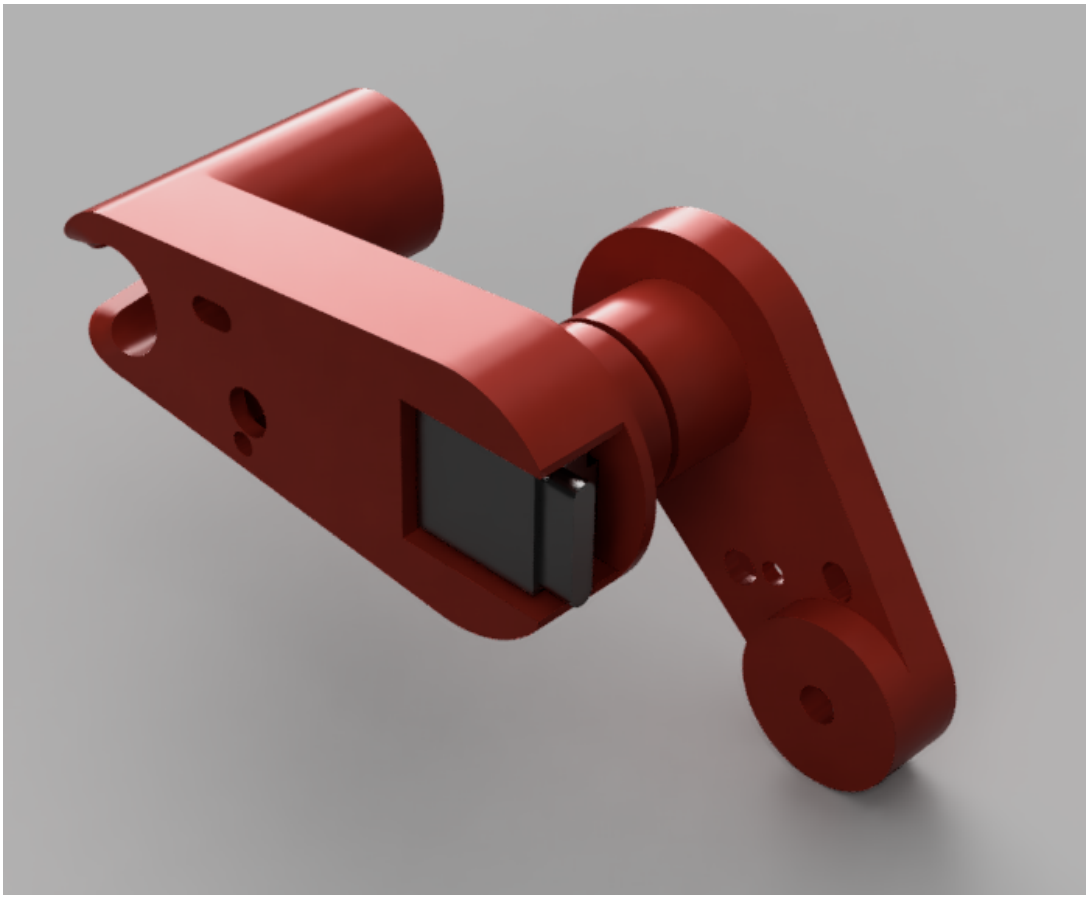

Figure 5.11: Under-actuated Adaptor

1.25, 1.5, 1.75, and 2 mm are manufactured. A cross-section view of the adaptor is given in Figure 5.12. In Figure 5.13, the easy-switch apparatus, a fixer is shown that is used to switch the mechanism from fully-actuated to under-actuated or vice-versa. The assembly of the adaptor is presented in Figures 5.14, 5.15 and 5.16. Finally, the under-actuated mechanism is shown in Figures 5.17, 5.18 and 5.19.

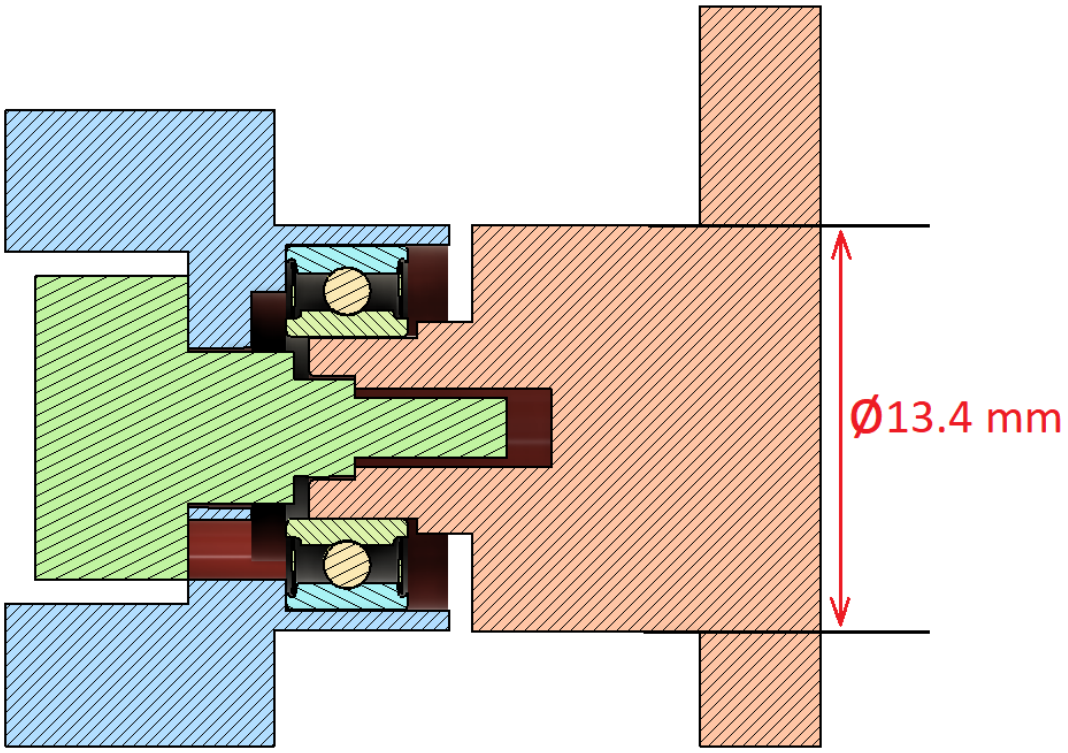

Figure 5.12: Under-actuated Adaptor Cross-Section

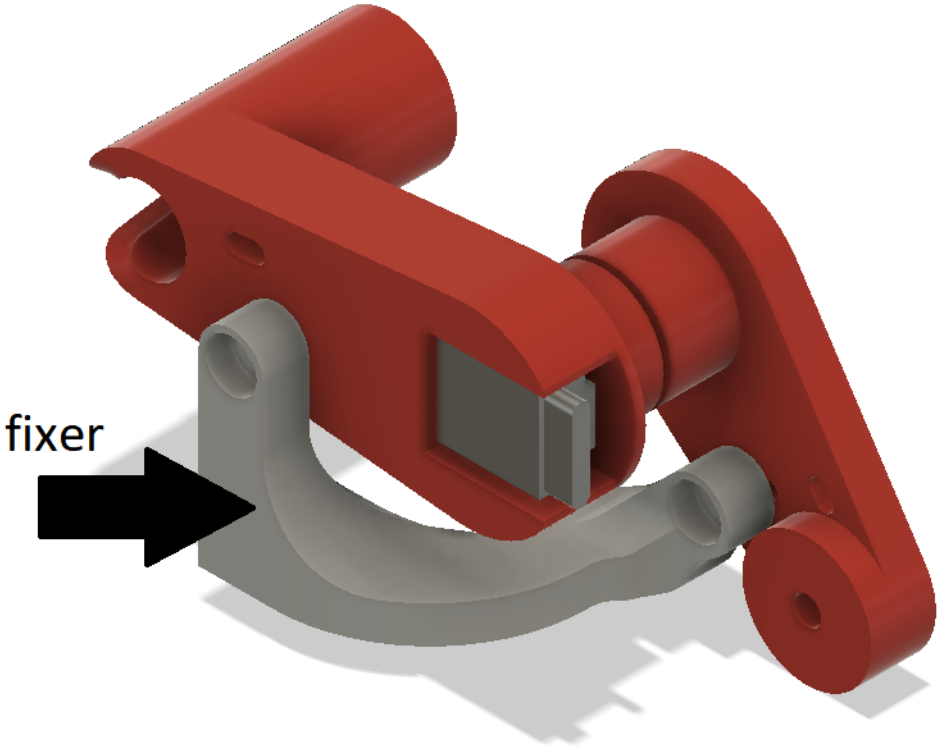

Figure 5.13: Under-actuated Adaptor Fixer

Figure 5.14: Under-actuated Adaptor View 1

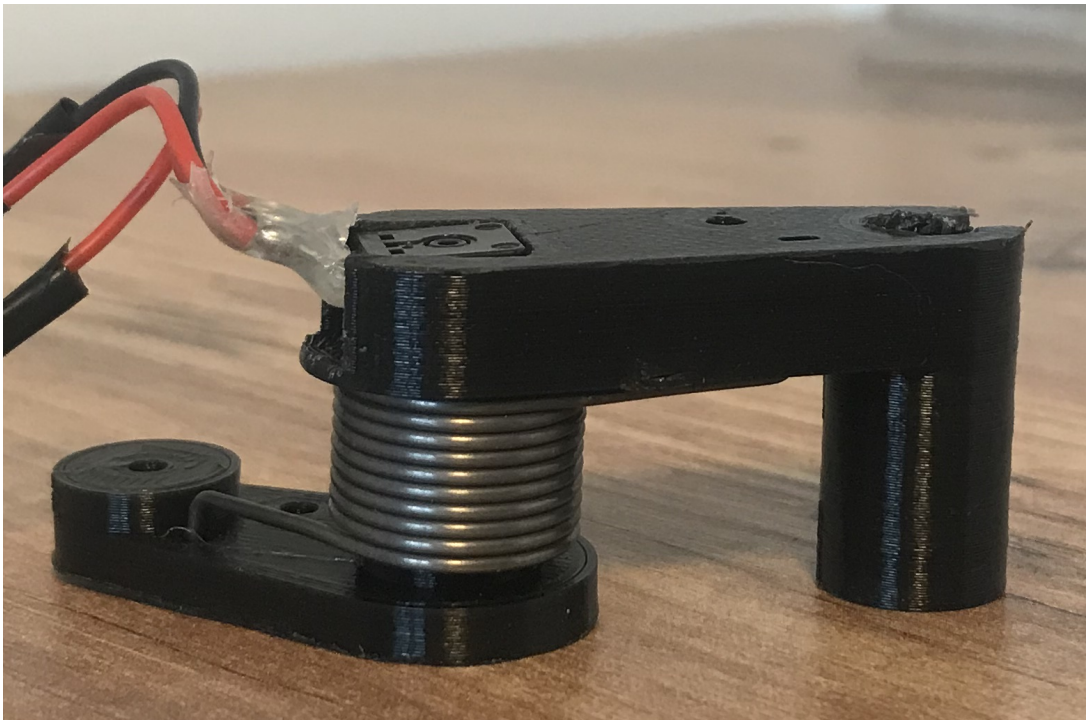

Figure 5.15: Under-actuated Adaptor View 2

Figure 5.16: Under-actuated Adaptor View 3

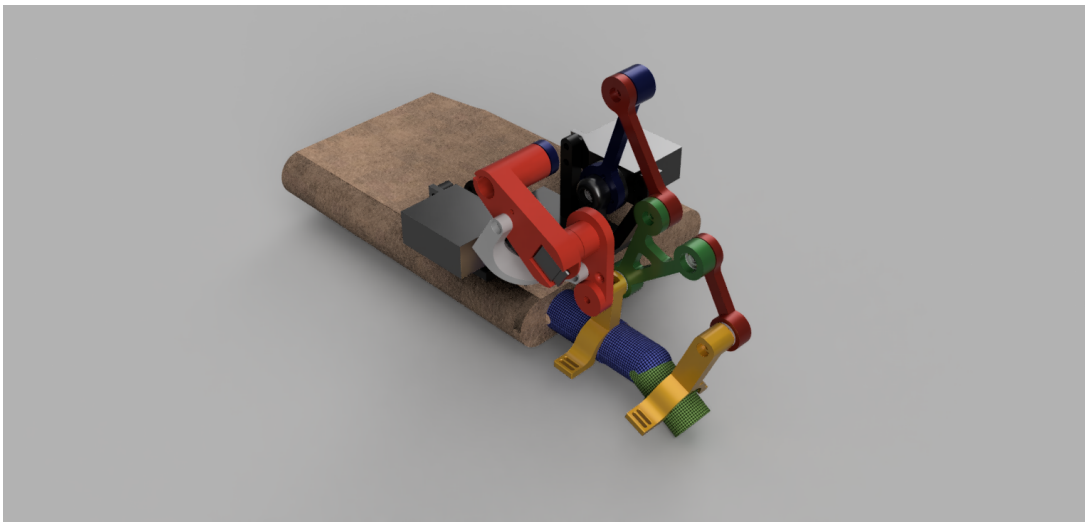

Figure 5.17: Under-Actuated Mechanism View 1

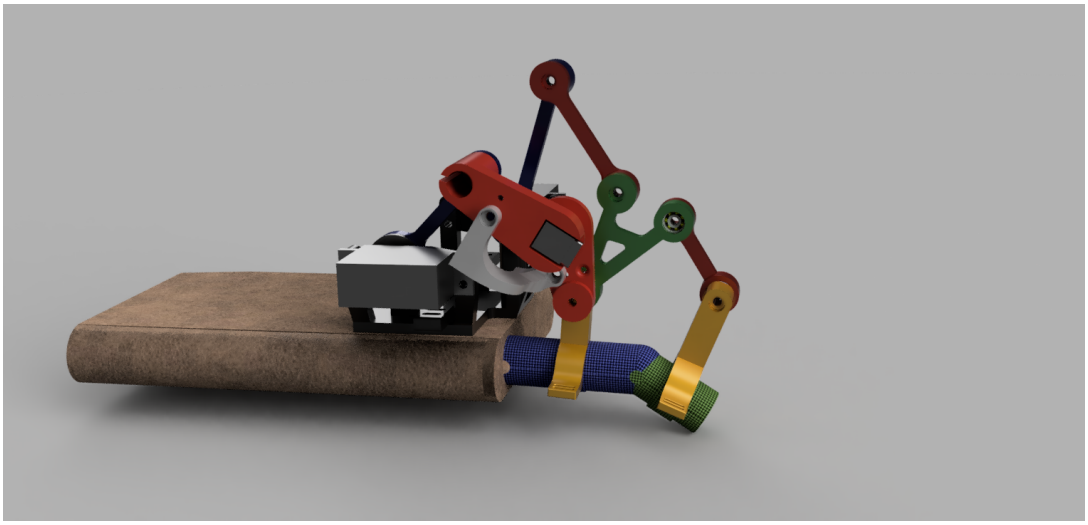

Figure 5.18: Under-Actuated Mechanism View 2

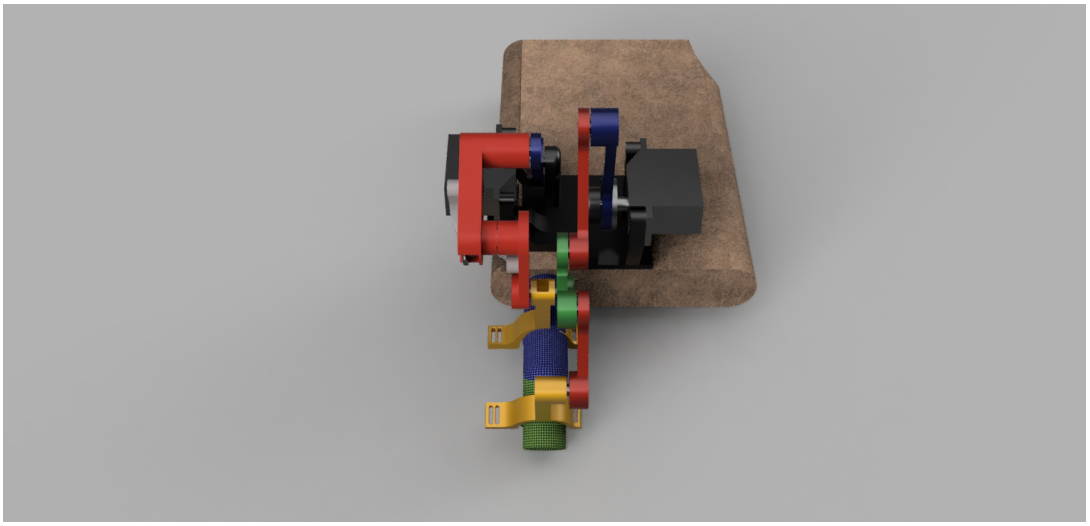

Figure 5.19: Under-Actuated Mechanism View 3

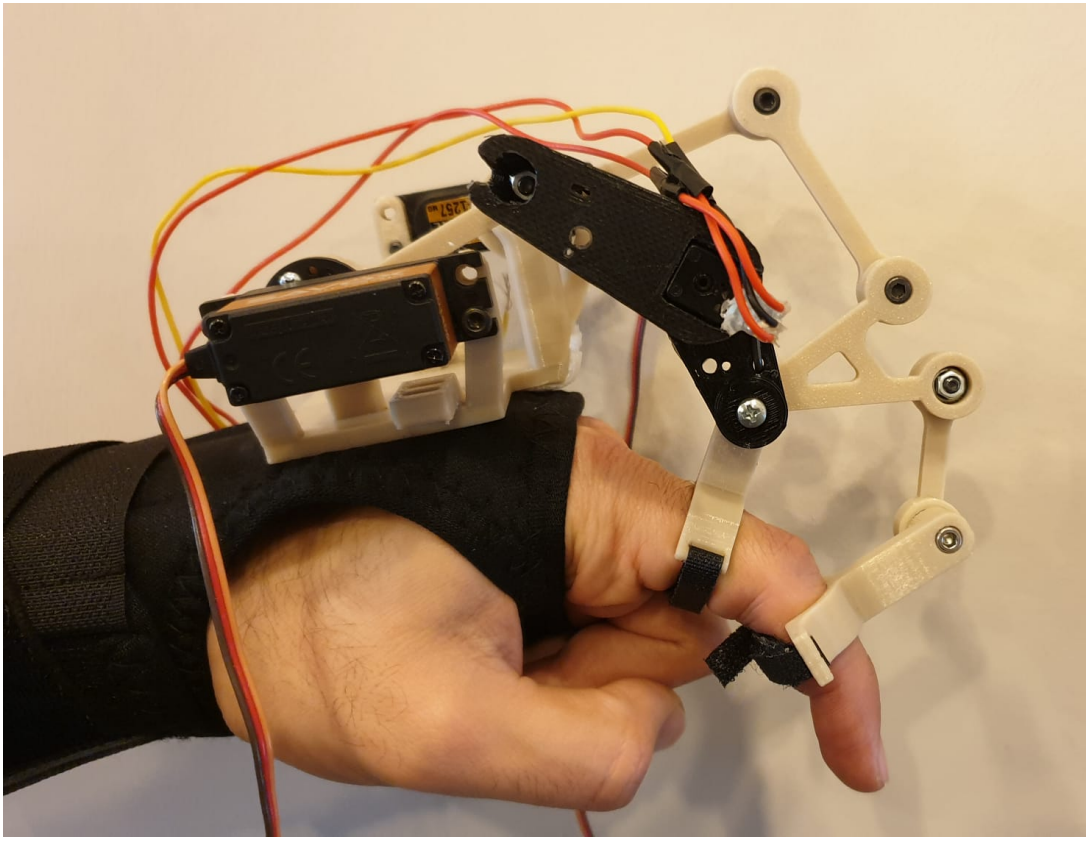

Figure 5.20: Manufactured Under-Actuated Mechanism

CHAPTER 6

DISCUSSION AND CONCLUSION

6.1 Discussion

It takes far more channeling to design an under-actuated mechanism than a fully-actuated one. Since the degree of actuation is less than the degree of freedom, it is not possible to define an under-actuated mechanism without using force equations. Therefore, the force equations are used to get this essential equation. These mechanisms can be sensitive to the environment because of this property.

Theoretically, the under-actuated mechanism should promote greater motor learning. This hypothesis has to be examined in real-world patient scenarios. Another important point is that a single-objective function only comes up with one solution, while a multi-objective function comes up with more than one solution. The designer has a selection from these solution sets. However, when the single-optimization problem is clearly specified, it can be used quite effectively. Additionally, the final product can be made using PLA additive manufacturing (3D printing). They are easy to make and incredibly stiff. Research involving actual patients, however, may have a different result.

6.2 Conclusion

In this thesis paper, a family of mechanisms is designed that is going to be used for rehabilitation purposes. The Global Isotropy Index is used to find the optimal mechanism. Primarily, a fully-actuated mechanism is produced. The fully-actuated mechanism is then used to design a family of under-actuated mechanisms with tor-

sional springs. A conventional mechanical torsion spring is used. Mechanism links are manufactured using 3D printers. An easy switch method is adapted to the mechanism so that it is possible to use the same mechanism not only in the fully-actuated type but also in the under-actuated type.

6.2.1 Future work

The following is a list of the upcoming works that would advance this thesis:

- In order to determine how accurate the virtual work calculations are, testing using motors must be performed.
- It is necessary to examine the differences between fully-actuated and under-actuated systems with real patient studies.
- In order to create a more user-friendly design, the data of the hand and fingers that are used as input for 3D design should be improved, such as finger segment diameters and palm altitude.
- Customizing the selection, crossover, and mutation functions allows for the specification of GA problems. Perfectly tailored functions may almost certainly ensure that the whole search space is checked.
- A topological optimization for the 3D design would be beneficial to reduce the mechanism's overall mass.
- It is possible to construct a compliant mechanism as an alternative to traditional springs.
- Instead of having a robust design for different users, the mechanism might work better if it had a few links that could be changed for different patients.

REFERENCES

[1] S. C. Johnston, S. Mendis, and C. D. Mathers, "Global variation in stroke burden and mortality: estimates from monitoring, surveillance, and modelling," *Lancet Neurol.*, vol. 8, pp. 345–354, Apr. 2009.

[2] SpinalCord.com, "Types of paralysis: Monoplegia, hemiplegia, paraplegia, and quadriplegia."

[3] R. A. Schmidt and T. D. Lee, *Motor learning and performance: From principles to application*. 2014.

[4] C. Pin-Barre and J. Laurin, "Physical exercise as a diagnostic, rehabilitation, and preventive tool: Influence on neuroplasticity and motor recovery after stroke," *Neural Plasticity*, vol. 2015, p. 608581, Nov 2015.

[5] J. A. Hosp and A. R. Luft, "Cortical plasticity during motor learning and recovery after ischemic stroke," *Neural Plast.*, vol. 2011, p. 871296, Oct. 2011.

[6] S. L. Small, G. Buccino, and A. Solodkin, "The mirror neuron system and treatment of stroke," *Dev. Psychobiol.*, vol. 54, pp. 293–310, Apr. 2012.

[7] L. M. Muratori, E. M. Lamberg, L. Quinn, and S. V. Duff, "Applying principles of motor learning and control to upper extremity rehabilitation," *Journal of Hand Therapy*, vol. 26, no. 2, pp. 94–103, 2013.

[8] C. Liu, J. Lu, H. Yang, and K. Guo, "Current state of robotics in hand rehabilitation after stroke: A systematic review," *Applied Sciences*, vol. 12, no. 9, 2022.

[9] J. Wang, J. Li, Y. Zhang, and S. Wang, "Design of an exoskeleton for index finger rehabilitation," in *2009 Annual International Conference of the IEEE Engineering in Medicine and Biology Society*, IEEE, Sept. 2009.

[10] S. C. Venema, *Experiments in surface perception using a fingertip haptic display*. PhD thesis, 1999.

[11] D. G. Kamper, T. George Hornby, and W. Z. Rymer, "Extrinsic flexor muscles generate concurrent flexion of all three finger joints," *Journal of Biomechanics*, vol. 35, no. 12, pp. 1581–1589, 2002.

[12] A. Turolla, O. A. Daud Albasini, R. Oboe, M. Agostini, P. Tonin, S. Paolucci, and Piron, *Haptic-based neurorehabilitation in poststroke patients: a feasibility prospective multicentre trial for robotics hand rehabilitation. Computational and mathematical methods in medicine*. 2013.

[13] S. C. Venema and B. Hannaford, "A probabilistic representation of human workspace for use in the design of human interface mechanisms," *IEEE ASME Trans. Mechatron.*, vol. 6, no. 3, pp. 286–294, 2001.

[14] F. Bullo and R. M. Murray, "Tracking for fully actuated mechanical systems: a geometric framework," *Automatica*, vol. 35, no. 1, pp. 17–34, 1999.

[15] S. S. Balli and S. Chand, "Transmission angle in mechanisms (triangle in mech)," *Mech. Mach. Theory*, vol. 37, pp. 175–195, Feb. 2002.

[16] C. Zhang, C. Rossi, W. He, and J. Colorado, "Virtual-work-based optimization design on compliant transmission mechanism for flapping-wing aerial vehicles," in *2016 International Conference on Manipulation, Automation and Robotics at Small Scales (MARSS)*, IEEE, July 2016.

[17] P. Boscariol, G. Boschetti, P. Gallina, and C. Passarini, "Spring design for motor torque reduction in articulated mechanisms," in *Advances in Service and Industrial Robotics*, Mechanisms and machine science, pp. 557–564, Cham: Springer International Publishing, 2018.

[18] S. Khatami, *Kinematic isotropy and robot design optimization using a genetic algorithm method*. PhD thesis, University of British Columbia, 2001.

[19] M. Kirćanski, "Kinematic isotropy and optimal kinematic design of planar manipulators and a 3-DOF spatial manipulator," *Int. J. Rob. Res.*, vol. 15, pp. 61–77, Feb. 1996.

[20] T. Yoshikawa, "Manipulability of robotic mechanisms," *Int. J. Rob. Res.*, vol. 4, pp. 3–9, June 1985.

[21] J. Kim and P. K. Khosla, "A multi-population genetic algorithm and its application to design of manipulators," in *Proceedings of the IEEE/RSJ International Conference on Intelligent Robots and Systems*, IEEE, 2005.

[22] C. A. Klein and B. E. Blaho, "Dexterity measures for the design and control of kinematically redundant manipulators," *Int. J. Rob. Res.*, vol. 6, pp. 72–83, June 1987.

[23] J.-O. Kim and K. Khosla, "Dexterity measures for design and control of manipulators," in *Proceedings IROS '91:IEEE/RSJ International Workshop on Intelligent Robots and Systems '91*, IEEE, 2002.

[24] C. A. Klein and T. A. Miklos, "Spatial robotic isotropy," *Int. J. Rob. Res.*, vol. 10, pp. 426–437, Aug. 1991.

[25] C. M. Gosselin, "Dexterity indices for planar and spatial robotic manipulators," in *Proceedings., IEEE International Conference on Robotics and Automation*, IEEE Comput. Soc. Press, 2002.

[26] O. Ma and J. Angeles, "The concept of dynamic isotropy and its applications to inverse kinematics and trajectory planning," in *Proceedings., IEEE International Conference on Robotics and Automation*, IEEE Comput. Soc. Press, 2002.

[27] J. Angeles, "The design of isotropic manipulator architectures in the presence of redundancies," *Int. J. Rob. Res.*, vol. 11, pp. 196–201, June 1992.

[28] L. J. Stocco, *Robot design optimization with haptic interface applications (Doctoral dissertation)*. 1999.

[29] R. Unal, G. Kiziltas, and V. Patoglu, "A multi-criteria design optimization framework for haptic interfaces," in *2008 Symposium on Haptic Interfaces for Virtual Environment and Teleoperator Systems*, pp. 231–238, 2008.

[30] A. Saltelli, "Sensitivity analysis for importance assessment," *Risk Anal.*, vol. 22, pp. 579–590, June 2002.

[31] O. Denizhan and M.-S. Chew, "Linkage mechanism optimization and sensitivity analysis of an automotive engine hood," *Int. j. automot. sci. technol.*, vol. 1, pp. 7–16, Mar. 2018.

[32] D. Xu, "Kinematic reliability and sensitivity analysis of the modified delta parallel mechanism," *Int. J. Adv. Robot. Syst.*, vol. 15, p. 172988141875910, Jan. 2018.

[33] J. Iqbal, H. Khan, N. G. Tsagarakis, and D. G. Caldwell, "A novel exoskeleton robotic system for hand rehabilitation-conceptualization to prototyping," *Biocybernetics and biomedical engineering*, vol. 34, no. 2, pp. 79–89, 2014.

[34] H. Lohninger, "Optimization Methods - Brute Force Approach." http://www.statistics4u.com/fundstat_eng/cc_optim_meth_brutefrc.html. [Online; accessed 2022-8-23].

[35] H. Lohninger, "Optimization Methods - Gradient Descent." http://www.statistics4u.com/fundstat_eng/cc_optim_meth_gradient.html. [Online; accessed 2022-12-20].

[36] H. Lohninger, "Optimization Methods - Monte Carlo Simulations." http://www.statistics4u.com/fundstat_eng/cc_optim_meth_montecarlo.html. [Online; accessed 2022-12-20].

[37] H. Lohninger, "Optimization Methods - Genetic Algorithms." http://www.statistics4u.com/fundstat_eng/cc_optim_meth_combi.html. [Online; accessed 2022-12-20].

[38] MathWorks, "Genetic algorithms and genetic programming." Accessed: 2022-8-23.

[39] MathWorks, "How the genetic algorithm works." Accessed: 2022-8-23.

[40] A. Dina, S. Danaila, M.-V. Pricop, and I. Bunescu, "Using genetic algorithms to optimize airfoils in incompressible regime," *INCAS BULL.*, vol. 11, pp. 79–90, Mar. 2019.

[41] O. de Weck, "Multidisciplinary system design and optimization," 2010.

[42] T. Murata and H. Ishibuchi, "MOGA: multi-objective genetic algorithms," in *Proceedings of 1995 IEEE International Conference on Evolutionary Computation*, IEEE, 2002.

[43] K. H. L. Heung, Z. Q. Tang, L. Ho, M. Tung, Z. Li, and R. K. Y. Tong, "Design of a 3d printed soft robotic hand for stroke rehabilitation and daily activities assistance," in *2019 IEEE 16th International Conference on Rehabilitation Robotics (ICORR)*, pp. 65–70, 2019.

[44] J.-S. Zhao, K. Zhou, and Z.-J. Feng, "A theory of degrees of freedom for mechanisms," *Mechanism and Machine Theory*, vol. 39, no. 6, pp. 621–643, 2004.

[45] U. Arnet, D. A. Muzykewicz, J. Fridén, and R. L. Lieber, "Intrinsic hand muscle function, part 1: creating a functional grasp," *J. Hand Surg. Am.*, vol. 38, pp. 2093–2099, Nov. 2013.

[46] H. M. Clayton, "Biomechanics of the distal interphalangeal joint," *Journal of Equine Veterinary Science*, vol. 30, no. 8, pp. 401–405, 2010.

[47] M. K. Ozgoren, *Kinematics of general spatial mechanical systems*. Standards Information Network, Mar. 2020.